Chapter 1
Field Emission from Quantum Wires of Nonparabolic Semiconductors

1.1 Introduction

The Fowler–Nordheim field emission (FNFE) is a well-known quantum-mechanical phenomenon that involves tunneling of electrons through a surface barrier due to the application of an intense external electric field. Normally, at field strengths of the order of 10^8 V/m (below the electrical breakdown), the potential barriers at the surfaces of metals and semiconductors usually become very thin and result in field emission of electrons due to the tunnel effect [1, 2]. This has been well investigated with reference to three-dimensional electron gases in metals and semiconductors and the FNFE from quantum-confined structures has also been studied in this context [3–37]. Some of significant features of the FNFE which have emerged from these investigations are as follows:

1. The FNFE increases with increasing electron concentration in bulk materials and are significantly influenced by the carrier energy spectra of different electronic materials.
2. The FNFE increases with increasing electric field.
3. The FNFE oscillates with film thickness for quantum-confined systems.
4. The FNFE oscillates with inverse quantizing magnetic field in the presence of magnetic quantization due to the Shubnikov–de Haas effect.
5. For various types of superlattices of different materials, the FNFE shows composite oscillations with different system variables.

In recent years, with the advent of fine lithographical methods [38, 39], molecular beam epitaxy [40], organometallic vapor-phase epitaxy [41], and other experimental techniques, the restriction of the motion of the carriers of bulk materials in one (quantum wells in ultrathin films, NIPI structures, inversion, and accumulation layers), two (quantum wires), and three (quantum dots, magnetosize quantized systems, magneto-accumulation layers, magneto-inversion layers quantum dot superlattices, magneto-quantum well superlattices, and magneto-NIPI structures) dimensions have in the last few years, attracted much attention not only for their

S. Bhattacharya and K.P. Ghatak, *Fowler–Nordheim Field Emission*, Springer Series in Solid-State Sciences 170, DOI 10.1007/978-3-642-20493-7_1,

potential in uncovering new phenomena in nanoscience, but also for their interesting quantum device applications [42–45]. In ultrathin films, the restriction of the motion of the carriers in the direction normal to the film (say, the z direction) may be viewed as carrier confinement in an infinitely deep 1D rectangular potential well, leading to quantization [known as quantum size effect (QSE)] of the wave vector of the carrier along the direction of the potential well, allowing 2D carrier transport parallel to the surface of the film representing new physical features not exhibited in bulk semiconductors [46–50]. The low-dimensional heterostructures based on various materials are widely investigated because of the enhancement of carrier mobility [51]. These properties make such structures suitable for applications in quantum well lasers [52], heterojunction FETs [53, 54], high-speed digital networks [55–58], high-frequency microwave circuits [59], optical modulators [60], optical switching systems [61], and other devices. The constant energy 3D wavevector space of bulk semiconductors becomes 2D wavevector surface in ultrathin films or quantum wells due to dimensional quantization. Thus, the concept of reduction of symmetry of the wavevector space and its consequence can unlock the physics of low-dimensional structures.

It is well known that in quantum wires (QWs), the restriction of the motion of the carriers along two directions may be viewed as carrier confinement by two infinitely deep 1D rectangular potential wells, along any two orthogonal directions leading to quantization of the wave vectors along the said directions, allowing 1D carrier transport [62–64]. With the help of modern fabrication techniques, such one-dimensional quantized structures have been experimentally realized and enjoy an enormous range of important applications in the realm of nanoscience in quantum regime. They have generated much interest in the analysis of nanostructured devices for investigating their electronic, optical, and allied properties [65–72]. Examples of such new applications are based on the different transport properties of ballistic charge carriers which include quantum resistors [73–75], resonant tunneling diodes and band filters [76, 77], quantum switches [78], quantum sensors [79, 80], quantum logic gates [81, 82], quantum transistors and subtuners [83, 84], heterojunction FETs [85], high-speed digital networks [86, 87], high-frequency microwave circuits [88], optical modulators [89], optical switching systems [90], and other nanoscale devices.

In this chapter, we shall study the FNFE from QWs of nonparabolic semiconductors having different band structures. At first we shall investigate the FNFE from QWs of nonlinear optical compounds which are being used in nonlinear optics and light-emitting diodes [91, 92]. The quasi-cubic model can be used to investigate the symmetric properties of both the bands at the zone center of wavevector space of the same compound.Including the anisotropic crystal potential in the Hamiltonian, and special features of the nonlinear optical compounds, Kildal [93] formulated the electron dispersion law under the assumptions of isotropic momentum matrix element and the isotropic spin–orbit splitting constant, respectively, although the anisotropies in the two aforementioned band constants are the significant physical features of the said materials [94–96]. In Sect. 1.2.1, the FNFE from QWs of nonlinear optical semiconductors has been investigated by considering the combined influence of the anisotropies of the said energy band constants together with the

inclusion of the crystal field splitting respectively within the framework of $\mathbf{k} \cdot \mathbf{p}$ formalism.

The III–V compounds find applications in infrared detectors [97], quantum dot light-emitting diodes [98], quantum cascade lasers [99], quantum well wires [100], optoelectronic sensors [101], high electron mobility transistors [102], etc. The electron energy spectrum of III–V semiconductors can be described by the three- and two-band models of Kane [103, 104], together with the models of Stillman et al. [105], Newson and Kurobe [106], and Palik et al. [107], respectively. In this context, it may be noted that the ternary and quaternary compounds enjoy the singular position in the entire spectrum of optoelectronic materials. The ternary alloy $Hg_{1-x}Cd_xTe$ is a classic narrow gap compound. The band gap of this ternary alloy can be varied to cover the spectral range from 0.8 to over 30 μm [108] by adjusting the alloy composition. $Hg_{1-x}Cd_xTe$ finds extensive applications in infrared detector materials and photovoltaic detector arrays in the 8–12 μm wave bands [109]. The above uses have generated the $Hg_{1-x}Cd_xTe$ technology for the experimental realization of high mobility single crystal with specially prepared surfaces. The same compound has emerged to be the optimum choice for illuminating the narrow subband physics because the relevant material constants can easily be experimentally measured [110]. Besides, the quaternary alloy $In_{1-x}Ga_xAs_yP_{1-y}$ lattice matched to InP, also finds wide use in the fabrication of avalanche photodetectors [111], heterojunction lasers [112], light-emitting diodes [113] and avalanche photodiodes [114], field effect transistors, detectors, switches, modulators, solar cells, filters, and new types of integrated optical devices are made from the quaternary systems [115]. It may be noted that all types of band models as discussed for III–V semiconductors are also applicable for ternary and quaternary compounds. In Sect. 1.2.2, the FNFE from QWs of III–V, ternary, and quaternary semiconductors has been studied in accordance with the said band models and the simplified results for wide gap materials having parabolic energy bands under certain limiting conditions have further been demonstrated as a special case and thus confirming the compatibility test.

The II–VI semiconductors are being used in nanoribbons, blue green diode lasers, photosensitive thin films, infrared detectors, ultrahigh-speed bipolar transistors, fiber optic communications, microwave devices, solar cells, semiconductor gamma-ray detector arrays, and semiconductor detector gamma camera and allow for a greater density of data storage on optically addressed compact discs [116–123]. The carrier energy spectra in II–VI compounds are defined by the Hopfield model [124] where the splitting of the two-spin states by the spin–orbit coupling and the crystalline field has been taken into account. Section 1.2.3 contains the investigation of the FNFE from QWs of II–VI compounds.

In recent years, Bismuth (Bi) nanolines have been fabricated and Bi also finds use in array of antennas, which leads to the interaction of electromagnetic waves with such Bi-nanowires [125, 126]. Several dispersion relations of the carriers have been proposed for Bi. Shoenberg [127] experimentally verified that the de Haas–Van Alphen and cyclotron resonance experiments supported the ellipsoidal parabolic model of Bi, although the magnetic field dependence of many physical properties

of Bi supports the two-band model [128]. The experimental investigations on the magneto-optical and the ultrasonic quantum oscillations support the Lax ellipsoidal nonparabolic model [129]. Kao [130], Dinger and Lawson [131], and Koch and Jensen [132] demonstrated that the Cohen model [133] is in conformity with the experimental results in a better way. Besides, the hybrid model of bismuth, as developed by Takaoka et al. also finds use in the literature [134]. McClure and Choi [135] derived a new model of Bi and they showed that it can explain the data for a large number of magneto-oscillatory and resonance experiments. In Sect. 1.2.4, the FNFE from QWs of Bi has been formulated in accordance with the aforementioned energy band models for the purpose of relative assessment. Besides, under certain limiting conditions all the results for all the models of 1D systems are reduced to the well-known result of the FNFE from QWs of wide gap materials. This above statement exhibits the compatibility test of our theoretical analysis.

Lead chalcogenides (PbTe, PbSe, and PbS) are IV–VI nonparabolic semiconductors whose studies over several decades have been motivated by their importance in infrared IR detectors, lasers, light-emitting devices, photovoltaics, and high-temperature thermoelectrics [136–140]. PbTe, in particular, is the end compound of several ternary and quaternary high-performance high-temperature thermoelectric materials [141–145]. It has been used not only as bulk but also as films [146–149], quantum wells [150], superlattices [151, 152], nanowires [153], colloidal and embedded nanocrystals [154–157], and PbTe films doped with various impurities have also been investigated [158–165]. These studies revealed some of the interesting features that had been seen in bulk PbTe, such as Fermi level pinning in the case of superconductivity [166]. In Sect. 1.2.5, the FNFE from QWs of IV–VI semiconductors has been studied taking PbTe as an example.

The stressed semiconductors are being investigated for strained silicon transistors, quantum cascade lasers, semiconductor strain gages, thermal detectors and strained-layer structures [167–170]. The FNFE from QWs of stressed compounds (taking stressed n-InSb as an example) has been investigated in Sect. 1.2.6. The vacuum deposited Tellurium (Te) has been used as the semiconductor layer in thin-film transistors (TFT) [171], which is being used in CO_2 laser detectors [172], electronic imaging, strain-sensitive devices [173, 174], and multichannel Bragg cell [175]. Section 1.2.7 contains the investigation of FNFE from QWs of Tellurium.

The n-gallium phosphide (n-GaP) finds applications in quantum dot light-emitting diode [176], high efficiency yellow solid-state lamps, light sources, and high peak current pulse for high gain tubes. The green and yellow light-emitting diodes made of nitrogen-doped n-GaP possess a longer device life at high drive currents [177–179]. In Sect. 1.2.8, the FNFE from QWs of n-GaP has been studied. The Platinum Antimonide ($PtSb_2$) is used in device miniaturization, colloidal nanoparticle synthesis, sensors, detector materials, and thermo-photovoltaic devices [180–182]. Section 1.2.9 explores the FNFE from QWs of $PtSb_2$. Bismuth telluride (Bi_2Te_3) was first identified as a material for thermoelectric refrigeration in 1954 [183] and its physical properties were later improved by the addition of bismuth selenide and antimony telluride to form solid solutions [184–188]. The alloys of Bi_2Te_3 are useful compounds for the thermoelectric industry and have been

investigated in the literature [184–188]. In Sect. 1.2.10, the FNFE from QWs of Bi_2Te_3 has been considered.

The usefulness of elemental semiconductor Germanium is already well known since the inception of transistor technology, and it is also being used in memory circuits, single photon detectors, single photon avalanche diode, ultrafast optical switch, THz lasers, and THz spectrometers [189–192]. In Sect. 1.2.11, the FNFE has been studied from QWs of Ge. Gallium Antimonide (GaSb) finds applications in the fiber optic transmission window, heterojunctions, and quantum wells. A complementary heterojunction field effect transistor in which the channels for the p-FET device and the n-FET device forming the complementary FET are formed from GaSb. The band gap energy of GaSb makes it suitable for low power operation [193–198]. In Sect. 1.2.12, the FNFE from QWs of GaSb has been studied. The II–V semiconductors are being used in photovoltaic cells constructed of single crystal semiconductor materials in contact with electrolyte solutions. Cadmium selenide shows an open-circuit voltage of 0.8 V and power conservation coefficient is nearly 6% for 720-nm light [199]. They are also used in ultrasonic amplification [200]. The development of an evaporated TFT using cadmium selenide as the semiconductor has also been reported [201, 202]. In Sect. 1.2.13, we shall study the FNFE from QWs of II–V semiconductors. Section 1.3 contains the result and discussions pertaining to this chapter. Section 1.4 contains open research problems.

1.2 Theoretical Background

1.2.1 The Field Emission from Quantum Wires of Nonlinear Optical Semiconductors

The form of $\mathbf{k}\cdot\mathbf{p}$ matrix for nonlinear optical compounds can be expressed extending Bodnar [94] as

$$H = \begin{bmatrix} H_1 & H_2 \\ H_2^+ & H_1 \end{bmatrix}, \tag{1.1}$$

where

$$H_1 \equiv \begin{bmatrix} E_{g_0} & 0 & P_{\|}k_z & 0 \\ 0 & (-2\Delta_{||}/3) & (\sqrt{2}\Delta_{\perp}/3) & 0 \\ P_{\|}k_z & (\sqrt{2}\Delta_{\perp}/3) & -(\delta + \frac{1}{3}\Delta_{\|}) & 0 \\ 0 & 0 & 0 & 0 \end{bmatrix}, \quad H_2 \equiv \begin{bmatrix} 0 & -f_{,+} & 0 & f_{,-} \\ f_{,+} & 0 & 0 & 0 \\ 0 & 0 & 0 & 0 \\ f_{,+} & 0 & 0 & 0 \end{bmatrix},$$

in which E_{g_0} is the band gap in the absence of any field, $P_{||}$ and $P_{\perp}$ are the momentum matrix elements parallel and perpendicular to the direction of crystal axis, respectively, δ is the crystal field splitting constant, and $\Delta_{||}$ and $\Delta_{\perp}$ are the

spin–orbit splitting constants parallel and perpendicular to the C-axis, respectively, $f_{,\pm} \equiv (P_\perp/\sqrt{2})(k_x \pm ik_y)$ and $i = \sqrt{-1}$. Thus, neglecting the contribution of the higher bands and the free electron term, the diagonalization of the above matrix leads to the dispersion relation of the conduction electrons in bulk specimens of nonlinear optical semiconductors as

$$\gamma(E) = f_1(E)k_s^2 + f_2(E)k_z^2, \tag{1.2}$$

where

$$\gamma(E) \equiv E\left(E + E_{g_0}\right)\left[(E + E_{g_0})(E + E_{g_0} + \Delta_{||}) + \delta\left(E + E_{g_0} + \frac{2}{3}\Delta_{||}\right) + \frac{2}{9}\left(\Delta_{||}^2 - \Delta_\perp^2\right)\right],$$

$$f_1(E) \equiv \frac{\hbar^2 E_{g_0}(E_{g_0} + \Delta_\perp)}{\left[2m_\perp^*\left(E_{g_0} + \frac{2}{3}\Delta_\perp\right)\right]}\left[\delta\left(E + E_{g_0} + \frac{1}{3}\Delta_{||}\right) + \left(E + E_{g_0}\right)\left(E + E_{g_0} + \frac{2}{3}\Delta_{||}\right) + \frac{1}{9}\left(\Delta_{||}^2 - \Delta_{||}^2\right)\right],$$

where E is the total energy of the electron as measured from the edge of the conduction band in the vertically upward direction in the absence of any quantization, $k_s^2 = k_x^2 + k_y^2$, $f_2(E) \equiv \dfrac{\hbar^2 E_{g_0}(E_{g_0} + \Delta_{||})}{\left[2m_{||}^*\left(E_{g_0} + \frac{2}{3}\Delta_{||}\right)\right]}\left[(E + E_{g_0})\left(E + E_{g_0} + \frac{2}{3}\Delta_{||}\right)\right]$, $h = h/2\pi$, h is the Planck's constant, and $m_{||}^*$ and $m_\perp^*$ are the longitudinal and transverse effective electron masses at the edge of the conduction band, respectively.

For two-dimensional quantization along the x and y directions, (1.2) assumes the form

$$k_z^2 = A_{11}(E, n_x, n_y), \tag{1.3}$$

where $A_{11}(E, n_x, n_y) = [f_2(E)]^{-1}[\gamma(E) - \phi_1(n_x, n_y) f_1(E)]$, $\phi_1(n_x, n_y) = \left(\dfrac{n_x\pi}{d_x}\right)^2 + \left(\dfrac{n_y\pi}{d_y}\right)^2$, $n_x = (1, 2, 3, \ldots)$, $n_y = (1, 2, 3, \ldots)$ are the size quantum numbers along the x and y directions, respectively, and d_x and d_y are the nanothickness along the x and y directions, respectively.

The quantized subband energy (E_{11}) is given by

$$\gamma(E_{11}) = f_1(E_{11})\phi_1(n_x, n_y). \tag{1.4}$$

The electron concentration per unit length can be expressed as

$$n_0 = \frac{2g_v}{\pi}\sum_{n_x=1}^{n_{x\max}}\sum_{n_y=1}^{n_{y\max}}\left[B_{11}\left(E_{F1D}, n_x, n_y\right) + B_{12}\left(E_{F1D}, n_x, n_y\right)\right], \tag{1.5}$$

where g_v is the valley degeneracy, $B_{11}(E_{F1D}, n_x, n_y) = [A_{11}(E_{F1D}, n_x, n_y)]^{1/2}$, $B_{12}(E_{F1D}, n_x, n_y) = \sum_{r=1}^{r_0} Z_{1D}(r)[B_{11}(E_{F1D}, n_x, n_y)]$, $Z_{1D}(r) = 2(k_B T)^{2r}(1-2^{1-2r})$ $\xi(2r)\frac{\partial^{2r}}{\partial E_{F1D}^{2r}}$, k_B is the Boltzmann constant, T is the temperature, r is the set of real positive integers whose upper limit is r_0, $\xi(2r)$ is the Zeta function of order $2r$ [203], and E_{F1D} is the Fermi energy in the presence of 2D quantization as measured from the edge of the conduction band in the vertically upward direction in the absence of any quantization.

The current (I) due to Fowler–Nordheim {FN}field emission can be written as

$$I = \frac{1}{2}\sum_{n_x=1}^{n_{x\max}}\sum_{n_y=1}^{n_{y\max}}\left[\int_{E_{11}}^{\infty}[e \cdot v n_1 t_{11}]\right], \tag{1.6a}$$

where e is the magnitude of the electron charge, v is the velocity of the electron and given by $v = (1/\hbar)(\partial E/\partial k_z)$, $n_1 = N_{1D}(E).f(E)dE$, $N_{1D}(E)$ is the 1D density-of-states function per subbands and can be written as $N_{1D}(E) = (2g_v/\pi)(\partial k_z/\partial E)$, $f(E)$ is the Fermi–Dirac occupation probability factor and is given by $f(E) = [1 + \exp(E - E_{F1D}/k_B T)]^{-1}$, and t_{11} is the transmission coefficient. From (1.6a), it appears that I is a function of the product of the carrier velocity, concentration, and transmission coefficient. These three quantities in turn depend totally on the dispersion relation of the material. As the basic **E–k** relation changes, all the aforementioned quantities will change and the current due to FN field emission will be different consequently. Thus, the field emission will change all together in 1D, 2D, and 3D quantization of the wave vector space encompassing the whole arena of quantized structures.

Thus, from (1.6a) one can write

$$I = \frac{1}{2}\sum_{n_x=1}^{n_{x\max}}\sum_{n_y=1}^{n_{y\max}}\left[\int_{E_{11}}^{\infty}\left[\frac{e}{\hbar}\frac{\partial E}{\partial k_z}.\frac{2g_v}{\pi}\frac{\partial k_z}{\partial E}f(E)\mathrm{d}E\right]t_{11}\right]. \tag{1.6b}$$

The term $\partial E/\partial k_z$ from velocity and the term $\partial k_z/\partial E$ from the density-of-states function per subbands cancel each other leaving the constant prefactor.

Therefore, (1.6b) assumes the form

$$I = \frac{e \cdot g_v}{\hbar\pi}\sum_{n_x=1}^{n_{x\max}}\sum_{n_y=1}^{n_{y\max}}\left[\int_{E_{11}}^{\infty}[f(E)\mathrm{d}E] \cdot t_{11}\right]. \tag{1.6c}$$

The term t_{11} in this case can be expressed by using the method as given in [204] as

$$t_{11} = \exp(-\beta_{11}) \tag{1.7}$$

in which

$$\beta_{11} = \frac{4\left[A_{11}\left(V_0, n_x, n_y\right)\right]^{3/2}}{3eF_{sz}\left[A'_{11}\left(V_0, n_x, n_y\right)\right]}. \tag{1.8}$$

F_{sz} is the electric field along the z-axis,

$A_{11}(V_0, n_x, n_y) = [f_2(V_0)]^{-1}[\gamma(V_0) - \phi_1(n_x, n_y) f_1(V_0)]$, V_0 is equal to the addition of the Fermi energy in the corresponding case and the work function ϕ_w of the material,

$$\begin{aligned}
f_2(V_0) &\equiv \frac{\hbar^2 E_{g_0}(E_{g_0} + \Delta_{||})}{\left[2m^*_{||}\left(E_{g_0} + \frac{2}{3}\Delta_{||}\right)\right]}\left[(V_0 + E_{g_0})\left(V_0 + E_{g_0} + \frac{2}{3}\Delta_{||}\right)\right], \\
\gamma(V_0) &\equiv V_0\left(V_0 + E_{g_0}\right)\Big[\left(V_0 + E_{g_0}\right)\left(V_0 + E_{g_0} + \Delta_{||}\right) \\
&\quad + \delta\left(V_0 + E_{g_0} + \frac{2}{3}\Delta_{||}\right) + \frac{2}{9}\left(\Delta^2_{||} - \Delta^2_{\perp}\right)\Big], \\
f_1(V_0) &\equiv \frac{\hbar^2 E_{g_0}(E_{g_0} + \Delta_{\perp})}{\left[2m^*_{\perp}\left(E_{g_0} + \frac{2}{3}\Delta_{\perp}\right)\right]}\Big[\delta\left(V_0 + E_{g_0} + \frac{1}{3}\Delta_{||}\right) \\
&\quad + \left(V_0 + E_{g_0}\right)\left(V_0 + E_{g_0} + \frac{2}{3}\Delta_{||}\right) + \frac{1}{9}\left(\Delta^2_{||} - \Delta^2_{||}\right)\Big], \\
A'_{11}(V_0, n_x, n_y) &= \Big[\frac{-A_{11}(V_0, n_x, n_y) f'_2(V_0)}{f_2(V_0)} + [f_2(V_0)]^{-1}[\gamma'(V_0) \\
&\quad - f'_1(V_0)\phi_1(n_x, n_y)]\Big], \\
f'_2(V_0) &= \left[[\hbar^2 E_{g0}(E_{g0} + \Delta_{\|})]\left[2m^*_{\|}\left(E_{g0} + \frac{2}{3}\Delta_{\|}\right)\right]^{-1}\right. \\
&\quad \left.\times\left[2V_0 + 2E_{g0} + \frac{2}{3}\Delta_{\|}\right]\right], \\
f'_1(V_0) &= \left[[\hbar^2 E_{g0}(E_{g0} + \Delta_{\perp})]\left[2m^*_{\perp}\left(E_{g0} + \frac{2}{3}\Delta_{\perp}\right)\right]^{-1}\right. \\
&\quad \left.\times\left[2V_0 + 2E_{g0} + \frac{2}{3}\Delta_{\|} + \delta\right]\right],
\end{aligned}$$

and

$$\gamma'(V_0) = \left[\frac{\gamma(V_0)(2V_0 + E_{g0})}{V_0(V_0 + E_{g0})} + (V_0(V_0 + E_{g0}))\left[2V_0 + 2E_{g0} + \Delta_{\|} + \delta\right]\right].$$

Thus, we can write

$$I = \frac{2g_v e k_B T}{h} \sum_{n_x=1}^{n_{x\max}} \sum_{n_y=1}^{n_{y\max}} F_0(\eta_{11})\, t_{11}, \tag{1.9}$$

where $\eta_{11} = (E_{F1D} - E_{11})/k_B T, F_0(\eta_{11})$ is the special case of the one-parameter Fermi–Dirac integral of order j which can be written as

$$F_j(\eta) = \left(\frac{1}{\Gamma(j+1)}\right) \int_0^\infty \frac{x^j \mathrm{d}x}{1 + \exp(x - \eta)}, \qquad j > -1 \tag{1.10}$$

or for all j, analytically continued as a complex contour integral around the negative x-axis

$$F_j(\eta) = \left(\frac{\Gamma(-j)}{2\pi\sqrt{-1}}\right) \int_{-\infty}^{+0} \frac{x^j \mathrm{d}x}{1 + \exp(-x - \eta)}, \tag{1.11}$$

where η is the dimensionless$x$ independent variable,

$$\Gamma(j+1) = j\Gamma(j),\ \Gamma\left(\frac{1}{2}\right) = \sqrt{\pi}, \text{ and } \Gamma(0) = 1..$$

Therefore, the field-emitted current is given by

$$I = \frac{2g_v e k_B T}{h} \sum_{n_x=1}^{n_{x\max}} \sum_{n_y=1}^{n_{y\max}} F_0(\eta_{11}) \exp(-\beta_{11}). \tag{1.12}$$

1.2.2 The Field Emission from Quantum Wires of III–V Semiconductors

The dispersion relation of the conduction electrons of III–V compounds are described by the models of Kane (both three and two bands) [103, 104], Stillman et al. [105], Newson and Kurobe [106], and Palik et al. [107], respectively. For the purpose of complete and coherent presentation, the FNFE from QWs of III–V semiconductors have also been investigated in accordance with the aforementioned different dispersion relations for indicating the relative comparison as follows:

1.2.2.1 The Three-Band Model of Kane

Under the conditions, $\delta = 0$, $\Delta_\parallel = \Delta_\perp = \Delta$ (isotropic spin–orbit splitting constant) and $m_\parallel^* = m_\perp^* = m_c$ (isotropic effective electron mass at the edge of the conduction band), (1.2) gets simplified into the form

$$\frac{\hbar^2 k^2}{2m_c} = I_{11}(E), \quad I_{11}(E) \equiv \frac{E\left(E+E_{g_0}\right)\left(E+E_{g_0}+\Delta\right)\left(E_{g_0}+\frac{2}{3}\Delta\right)}{E_{g_0}(E_{g_0}+\Delta)\left(E+E_{g_0}+\frac{2}{3}\Delta\right)}, \tag{1.13}$$

which is known as the three-band model of Kane [103, 104] and is often used to study the electronic properties of III–V, ternary, and quaternary semiconductors.

The 1D E–k_z relation can be expressed as

$$k_z^2 = A_{12}(E, n_x, n_y), \tag{1.14}$$

where $A_{12}(E, n_x, n_y) = \frac{2m_c}{\hbar^2} I_{11}(E) - \phi_1(n_x, n_y)$.

The quantized subband energy (E_{12}) is given by

$$I_{11}(E_{12}) = \left[\frac{\hbar^2}{2m_c}\right] \phi_1(n_x, n_y). \tag{1.15}$$

The electron concentration per unit length can be written as

$$n_0 = \frac{2g_{\mathrm{v}}}{\pi} \sum_{n_x=1}^{n_{x\max}} \sum_{n_y=1}^{n_{y\max}} \left[B_{13}\left(E_{\mathrm{F1D}}, n_x, n_y\right) + B_{14}\left(E_{\mathrm{F1D}}, n_x, n_y\right)\right], \tag{1.16}$$

where $B_{13}\left(E_{\mathrm{F1D}}, n_x, n_y\right) = \left[A_{12}\left(E_{\mathrm{F1D}}, n_x, n_y\right)\right]^{1/2}$ and $B_{14}(E_{\mathrm{F1D}}, n_x, n_y) = \sum_{r=1}^{r_0} Z_{1\mathrm{D}}(r)[B_{13}(E_{\mathrm{F1D}}, n_x, n_y)]$.

The field-emitted current can be expressed as

$$I = \frac{2g_{\mathrm{v}} e k_{\mathrm{B}} T}{h} \sum_{n_x=1}^{n_{x\max}} \sum_{n_y=1}^{n_{y\max}} F_0(\eta_{12})\, t_{12}, \tag{1.17}$$

where $\eta_{12} = (E_{\mathrm{F1D}} - E_{12})/k_{\mathrm{B}}T$, $t_{12} = \exp(-\beta_{12})$, $\beta_{12} = \frac{4}{3}[A_{12}(V_0, n_x, n_y)]^{3/2} \cdot [eF_{sz}A'_{12}(V_0)]^{-1}$,

$$A_{12}(V_0, n_x, n_y) = \left[\frac{2m_c}{\hbar^2} I_{11}(V_0) - \phi_1(n_x, n_y)\right],$$

$$I_{11}(V_0) \equiv \frac{V_0(V_0+E_{g_0})(V_0+E_{g_0}+\Delta)\left(E_{g_0}+\frac{2}{3}\Delta\right)}{E_{g_0}(E_{g_0}+\Delta)\left(V_0+E_{g_0}+\frac{2}{3}\Delta\right)} \quad \text{and}$$

$$A'_{12}(V_0) = \left[\frac{2m_c}{\hbar^2} I_{11}(V_0)\left[\frac{1}{V_0} + \frac{1}{V_0+E_{g0}} + \frac{1}{V_0+E_{g0}+\Delta} - \frac{1}{V_0+E_{g0}+(2/3)\Delta}\right]\right].$$

Therefore, the field-emitted current is given by

$$I = \frac{2g_v e k_B T}{h} \sum_{n_x=1}^{n_{x\max}} \sum_{n_y=1}^{n_{y\max}} F_0(\eta_{12}) \exp(-\beta_{12}). \tag{1.18}$$

1.2.2.2 Two-Band Model of Kane

Under the inequalities $\Delta \gg E_{g_0}$ or $\Delta \ll E_{g_0}$, (1.13) assumes the form

$$E(1 + \alpha E) = (\hbar^2 k^2 / 2m_c), \quad \alpha \equiv 1/E_{g_0}. \tag{1.19}$$

Equation (1.19) is known as the two-band model of Kane where α is known as band nonparabolicity parameter and should be as such for studying the electronic properties of the semiconductors whose band structures obey the above inequalities [103, 104].

The 1D E–k_z relation can be expressed as

$$k_z^2 = A_{13}(E, n_x, n_y), \tag{1.20}$$

where $A_{13}(E, n_x, n_y) = \left[\frac{2m_c}{\hbar^2}\{E(1 + \alpha E)\} - \phi_1(n_x, n_y)\right]$.

The quantized subband energy (E_{12}) is given by

$$E_{13}(1 + \alpha E_{13}) = \left[\frac{\hbar^2}{2m_c}\right] \phi_1(n_x, n_y). \tag{1.21}$$

The electron concentration per unit length can be written as

$$n_0 = \frac{2g_v}{\pi} \sum_{n_x=1}^{n_{x\max}} \sum_{n_y=1}^{n_{y\max}} \left[B_{15}\left(E_{F1D}, n_x, n_y\right) + B_{16}\left(E_{F1D}, n_x, n_y\right)\right], \tag{1.22}$$

where $B_{15}\left(E_{F1D}, n_x, n_y\right) = \left[A_{13}(E_{F1D}, n_x, n_y)\right]^{1/2}$ and

$$B_{16}(E_{F1D} n_x, n_y) = \sum_{r=1}^{r_0} Z_{1D}(r) \left[B_{15}\left(E_{F1D}, n_x, n_y\right)\right].$$

The field-emitted current can be expressed as

$$I = \frac{2g_v e k_B T}{h} \sum_{n_x=1}^{n_{x\max}} \sum_{n_y=1}^{n_{y\max}} F_0(\eta_{13}) t_{13}, \tag{1.23}$$

where $\eta_{13} = (E_{F1D} - E_{13})/k_B T$, $t_{13} = \exp(-\beta_{13})$, $\beta_{13} = \frac{4}{3}\left[A_{13}\left(V_0, n_x, n_y\right)\right]^{3/2} \cdot \left[eF_{sz} A'_{13}(V_0)\right]^{-1}$, and $A'_{13}(V_0) = \frac{2m_c}{\hbar^2}(1 + 2\alpha V_0)$.

Therefore, the field-emitted current assumes the from

$$I = \frac{2g_v e k_B T}{h} \sum_{n_x=1}^{n_{x\max}} \sum_{n_y=1}^{n_{y\max}} F_0(\eta_{13}) \exp(-\beta_{13}). \tag{1.24}$$

1.2.2.3 Parabolic Energy Bands

The expressions for the electron concentration per unit length and the FNFE from QWs having parabolic energy bands can, respectively, be written as

$$n_0 = \frac{2g_v \sqrt{2\pi m_c k_B T}}{h} \sum_{n_x=1}^{n_{x\max}} \sum_{n_y=1}^{n_{y\max}} F_{-1/2}(\eta_{14}), \tag{1.25}$$

$$I = \frac{2g_v e k_B T}{h} \sum_{n_x=1}^{n_{x\max}} \sum_{n_y=1}^{n_{y\max}} F_0(\eta_{14}) \exp\left[-\frac{4}{3eF_{sz}} \left(\frac{2m_c}{\hbar^2} \right)^{1/2} V_0^{3/2} \left\{ 1 - \frac{\hbar^2 \phi_1(n_x, n_y)}{2m_c V_0} \right\}^{3/2} \right], \tag{1.26}$$

where $\eta_{14} = \left[E_{F1D} - \frac{\hbar^2 \phi_1(n_x, n_y)}{2m_c} \right] [k_B T]^{-1}$.

Converting the summations over n_x and n_y to the corresponding integrations, (1.26) gets transformed as

$$J = \frac{g_v e^2 F_{sz}^2}{8\pi h \phi_w} \exp\left\{ -\frac{4}{3eF_{sz}} \left(\frac{2m_c}{\hbar^2} \right)^{1/2} \phi_w^{3/2} \right\}. \tag{1.27}$$

Equation (1.27) is the well-known expression of the FNFE from bulk semiconductors having parabolic energy bands [205, 206].

1.2.2.4 The Model of Stillman et al.

In accordance with the model of Stillman et al. [105], the electron dispersion law of III–V materials assumes the form

$$E = \bar{t}_{11} k^2 - \bar{t}_{12} k^4, \tag{1.28}$$

where $\bar{t}_{11} \equiv \frac{\hbar^2}{2m_c}$, $\bar{t}_{12} \equiv \left(1 - \frac{m_c}{m_0}\right)^2 \left(\frac{\hbar^2}{2m_c}\right)^2 \left[\left(3E_{g_0} + 4\Delta + \frac{2\Delta^2}{E_{g_0}} \right) . \left\{ (E_{g_0} + \Delta)(2\Delta + 3E_{g_0}) \right\}^{-1} \right]$, and m_0 is the free electron mass.

Equation (1.28) can be expressed as

$$\frac{\hbar^2 k^2}{2m_c} = I_{12}(E), \tag{1.29}$$

where $I_{12}(E) \equiv a_{11}[1-(1-a_{12}E)^{1/2}]$ and $a_{11} \equiv \left(\frac{\hbar^2 \bar{t}_{11}}{4m_c \bar{t}_{12}}\right)$, and $a_{12} \equiv \frac{4\bar{t}_{12}}{\bar{t}_{11}^2}$.

The 1D E–k_z relation can be written as

$$k_z^2 = A_{14}\left(E, n_x, n_y\right), \tag{1.30}$$

where $A_{14}(E, n_x, n_y) = \left[\frac{2m_c}{\hbar^2}\{I_{12}(E)\} - \phi_1(n_x, n_y)\right]$.

The quantized subband energy (E_{14}) is given by

$$I_{12}(E_{14}) = \left[\frac{\hbar^2}{2m_c}\right]\phi_1\left(n_x, n_y\right). \tag{1.31}$$

The electron concentration per unit length can be expressed as

$$n_0 = \frac{2g_v}{\pi}\sum_{n_x=1}^{n_{x\max}}\sum_{n_y=1}^{n_{y\max}}\left[B_{17}\left(E_{F1D}, n_x, n_y\right) + B_{18}\left(E_{F1D}, n_x, n_y\right)\right], \tag{1.32}$$

where $B_{17}\left(E_{F1D}, n_x, n_y\right) = \left[A_{14}\left(E_{F1D}, n_x, n_y\right)\right]^{1/2}$ and $B_{18}\left(E_{F1D}, n_x, n_y\right) = \sum_{r=1}^{r_0} Z_{1D}(r)\left[B_{17}\left(E_{F1D}, n_x, n_y\right)\right]$.

The field-emitted current can be written as

$$I = \frac{2g_v e k_B T}{h}\sum_{n_x=1}^{n_{x\max}}\sum_{n_y=1}^{n_{y\max}} F_0(\eta_{15})\exp(-\beta_{15}), \tag{1.33}$$

where $\eta_{15} = \left(E_{F1D} - E_{14}\right)/k_B T, \beta_{15} = \frac{4}{3}\left[A_{14}\left(V_0, n_x, n_y\right)\right]^{3/2}\cdot[eF_{sz}A'14\,(V_0)]^{-1}$, $A_{14}(V_0, n_x, n_y) = \left[\frac{2m_c}{\hbar^2}\{I_{12}(V_0)\} - \phi_1(n_x, n_y)\right]$, $A'_{14}(V_0) = \frac{2m_c}{\hbar^2}I'_{12}(V_0)$, and $I'_{12}(V_0) = \left(\frac{a_{11}a_{12}}{2}\right)(1-a_{12}V_0)^{-1/2}$.

1.2.2.5 The Model of Newson and Kurobe

In accordance with the model of Newson and Kurobe [106], the electron dispersion law in this case assumes the form

$$E = a_{13}k_z^4 + \left[\frac{\hbar^2}{2m_c} + a_{14}k_s^2\right]k_z^2 + \frac{\hbar^2}{2m_c}k_s^2 + a_{14}k_x^2k_y^2 + a_{13}\left(k_x^4 + k_y^4\right), \quad (1.34)$$

where a_{13} is the nonparabolicity constant, $a_{14}(\equiv 2a_{13} + a_{15})$, and a_{15} is known as the warping constant.

The 1D E–k_z relation can be expressed as

$$k_z^2 = A_{15}(E, n_x, n_y), \quad (1.35)$$

where $A_{15}(E, n_x, n_y) = (2a_{13})^{-1}[-\overline{L_1}(n_x, n_y) + [\{\overline{L_1}(n_x, n_y)\}^2 - 4a_{13}[\overline{L_2}(n_x, n_y) - E)]^{1/2}]$, $\overline{L_1}(n_x, n_y) = \frac{\hbar^2}{2m_c} + a_{14}\left[\left(\frac{n_x\pi}{d_x}\right) + \left(\frac{n_y\pi}{d_y}\right)^2\right]$, and $\overline{L_2}(n_x, n_y) = \left[\frac{\hbar^2}{2m_c}\phi_1(n_x, n_y) + a_{14}\left(\frac{n_x\pi}{d_x}\cdot\frac{n_y\pi}{d_y}\right)^2 + a_{13}\left[\left(\frac{n_x\pi}{d_x}\right)^4 + \left(\frac{n_y\pi}{d_y}\right)^4\right]\right]$.

The quantized subband energy (E_{16}) is given by

$$E_{16} = \overline{L_2}(n_x, n_y). \quad (1.36)$$

The electron concentration per unit length can be written as

$$n_0 = \frac{2g_v}{\pi}\sum_{n_x=1}^{n_{x\max}}\sum_{n_y=1}^{n_{y\max}}\left[B_{19}\left(E_{F1D}, n_x, n_y\right) + B_{20}\left(E_{F1D}, n_x, n_y\right)\right], \quad (1.37)$$

where $B_{19}\left(E_{F1D}, n_x, n_y\right) = \left[A_{15}\left(E_{F1D}, n_x, n_y\right)\right]^{1/2}$ and

$$B_{20}(E_{F1D}, n_x, n_y) = \sum_{r=1}^{r_0} Z_{1D}(r)[B_{19}(E_{F1D}, n_x, n_y)]. \quad (1.38)$$

The field-emitted current assumes the form

$$I = \frac{2g_v e k_B T}{h}\sum_{n_x=1}^{n_{x\max}}\sum_{n_y=1}^{n_{y\max}} F_0(\eta_{16})\exp(-\beta_{16}), \quad (1.39)$$

where $\eta_{16} = (E_{F1D} - E_{16})/k_BT$, $\beta_{16} = \frac{4}{3}\left[A_{15}(V_0, n_x, n_y)\right]^{3/2}\cdot\left[eF_{sz}A'_{15}(V_0, n_x, n_y)\right]^{-1}$, and $A'_{15}(V_0, n_x, n_y) = [\{\overline{L_1}(n_x, n_y)\}^2 - 4a_{13}[\overline{L_2}(n_x, n_y) - V_0)]^{-1/2}]$.

1.2.2.6 Model of Palik et al.

The energy spectrum of the conduction electrons in III–V semiconductors up to the fourth order in effective mass theory, taking into account the interactions of heavy hole, light hole, and the split-off holes can be expressed in accordance with the model of Palik et al. [107] as

$$E = \frac{\hbar^2 k^2}{2m_c} - \overline{B}_{11} k^4, \tag{1.40}$$

where $\overline{B}_{11} = \left[\frac{\hbar^4}{4E_{g_0}(m_c)^2}\right]\left[\frac{1+\frac{x_{11}^2}{2}}{1+\frac{x_{11}}{2}}\right](1-y_{11})^2, x_{11} = \left[1+\left(\frac{\Delta}{E_{g0}}\right)\right],^{-1}$ and $y_{11} = \frac{m_c}{m_o}$.

Equation (1.40) gets simplified as

$$\frac{\hbar^2 k^2}{2m_c} = I_{13}(E), \tag{1.41}$$

where $I_{13}(E) = \bar{b}_{12}\left[\bar{a}_{12} - \left((\bar{a}_{12})^2 - 4E\overline{B}_{11}\right)^{1/2}\right]$ and $\bar{a}_{12} = \left(\frac{\hbar^2}{2m_c}\right)$, and $\bar{b}_{12} = \left[\frac{\bar{a}_{12}}{2\overline{B}_{11}}\right]$.

The 1D E–k_z relation can be written as

$$k_z^2 = A_{16}(E, n_x, n_y), \tag{1.42}$$

where $A_{16}(E, n_x, n_y) = \left[\frac{2m_c}{\hbar^2}\{I_{13}(E)\} - \phi_1(n_x, n_y)\right]$.

The electron concentration per unit length can be expressed as

$$n_0 = \frac{2g_v}{\pi}\sum_{n_x=1}^{n_{x\max}}\sum_{n_y=1}^{n_{y\max}}\left[B_{21}\left(E_{\text{F1D}}, n_x, n_y\right) + B_{22}\left(E_{\text{F1D}}, n_x, n_y\right)\right], \tag{1.43}$$

where $B_{21}\left(E_{\text{F1D}}, n_x, n_y\right) = \left[A_{16}\left(E_{\text{F1D}}, n_x, n_y\right)\right]^{1/2}$ and $B_{22}\left(E_{\text{F1D}}, n_x, n_y\right) = \sum_{r=1}^{r_0} Z_{1\text{D}}(r)\left[B_{21}\left(E_{\text{F1D}}, n_x, n_y\right)\right]$.

The field-emitted current can be written as

$$I = \frac{2g_v e k_B T}{h}\sum_{n_x=1}^{n_{x\max}}\sum_{n_y=1}^{n_{y\max}} F_0\left(\eta_{16}\right)\exp(-\beta_{16}), \tag{1.44}$$

where $\eta_{16} = \left(E_{\text{F1D}} - E_{17}\right)/k_B T$ and E_{17} is the root of

$$\frac{\hbar^2}{2m_c}\phi_1(n_x, n_y) = I_{13}(E_{17}), \tag{1.45}$$

where $\beta_{16} = \frac{4}{3}\left[A_{16}\left(V_0, n_x, n_y\right)\right]^{3/2} \cdot \left[eF_{sz}A'_{16}(V_0)\right]^{-1}$, $A'_{16}(V_0) = \frac{2m_c}{\hbar^2} I'_{13}(V_0)$, and $I'_{13}(V_0) = 2\bar{b}_{12}\overline{B}_{11}\left[(\bar{a}_{12})^2 - 4V_0\overline{B}_{11}\right]^{-1/2}$.

1.2.3 The Field Emission from Quantum Wires of II–VI Semiconductors

The carrier energy spectra in bulk specimens of II–VI compounds in accordance with Hopfield model [124] can be written as

$$E = A_0 k_s^2 + B_0 k_z^2 \pm C_0 k_s, \tag{1.46}$$

where $A_0 \equiv \hbar^2/2m_\perp^*$, $B_0 \equiv \hbar^2/2m_\parallel^*$, and C_0 represents the splitting of the two-spin states by the spin–orbit coupling and the crystalline field.

The 1D dispersion relation for quantum wires of II–VI semiconductors can be expressed as

$$E = B_0 k_z^2 + G_{3,\pm}(n_x, n_y), \tag{1.47}$$

where $G_{3,\pm}\left(n_x, n_y\right) \equiv \left[A_0\left\{\left(\frac{\pi n_x}{d_x}\right)^2 + \left(\frac{\pi n_y}{d_y}\right)^2\right\} \pm C_0\left\{\left(\frac{\pi n_x}{d_x}\right)^2 + \left(\frac{\pi n_y}{d_y}\right)^2\right\}^{1/2}\right]$.

The FNFE in this case is given by

$$I = \frac{e g_v k_B T}{h} \sum_{n_x=1}^{n_{x\max}} \sum_{n_y=1}^{n_{y\max}} \left[\left\{F_0\left\{(k_B T)^{-1}\left[E_{F1D} - \left[G_{3,+}\left(n_x, n_y\right)\right]\right]\right\} \times \exp\left(-\overline{\beta}_{016,+}\right)\right\} + F_0\left\{(k_B T)^{-1}\left[E_{F1D} - \left[G_{3,-}\left(n_x, n_y\right)\right]\right]\right\} \exp\left(-\overline{\beta}_{016,-}\right)\right] \tag{1.48}$$

and $\overline{\beta}_{016,\pm} = \frac{4}{3}\left[\left(V_0 - G_{3,\pm}\left(n_x, n_y\right)\right)\right]^{3/2} \cdot [eF_{sz}\hbar]^{-1}\sqrt{2m_\parallel^*}$.

The 1D electron statistics can be written as

$$n_{1D} = \frac{g_v}{\pi\sqrt{B_0}} \sum_{n_x=1}^{n_{x\max}} \sum_{n_y=1}^{n_{y\max}} \left[t_7\left(E_{F1D}, n_x, n_y\right) + t_8\left(E_{F1D}, n_x, n_y\right)\right], \tag{1.49}$$

where $t_7\left(E_{F1D}, n_x, n_y\right) \equiv \left[E_{F1D} - \left[G_{3,+}\left(n_x, n_y\right)\right]\right]^{1/2} + \left[E_{F1D} - \left[G_{3,-}\left(n_x, n_y\right)\right]\right]^{1/2}$ and $t_8\left(E_{F1D}, n_x, n_y\right) = \sum_1^0 Z_{1D}(r)\left[t_7(E_{F1D}, n_x, n_y)\right]$

1.2.4 The Field Emission from Quantum Wires of Bismuth

1.2.4.1 The McClure and Choi Model

The dispersion relation of the carriers in Bi can be written, following the McClure and Choi [135], as

$$E\left(1+\alpha E\right)=\frac{p_x^2}{2m_1}+\frac{p_y^2}{2m_2}+\frac{p_z^2}{2m_3}+\frac{p_y^2}{2m_2}\alpha E\left\{1-\left(\frac{m_2}{m_2'}\right)\right\}+\frac{p_y^4\alpha}{4m_2m_2'}-\frac{\alpha p_x^2p_y^2}{4m_1m_2}-\frac{\alpha p_y^2p_z^2}{4m_2m_3},\tag{1.50}$$

where $p_i\equiv\hbar k_i, i=x,y,z$, m_1, m_2, and m_3 are the effective carrier masses at the band edge along the x, y, and z directions, respectively, and m_2' is the effective mass tensor component at the top of the valence band (for electrons) or at the bottom of the conduction band (for holes).

The 1D dispersion relation of the carriers in Bi in this case assumes the form

$$E\left(1+\alpha E\right)=\left\{\frac{\hbar^2k_x^2}{2m_1}\left[1-\frac{\alpha\hbar^2}{2m_2}\left(\frac{\pi n_y}{d_y}\right)^2\right]+G_{12}+\frac{\hbar^2}{2m_2}\alpha E\left\{1-\left(\frac{m_2}{m_2'}\right)\right\}\left(\frac{\pi n_y}{d_y}\right)^2\right\},\tag{1.51}$$

where $n_z=1,2,3,\ldots$ is the size quantum number along the z direction, d_z is the nanothickness along the z direction, and

$$G_{12}\equiv\left\{\frac{\hbar^2}{2m_2}\left(\frac{\pi n_y}{d_y}\right)^2+\frac{\hbar^2}{2m_3}\left(\frac{\pi n_z}{d_z}\right)^2+\frac{\alpha\hbar^4}{4m_2m_2'}\left(\frac{\pi n_y}{d_y}\right)^4-\frac{\alpha}{4m_2m_3}\left(\frac{\hbar^2n_yn_z\pi^2}{d_yd_z}\right)^2\right\}.$$

Using (1.51), the 1D electron statistics can be expressed as

$$n_{1D}=\frac{2g_v}{\pi}\frac{\sqrt{2m_1}}{\hbar}\sum_{n_y=1}^{n_{y\max}}\sum_{n_z=1}^{n_{z\max}}\left[t_{27}\left(E_{F1D},n_y,n_z\right)+t_{28}\left(E_{F1D},n_y,n_z\right)\right],\tag{1.52}$$

where

$$t_{27}\left(E_{F1D},n_y,n_z\right)\equiv\left\{\left[1-\frac{\alpha\hbar^2}{2m_2}\left(\frac{\pi n_y}{d_y}\right)^2\right]^{-1/2}\left[E_{F1D}\left(1+\alpha E_{F1D}\right)-G_{12}-\frac{\hbar^2}{2m_2}\alpha E_{F1D}\left\{1-\left(\frac{m_2}{m_2'}\right)\right\}\left(\frac{\pi\hbar n_y}{d_y}\right)^2\right]^{1/2}\right\}$$

and

$$t_{28}\left(E_{\mathrm{F1D}}, n_y, n_z\right) \equiv \sum_{r=1}^{s_o} Z_{1\mathrm{D}}(r)\left[t_{27}\left(E_{\mathrm{F1D}}, n_y, n_z\right)\right].$$

The field-emitted current is given by

$$I = \frac{2g_{\mathrm{v}} e k_{\mathrm{B}} T}{h} \sum_{n_z=1}^{n_{z\max}} \sum_{n_y=1}^{n_{y\max}} F_0(\eta_{17}) \exp(-\beta_{17}), \tag{1.53}$$

where $\eta_{17} = \dfrac{E_{\mathrm{F1D}} - E_{19}}{k_{\mathrm{B}} T}$ and E_{19} is the root of

$$E_{19}\left(1 + \alpha E_{19}\right) = \left\{ G_{12} + \frac{\hbar^2}{2m_2} \alpha E_{19} \left\{ 1 - \left(\frac{m_2}{m_2'}\right) \right\} \left(\frac{\pi n_y}{d_y}\right)^2 \right\}, \tag{1.54}$$

$$\beta_{17} = \frac{4}{3}[A_{17}(V_0, n_z, n_y)]^{3/2} \cdot [eF_{sz} A_{17}'(V_{0,} n_z, n_y)]^{-1},$$

$$\left[1 - \frac{\alpha\hbar^2}{2m_2}\left(\frac{\pi n_y}{d_y}\right)^2\right]^{-1} \left[V_0\left(1 + \alpha V_0\right) - G_{12} - \left\{ \frac{\hbar^2}{2m_2} \alpha V_0 \left\{ 1 - \left(\frac{m_2}{m_2'}\right) \right\} \times \left(\frac{\pi n_y}{d_y}\right)^2 \right\} \right] \left(\frac{\hbar^2}{2m_1}\right)^{-1} = A_{17}\left(V_{0,} n_{y,} n_z\right),$$

and

$$\left[1 - \frac{\alpha\hbar^2}{2m_2}\left(\frac{\pi n_y}{d_y}\right)^2\right]^{-1} \left[\left(1 + 2\alpha V_0\right) - \left\{ \frac{\hbar^2}{2m_2} \alpha \left\{ 1 - \left(\frac{m_2}{m_2'}\right) \right\} \left(\frac{\pi n_y}{d_y}\right)^2 \right\} \right] \times \left(\frac{\hbar^2}{2m_1}\right)^{-1} = A_{17}'\left(V_{0,} n_{y,} n_z\right).$$

1.2.4.2 The Hybrid Model

The dispersion relation of the carriers in bulk specimens of Bi in accordance with the Hybrid model can be written as [134]

$$E\left(1 + \alpha E\right) = \frac{\theta_0\left(E\right)\left(\hbar k_y\right)^2}{2M_2} + \frac{\alpha\gamma_0\hbar^4 k_y^4}{4M_2^2} + \frac{\hbar^2 k_x^2}{2m_1} + \frac{\hbar^2 k_z^2}{2m_3}, \tag{1.55}$$

where $\theta_0(E) \equiv [1 + \alpha E(1 - \gamma_0) + \overline{\delta}_0]$, $\gamma_0 \equiv \frac{M_2}{m_2}$, $\overline{\delta}_0 \equiv \frac{M_2}{M_2'}$, and the other notations are defined in [134].

The 1D dispersion relation in this case assumes the form

$$E\left(1+\alpha E\right)=\frac{\hbar^2 k_x^2}{2m_1}+G_{14}+\frac{\hbar^2}{2M_2}\left(\frac{\pi n_y}{d_y}\right)^2\alpha E\left(1-\gamma_0\right), \tag{1.56}$$

where $G_{14}=\left[\frac{\hbar^2}{2m_3}\left(\frac{\pi n_z}{d_z}\right)^2+\frac{\hbar^2}{2M_2}\left(\frac{\pi n_y}{d_y}\right)^2\left(1+\bar{\delta}_0\right)+\frac{\alpha\gamma_0\hbar^4}{4M_2^2}\left(\frac{\pi n_y}{d_y}\right)^4\right]$.

The use of (1.56) leads to the expression for the electron concentration per unit length as

$$n_{\mathrm{D1}}=\frac{2g_{\mathrm{v}}}{\pi}\frac{\sqrt{2m_1}}{\hbar}\sum_{n_y=1}^{n_{y\max}}\sum_{n_z=1}^{n_{z\max}}\left[t_{31}\left(E_{\mathrm{F1D}},n_y,n_z\right)+t_{32}\left(E_{\mathrm{F1D}},n_y,n_z\right)\right], \tag{1.57}$$

where

$$t_{31}\left(E_{F1\mathrm{D}},n_y,n_z\right)\equiv\left[E_{\mathrm{F1D}}\left(1+\alpha E_{1\mathrm{DF}}\right)-G_{14}-\frac{\hbar^2}{2M_2}\left(\frac{\pi n_y}{d_y}\right)^2\alpha E_{\mathrm{F1D}}\left(1-\gamma_0\right)\right]^{1/2},$$

and $t_{32}\left(E_{\mathrm{F1D}},n_y,n_z\right)\equiv\sum_{r=1}^{s_o}Z_{1\mathrm{D}}(r)\left[t_{31}\left(E_{\mathrm{F1D}},n_y,n_z\right)\right]$.

The field-emitted current is given by

$$I=\frac{2g_{\mathrm{v}}ek_{\mathrm{B}}T}{h}\sum_{n_z=1}^{n_{z\max}}\sum_{n_y=1}^{n_{y\max}}F_0(\eta_{18})\exp(-\beta_{18}), \tag{1.58}$$

where $\eta_{18}=\frac{E_{\mathrm{F1D}}-E_{20}}{k_BT}$.

E_{20} is the root of

$$E_{20}\left(1+\alpha E_{20}\right)=G_{14}+\frac{\hbar^2}{2M_2}\left(\frac{\pi n_y}{d_y}\right)^2\alpha E_{20}\left(1-\gamma_0\right), \tag{1.59}$$

$$\beta_{18}=\frac{4}{3}[A_{18}(V_0,n_z,n_y)]^{3/2}\cdot[eF_{sz}A'_{18}(V_0,n_z,n_y)]^{-1},$$

$$\left[V_0\left(1+\alpha V_0\right)-G_{14}-\left\{\frac{\hbar^2}{2M_2}\alpha V_0\left\{1-\gamma_0\right\}\left(\frac{\pi n_y}{d_y}\right)^2\right\}\right]\left(\frac{\hbar^2}{2m_1}\right)^{-1}$$

$$=A_{18}\left(V_0,n_y,n_z\right),$$

$$\text{and}\left[\left(1+2\alpha V_0\right)-\left\{\frac{\hbar^2}{2M_2}\alpha\left\{1-\gamma_0\right\}\left(\frac{\pi n_y}{d_y}\right)^2\right\}\right]\left(\frac{\hbar^2}{2m_1}\right)^{-1}=A'_{18}\left(V_0,n_y,n_z\right).$$

1.2.4.3 The Cohen Model

In accordance with the Cohen model [133], the dispersion law of the carriers in Bi is given by

$$E\left(1+\alpha E\right)=\frac{p_x^2}{2m_1}+\frac{p_z^2}{2m_3}-\frac{\alpha E p_y^2}{2m_2'}+\frac{p_y^2(1+\alpha E)}{2m_2}+\frac{\alpha p_y^4}{4m_2m_2'}. \tag{1.60}$$

The 1D carrier dispersion law in this case can be written as

$$\alpha E^2+El_7-G_{15}=\frac{\hbar^2k_x^2}{2m_1}, \tag{1.61}$$

where $l_7=\left[1-\frac{\alpha\hbar^2}{2m_2}\left(\frac{\pi n_y}{d_y}\right)^2+\frac{\alpha\hbar^2}{2m_2'}\left(\frac{\pi n_y}{d_y}\right)^2\right]$

and $G_{15}=\left[\frac{\hbar^2}{2m_3}\left(\frac{\pi n_z}{d_z}\right)^2+\frac{\hbar^2}{2m_2}\left(\frac{\pi n_y}{d_y}\right)^2+\frac{\alpha\hbar^4}{4m_2m_2'}\left(\frac{\pi n_y}{d_y}\right)^4\right]$.

The 1D electron concentration per unit length assumes the form

$$n_{1D}=\frac{2g_v}{\pi}\frac{\sqrt{2m_1}}{\hbar}\sum_{n_y=1}^{n_{y\max}}\sum_{n_z=1}^{n_{z\max}}\left[t_{35}\left(E_{F1D},n_y,n_z\right)+t_{36}\left(E_{F1D},n_y,n_z\right)\right], \tag{1.62}$$

where $t_{35}\left(E_{F1D},n_y,n_z\right)=\left[\alpha E_{F1D}^2+E_{F1D}l_7-G_{15}\right]^{1/2}$ and $t_{36}\left(E_{F1D},n_y,n_z\right)=\sum_{r=1}^{s_o}Z_{1D}\left(r\right)\left[t_{35}\left(E_{F1D},n_y,n_z\right)\right]$.

The field-emitted current is given by

$$I=\frac{2g_v e k_B T}{h}\sum_{n_z=1}^{n_{z\max}}\sum_{n_y=1}^{n_{y\max}}F_0(\eta_{19})\exp(-\beta_{19}), \tag{1.63}$$

where $\eta_{19}=\frac{E_{F1D}-E_{21}}{k_BT}$.

E_{21} is the root of

$$E_{21}\left(l_7+\alpha E_{21}\right)=G_{15}, \tag{1.64}$$

$$\beta_{19}=\tfrac{4}{3}[A_{21}(V_0,n_z,n_y)]^{3/2}\cdot[eF_{sz}A_{21}'(V_0,n_z,n_y)]^{-1},$$

$$[V_0(l_7+\alpha V_0)-G_{15}]\left(\frac{\hbar^2}{2m_1}\right)^{-1}=A_{21}(V_0,n_y,n_z),\quad\text{and}$$

$$[(l_7+2\alpha V_0)]\left(\frac{\hbar^2}{2m_1}\right)^{-1}=A_{21}'(V_0,n_y,n_z).$$

1.2.4.4 The Lax Model

The electron energy spectra in bulk specimens of Bi in accordance with the Lax model can be written as [129]

$$E\left(1+\alpha E\right)=\frac{p_x^2}{2m_1}+\frac{p_y^2}{2m_2}+\frac{p_z^2}{2m_3}. \tag{1.65}$$

The 1D dispersion relation in this case can be expressed as

$$E\left(1+\alpha E\right)=\frac{\hbar^2 k_x^2}{2m_1}+G_{16}, \tag{1.66}$$

where $G_{16}=\frac{\hbar^2}{2m_2}\left(\frac{\pi n_y}{d_y}\right)^2+\frac{\hbar^2}{2m_3}\left(\frac{\pi n_z}{d_z}\right)^2$.
The 1D electron statistics is given by

$$n_{1D}=\frac{2g_v}{\pi}\frac{\sqrt{2m_1}}{\hbar}\sum_{n_y=1}^{n_{y\max}}\sum_{n_z=1}^{n_{z\max}}\left[t_{37}\left(E_{F1D},n_y,n_z\right)+t_{38}\left(E_{F1D},n_y,n_z\right)\right], \tag{1.67}$$

where $t_{37}\left(E_{F1D},n_y,n_z\right)=\left[E_{F1D}\left(1+\alpha E_{F1D}\right)-G_{16}\right]^{1/2}$ and $t_{38}\left(E_{F1D},n_y,n_z\right)=\sum_{r=1}^{s_o}Z_{1D}\left(r\right)\left[t_{37}\left(E_{F1D},n_y,n_z\right)\right]$.

The field-emitted current in this case assumes the form

$$I=\frac{2g_v e k_B T}{h}\sum_{n_z=1}^{n_{z\max}}\sum_{n_y=1}^{n_{y\max}}F_0(\eta_{20})\exp(-\beta_{20}), \tag{1.68}$$

where $\eta_{20}=\frac{E_{F1D}-E_{22}}{k_B T}$.
E_{22} is the root of

$$E_{22}\left(l_7+\alpha E_{22}\right)=G_{16}, \tag{1.69}$$

$$\beta_{20}=\tfrac{4}{3}\left[A_{22}(V_0,n_z,n_y)\right]^{3/2}\cdot\left[eF_{sz}A'_{22}(V_0)\right]^{-1},$$

$$\left[V_0\left(1+\alpha V_0\right)-G_{16}\right]\left(\frac{\hbar^2}{2m_1}\right)^{-1}=A_{22}\left(V_{0,}n_{y,}n_z\right),\quad\text{and}$$

$$\left[\left(1+2\alpha V_0\right)\right]\left(\frac{\hbar^2}{2m_1}\right)^{-1}=A'_{22}\left(V_0\right).$$

It may be noted that under the conditions $\alpha\to 0$, $M'_2\to\infty$ and isotropic effective electron mass at the edge of the conduction band, all models of Bismuth convert into isotropic parabolic energy bands. Thus under the aforementioned conditions and the conversion of the summations over the quantum numbers to the corresponding integrations, all the equations for FNFE for Bismuth lead to the well-known expression of the FNFE as given by (1.27).

1.2.5 The Field Emission from Quantum Wires of IV–VI Semiconductors

The dispersion relation of the conduction electrons in IV–VI semiconductors can be expressed in accordance with Dimmock [207] as

$$\left[\overline{\varepsilon} - \frac{E_{g0}}{2} - \frac{\hbar^2 k_s^2}{2m_t^-} - \frac{\hbar^2 k_z^2}{2m_l^-}\right]\left[\overline{\varepsilon} + \frac{E_{g0}}{2} + \frac{\hbar^2 k_s^2}{2m_t^-} + \frac{\hbar^2 k_z^2}{2m_l^-}\right] = P_\perp^2 k_s^2 + P_{||}^2 k_z^2, \tag{1.70}$$

where $\overline{\varepsilon}$ is the energy as measured from the center of the band gap E_{g_0}, and $m_t^{\pm}$ and $m_l^{\pm}$ represent the contributions to the transverse and longitudinal effective masses of the external L_6^+ and L_6^- bands arising from the $\overrightarrow{k}.\overrightarrow{p}$ perturbations with the other bands taken to the second order.

Using $\varepsilon = E + \left(E_{g_0}/2\right)$, $P_\perp^2 = \dfrac{\hbar^2 E_{g_0}}{2m_t^*}$, and $P_{||}^2 = \dfrac{\hbar^2 E_{g_0}}{2m_l^*}$ (m_t^* and m_l^* are the transverse and longitudinal effective electron masses at $k = 0$) in (1.70), we can write

$$\left[E - \frac{\hbar^2 k_s^2}{2m_t^-} - \frac{\hbar^2 k_z^2}{2m_l^-}\right]\left[1 + \alpha E + \alpha\frac{\hbar^2 k_s^2}{2m_t^+} + \alpha\frac{\hbar^2 k_z^2}{2m_l^+}\right] = \frac{\hbar^2 k_s^2}{2m_t^*} + \frac{\hbar^2 k_z^2}{2m_l^*}. \tag{1.71}$$

The 1D dispersion relation can be expressed from (1.71) as

$$k_z^2 = A_{23}(E, n_x, n_y), \tag{1.72}$$

where $A_{23}(E, n_x, n_y) = (2h_4)^{-1}\left[h_6\left(E, n_x, n_y\right) - \left[h_6^2\left(E, n_x, n_y\right) + 4h_4h_7\left(E, n_x, n_y\right)\right]^{1/2}\right]$, $h_4 = \left[\dfrac{\alpha\hbar^4}{4x_3x_6}\right]$,

$$x_3 = \frac{3m_t^-m_l^-}{2m_l^- + m_t^-}, \quad x_6 = \frac{3m_t^+m_l^+}{2m_l^+ + m_t^+},$$

$$h_6\left(E, n_x, n_y\right) = \left[\frac{\alpha E\hbar^2}{2x_6} - \frac{\alpha\hbar^2}{2x_6}\left[\left(\frac{\pi n_x}{d_x}\right)^2\frac{\hbar^2}{2x_1} + \left(\frac{\pi n_y}{d_y}\right)^2\frac{\hbar^2}{2x_2}\right] - \right.$$

$$\left.\frac{\alpha\hbar^2}{2x_3}\left[\left(\frac{\pi n_x}{d_x}\right)^2\frac{\hbar^2}{2x_4} + \left(\frac{\pi n_y}{d_y}\right)^2\frac{\hbar^2}{2x_5}\right] - \frac{\hbar^2}{2m_3} - \frac{(1+\alpha E)\hbar^2}{2x_3}\right],$$

$$x_1 = m_t^-, \quad x_2 = \frac{m_t^- + 2m_l^-}{3}, \quad x_4 = m_t^+, \quad x_5 = \frac{m_t^+ + 2m_l^+}{3}, \quad m_3 = \frac{3m_t^*m_l^*}{m_t^* + 2m_l^*},$$

$$h_7\left(E,n_x,n_y\right)=\left[E\left(1+\alpha E\right)+\alpha E\left[\left(\frac{\pi n_x}{d_x}\right)^2\frac{\hbar^2}{2x_4}+\left(\frac{\pi n_y}{d_y}\right)^2\frac{\hbar^2}{2x_5}\right]\right.$$
$$-\left(1+\alpha E\right)\left[\left(\frac{\pi n_x}{d_x}\right)^2\frac{\hbar^2}{2x_1}+\left(\frac{\pi n_y}{d_y}\right)^2\frac{\hbar^2}{2x_2}\right]-\alpha\left[\left(\frac{\pi n_x}{d_x}\right)^2\frac{\hbar^2}{2x_1}\right.$$
$$\left.+\left(\frac{\pi n_y}{d_y}\right)^2\frac{\hbar^2}{2x_2}\right]\left[\left(\frac{\pi n_x}{d_x}\right)^2\frac{\hbar^2}{2x_4}+\left(\frac{\pi n_y}{d_y}\right)^2\frac{\hbar^2}{2x_5}\right]$$
$$\left.-\left[\left(\frac{\pi n_x}{d_x}\right)^2\frac{\hbar^2}{2m_1}+\left(\frac{\pi n_y}{d_y}\right)^2\frac{\hbar^2}{2m_2}\right]\right],$$
$$\times m_1=m_t^*,\quad\text{and}\quad m_2=\frac{m_t^*+2m_l^*}{3}.$$

The electron concentration is given by

$$n_0=\frac{2g_{\mathrm{v}}}{\pi}\sum_{n_x=1}^{n_{x\max}}\sum_{n_y=1}^{n_{y\max}}\left[B_{32}(E_{\mathrm{F1D}},n_x,n_y)+B_{33}(E_{\mathrm{F1D}},n_x,n_y)\right],\tag{1.73}$$

where $B_{32}(E_{\mathrm{F1D}},n_x,n_y)=[A_{23}(E_{\mathrm{F1D}},n_x,n_y)]^{1/2}$ and $B_{33}(E_{\mathrm{F1D}},n_x,n_y)=\sum_{r=1}^{r_0}Z_{1\mathrm{D}}(r)[B_{32}(E_{\mathrm{F1D}},n_x,n_y)]$.

The field-emitted current can be written as

$$I=\frac{2g_{\mathrm{v}}ek_{\mathrm{B}}T}{h}\sum_{n_x=1}^{n_{x\max}}\sum_{n_y=1}^{n_{y\max}}F_0(\eta_{22})\exp(-\beta_{22}),\tag{1.74}$$

where $\eta_{22}=\dfrac{E_{\mathrm{F1D}}-\overline{E_{22}}}{k_{\mathrm{B}}T}$.

The subband energy $\overline{E_{22}}$ assumes the form

$$\overline{E_{22}}=(2\alpha)^{-1}\left[-\zeta_{70}(n_x,n_y)+[\zeta_{70}^2(n_x,n_y)+4\alpha\zeta_{71}(n_x,n_y)]^{1/2}\right]\tag{1.75}$$

in which

$$\zeta_{70}\left(n_x,n_y\right)=\left[1+\alpha\left[\left(\frac{\pi n_x}{d_x}\right)^2\frac{\hbar^2}{2x_4}+\left(\frac{\pi n_y}{d_y}\right)^2\frac{\hbar^2}{2x_5}\right]\right.$$
$$\left.-\alpha\left[\left(\frac{\pi n_x}{d_x}\right)^2\frac{\hbar^2}{2x_1}+\left(\frac{\pi n_y}{d_y}\right)^2\frac{\hbar^2}{2x_2}\right]\right],$$

$$\zeta_{71}\left(n_x, n_y\right) = \left[\left[\left(\frac{\pi n_x}{d_x}\right)^2 \frac{\hbar^2}{2x_1} + \left(\frac{\pi n_y}{d_y}\right)^2 \frac{\hbar^2}{2x_2}\right] + \alpha\left[\left(\frac{\pi n_x}{d_x}\right)^2 \frac{\hbar^2}{2x_1} + \left(\frac{\pi n_y}{d_y}\right)^2 \frac{\hbar^2}{2x_2}\right]\left[\left(\frac{\pi n_x}{d_x}\right)^2 \frac{\hbar^2}{2x_4} + \left(\frac{\pi n_y}{d_y}\right)^2 \frac{\hbar^2}{2x_5}\right] + \left[\left(\frac{\pi n_x}{d_x}\right)^2 \frac{\hbar^2}{2m_1} + \left(\frac{\pi n_y}{d_y}\right)^2 \frac{\hbar^2}{2m_2}\right]\right],$$

$$\beta_{22} = \frac{4}{3}\left[A_{23}(V_0, n_x, n_y)\right]^{3/2} \cdot \left[eF_{sz}A'_{23}(V_0, n_x, n_y)\right]^{-1},$$

$$A'_{23}(V_0, n_x, n_y) = (2h_4)^{-1}\left[h'_6 - \frac{h_6\left(V_0, n_x, n_y\right)h'_6 + 2h_4h'_7\left(V_0, n_x, n_y\right)}{\left[h_6^2\left(V_0, n_x, n_y\right) + 4h_4h_7\left(V_0, n_x, n_y\right)\right]^{1/2}}\right],$$

$$h'_6 = \frac{\alpha\hbar^2}{2}\left(\frac{1}{x_6} - \frac{1}{x_3}\right),$$

and

$$h'_7(V_0, n_x, n_y) = \left[1 + 2\alpha V_0 + \alpha\left[\frac{\hbar^2}{2x_4}\left(\frac{\pi n_x}{d_x}\right)^2 + \left(\frac{\pi n_y}{d_y}\right)^2 \frac{\hbar^2}{2x_5}\right] - \alpha\left[\frac{\hbar^2}{2x_1}\left(\frac{\pi n_x}{d_x}\right)^2 + \left(\frac{\pi n_y}{d_y}\right)^2 \frac{\hbar^2}{2x_2}\right]\right].$$

1.2.6 The Field Emission from Quantum Wires of Stressed Semiconductors

The dispersion relation of the conduction electrons in bulk specimens of stressed semiconductors can be written as [208–211]

$$\frac{k_x^2}{[a^*(E)]^2} + \frac{k_y^2}{[b^*(E)]^2} + \frac{k_z^2}{[c^*(E)]^2} = 1, \tag{1.76}$$

where

$$\left[a^*(E)\right]^2 = \frac{K_0(E)}{M_0(E) + \frac{1}{2}N_0(E)},$$

$$K_0(E) = \left[E - C_1\varepsilon - \frac{2C_2^2\varepsilon_{xy}^2}{3E'_{g_0}(E)}\right]\left(\frac{3E'_{g_0}(E)}{2B_2^2}\right).$$

C_1 is the conduction band deformation potential constant, ε is the trace of the strain tensor $\hat{\varepsilon}$ which can be written as $\hat{\varepsilon} = \begin{bmatrix} \varepsilon_{xx} & \varepsilon_{xy} & 0 \\ \varepsilon_{xy} & \varepsilon_{yy} & 0 \\ 0 & 0 & \varepsilon_{zz} \end{bmatrix}$, C_2 is a constant which describes the strain interaction between the conduction and valance bands, $E'_{g_0}(E) = E_{g_0} + E - C_1\varepsilon$, E_{g_0} is the band gap in the absence of stress, B_2 is the momentum matrix element,

$$M_0(E) = \left[1 - \frac{(\bar{a}_0 + C_1)\,\varepsilon}{E'_{g_0}(E)} + \frac{3\bar{b}_0\varepsilon_{xx}}{2E'_{g_0}(E)} - \frac{\bar{b}_0\varepsilon}{2E'_{g_0}(E)}\right], \quad \bar{a}_0 = -\frac{1}{3}\left(\bar{b}_0 + 2\bar{m}\right),$$

$\bar{a}_0 = -\frac{1}{3}\left(\bar{l} + 2\bar{m}\right)$ $\bar{b}_0 = \frac{1}{3}\left(\bar{l} - \bar{m}\right)$, and $\bar{d}_0 = \frac{2\bar{n}}{\sqrt{3}}, \bar{l}, \bar{m}, \bar{n}$ are the matrix elements of the strain perturbation operator, $N_0(E) = \left(\bar{d}_0\sqrt{3}\right)\frac{\varepsilon_{xy}}{E'_{g_0}(E)}$,

$$\left[b^*(E)\right]^2 = \frac{K_0(E)}{M_0(E) - \frac{1}{2}N_0(E)}, \quad \left[c^*(E)\right]^2 = \frac{K_0(E)}{L_0(E)}, \quad \text{and}$$

$$L_0(E) = \left[1 - \frac{(\bar{a}_0 + C_1)\,\varepsilon}{E'_{g_0}(E)} + \frac{3\bar{b}_0\varepsilon_{zz}}{2E'_{g_0}(E)} - \frac{\bar{b}_0\varepsilon}{2E'_{g_0}(E)}\right].$$

The 1D dispersion relation of the carriers in stressed materials in this case can be written as

$$k_z^2 = A_{24}(E, n_x, n_y), \tag{1.77}$$

where $A_{24}(E, n_x, n_y) = [c^*(E)]^2\left[1 - \left(\frac{\pi n_x}{d_x}\right)^2[a^*(E)]^{-2} - \left(\frac{\pi n_y}{d_y}\right)^2[b^*(E)]^{-2}\right]$.

The subband energy E_{23} assumes the form

$$\left[\left(\frac{\pi n_x}{d_x}\right)^2\left[a^*(E)\right]^{-2} + \left(\frac{\pi n_y}{d_y}\right)^2\left[b^*(E)\right]^{-2}\right] = 1. \tag{1.78}$$

Using (1.77), the 1D electron statistics can be expressed as

$$n_{1D} = \frac{2g_v}{\pi}\sum_{n_y=1}^{n_{y\max}}\sum_{n_z=1}^{n_{z\max}}\left[B_{34}\left(E_{F1D}, n_y, n_z\right) + B_{35}\left(E_{F1D}, n_y, n_z\right)\right], \tag{1.79}$$

where $B_{34}\left(E_{F1D}, n_y, n_z\right) = \sqrt{A_{24}(E_{F1D}, n_x, n_y)}$ and $B_{35}\left(E_{F1D}, n_x, n_y\right) = \sum_{r=1}^{s_o} Z_{1D}(r)\left[B_{34}\left(E_{F1D}, n_y, n_z\right)\right]$.

The field-emitted current is given by

$$I = \frac{2g_{\mathrm{v}}ek_{\mathrm{B}}T}{h}\sum_{n_x=1}^{n_{x\max}}\sum_{n_y=1}^{n_{y\max}} F_0(\eta_{23})\exp(-\beta_{23}), \tag{1.80}$$

where

$$\eta_{23} = \frac{E_{\mathrm{F1D}} - E_{23}}{k_{\mathrm{B}}T}, \quad \beta_{23} = \frac{4}{3}\left[A_{24}(V_0, n_x, n_y)\right]^{3/2}\cdot\left[eF_{sz}A'_{24}(V_0, n_x, n_y)\right]^{-1},$$

$$A'_{24}\left(V_0, n_x, n_y\right) = \left[\frac{K'_0(V_0)}{L_0(V_0)} - \frac{K_0(V_0)L'_0(V_0)}{L_0^2(V_0)} - \left(\frac{n_x\pi}{d_x}\right)^2\frac{\left[M'_0(V_0) + \frac{1}{2}N'_0(V_0)\right]}{L_0(V_0)}\right.$$
$$+\left(\frac{n_x\pi}{d_x}\right)^2\cdot\frac{L'_0(V_0)}{L_0^2(V_0)}\left[M_0(V_0) + \frac{1}{2}N_0(V_0)\right] + \left(\frac{n_y\pi}{d_y}\right)^2\cdot\frac{L'_0(V_0)}{L_0^2(V_0)}$$
$$\left.\times\left[M_0(V_0) - \frac{1}{2}N_0(V_0)\right] - \left(\frac{n_y\pi}{d_y}\right)^2\cdot\frac{1}{L_0(V_0)}\left[M'_0(V_0) - \frac{1}{2}N'_0(V_0)\right]\right],$$

$$K'_0\left(V_0\right) = \left[\left[1 + \frac{2C_2^2\varepsilon_{xy}^2}{3\{E'_{g_0}(V_0)\}^2}\right]\left(\frac{3E'_{g_0}(V_0)}{2B_2^2}\right)\right.$$
$$\left.+\left[V_0 - C_1\varepsilon - \frac{2C_2^2\varepsilon_{xy}^2}{3E'_{g_0}(V_0)}\right]\left(\frac{3}{2B_2^2}\right)\right],$$

$$M'_0\left(V_0\right) = \left[\frac{(\bar{a}_0 + C_1)\,\varepsilon}{(E'_{g_0}(V_0))^2} - \frac{3\bar{b}_0\varepsilon_{xx}}{2(E'_{g_0}(V_0))^2} + \frac{\bar{b}_0\varepsilon}{2(E'_{g_0}(V_0))^2}\right], \quad \text{and}$$

$$N'_0\left(V_0\right) = -\left(\bar{d}_0\sqrt{3}\right)\frac{\varepsilon_{xy}}{(E'_{g_0}(V_0))^2}.$$

1.2.7 The Field Emission from Quantum Wires of Tellurium

The dispersion relation of the conduction electrons in Te can be expressed as [212]

$$E = \psi_1 k_z^2 + \psi_2 k_s^2 \pm [\psi_3^2 k_z^2 + \psi_4^2 k_s^2]^{1/2}, \tag{1.81}$$

where ψ_1, ψ_2, ψ_3, and ψ_4 are system constants.

From (1.81), the1D dispersion relation can be written as

$$k_z^2 = A_{25,\pm}(E, n_x, n_y), \tag{1.82}$$

where

$$A_{25,\pm}(E,n_x,n_y)=\left[\left(\psi_5(E)-\psi_6k_s^2\pm\psi_7\left[\psi_8(E)-k_s^2\right]^{1/2}\right],\ \ k_s^2=\phi_1(n_x,n_y),$$

$$\psi_5(E)=\left[\frac{E}{\psi_1}+\frac{E}{2\psi_1^2}\right],\ \ \psi_6=\frac{\psi_2}{\psi_1},\ \ \psi_7=(2\psi_1^2)^{-1}\left[4\psi_3^2\psi_1\psi_2-4\psi_1^2\psi_4^2\right]^{1/2},\ \text{and}$$

$$\psi_8(E)=\left[\frac{\psi_4^4+4E\psi_3^2\psi_1}{4\psi_3^2\psi_1\psi_2-4\psi_1^2\psi_4^2}\right].$$

The subband energies are given by

$$E_{26,\pm}=\psi_2\phi_1\left(n_x,n_y\right)\pm\psi_4\left(\phi_1\left(n_x,n_y\right)\right)^{1/2}. \tag{1.83}$$

The electron concentration per unit length can be expressed as

$$n_0=\frac{g_v}{\pi}\sum_{n_x=1}^{n_{x\max}}\sum_{n_y=1}^{n_{y\max}}\left[B_{36,\pm}\left(E_{F1D},n_x,n_y\right)+B_{37,\pm}\left(E_{F1D},n_x,n_y\right)\right], \tag{1.84}$$

where $B_{36,\pm}\left(E_{F1D},n_x,n_y\right)=\sqrt{A_{25,+}(E_{F1D},n_x,n_y)}+\sqrt{A_{25,-}(E_{F1D},n_x,n_y)}$ and

$$B_{37,\pm}\left(E_{F1D},n_x,n_y\right)=\sum_{r=1}^{s_o}Z_{1D}(r)\left[B_{36,+}\left(E_{F1D},n_x,n_y\right)+B_{36,-}\left(E_{F1D},n_x,n_y\right)\right].$$

The field-emitted current assumes the form

$$I=\frac{g_v e k_B T}{h}\sum_{n_x=1}^{n_{x\max}}\sum_{n_y=1}^{n_{y\max}}\left[F_0(\eta_{24,+})\exp(-\beta_{24,+})+F_0(\eta_{24,-})\exp(-\beta_{24,-})\right], \tag{1.85}$$

where $\eta_{24,\pm}=\dfrac{E_{F1D}-E_{26,\pm}}{k_BT},\beta_{24,\pm}=\dfrac{4}{3}\left[A_{25,\pm}\left(V_0,n_x,n_y\right)\right]^{3/2}\cdot\left[eF_{sz}A'_{25,\pm},\right.$
$\left.(V_0n_x,n_y)\ \right]^{-1}, A'_{25,\pm}\left(V_0,n_x,n_y\right)=\left[\frac{1}{\psi_1}\pm\dfrac{\psi_7}{2}\left[\psi_8(V_0)-\phi_1\left(n_x,n_y\right)\right]^{-1/2}\psi'_8(V_0)\right]$,
and $\psi'_8(V_0)=\left[\frac{4\psi_3^2\psi_1}{4\psi_3^2\psi_1\psi_2-4\psi_1^2\psi_4^2}\right]$

1.2.8 The Field Emission from Quantum Wires of Gallium Phosphide

The energy spectrum of the conduction electrons in n-GaP can be written as [213]

$$E=\frac{\hbar^2k_s^2}{2m_\perp^*}+\frac{\hbar^2}{2m_{||}^*}\left[\overline{A}'k_s^2+k_z^2\right]-\left[\frac{\hbar^4k_0^2}{m_{||}^{*2}}\left(k_s^2+k_z^2\right)+|V_G|^2\right]^{1/2}+|V_G|, \tag{1.86}$$

where k_0 and $|V_G|$ are constants of the energy spectrum and $\overline{A}' = 1$. The 1D dispersion relation assumes the form

$$k_z^2 = A_{26}(E, n_x, n_y), \tag{1.87}$$

where

$$A_{26}\left(E, n_x, n_y\right) = \left[t_1 E + t_2 - t_3\phi_1\left(n_x, n_y\right) - \left[t_4\phi_1\left(n_x, n_y\right) + t_6 E + t_5\right]^{1/2}\right],$$

$$t_1 = (b_0)^{-1}$$

$$b_0 = \left(\hbar^2/2m_{\|}^*\right),\ \ t_2 = \left[-2b_0 D_0 + C\right]\left[2b_0^2\right]^{-1},\ \ D_0 = \left|V_g\right|,\ \ C = \left(\hbar^2 k_0/m_{\|}^*\right)^2,$$

$$t_3 = \left(a_0/b_0\right),\ \ a_0 = \left[\left(\hbar^2/2m_{\perp}^*\right) + \left(A\hbar^2/2m_{\|}^*\right)\right],\ \ t_4 = \left(\bar{a}_1/\left(4b_0^4\right)\right),$$

$$\bar{a} = 4b_0 C\left(b_0 - C\right),$$

$$t_6 = \left(\bar{a}_3/\left(4b_0^4\right)\right),\ \ \bar{a}_3 = 4Cb_0,\ \ t_5 = \left(\bar{a}_2/\left(4b_0^4\right)\right),\ \text{and}$$

$$\bar{a}_2 = \left[C^2 + 4b_0^2 D_0^2 - 4b_0 C D_0\right].$$

The subband energy E_{27} can be written as

$$E_{27} = a_0\phi_1(n_x, n_y) - (C\phi_1(n_x, n_y) + D_0^2)^{1/2} + D_0. \tag{1.88}$$

The electron concentration per unit length can be expressed as

$$n_0 = \frac{2g_{\mathrm{v}}}{\pi}\sum_{n_x=1}^{n_{x\max}}\sum_{n_y=1}^{n_{y\max}}\left[B_{38}\left(E_{\mathrm{F1D}}, n_x, n_y\right) + B_{39}\left(E_{\mathrm{F1D}}, n_x, n_y\right)\right], \tag{1.89}$$

where $B_{38}\left(E_{\mathrm{F1D}}, n_x, n_y\right) = \sqrt{A_{26}(E_{\mathrm{F1D}}, n_x, n_y)}$ and $B_{39}\left(E_{\mathrm{F1D}}, n_x, n_y\right) = \sum_{r=1}^{s_o} Z_{1\mathrm{D}}(r)\left[B_{38}\left(E_{\mathrm{F1D}}, n_x, n_y\right)\right]$.

The field-emitted current assumes the form

$$I = \frac{2g_{\mathrm{v}} e k_{\mathrm{B}} T}{h}\sum_{n_x=1}^{n_{x\max}}\sum_{n_y=1}^{n_{y\max}}\left[F_0(\eta_{26})\exp(-\beta_{26})\right], \tag{1.90}$$

where $\eta_{26} = \dfrac{E_{\mathrm{F1D}} - E_{27}}{k_{\mathrm{B}}T}$, $\beta_{26} = \dfrac{4}{3}\left[A_{26}\left(V_0, n_x, n_y\right)\right]^{3/2}\cdot\left[eF_{sz}A'_{26}\left(V_0, n_x, n_y\right)\right]^{-1}$, and $A'_{26}\left(V_0, n_x, n_y\right) = \left[t_1 - \dfrac{1}{2}t_6\left[t_4\phi_1\left(n_x, n_y\right) + t_6 V_0 + t_5\right]^{-1/2}\right]$.

1.2.9 The Field Emission from Quantum Wires of Platinum Antimonide

The dispersion relation for n − $PtSb_2$ is given by [214]

$$\left[E+\overline{\lambda_0}\frac{(\overline{a})^2}{4}k^2-\overline{l}\frac{(\overline{a})^2}{4}k_s^2\right]\left[E+\overline{\delta_0}-\overline{\nu}\frac{(\overline{a})^2}{4}k^2-\overline{n}\frac{(\overline{a})^2}{4}k_s^2\right]=\frac{I\,(\overline{a})^4}{16}k^4, \tag{1.91}$$

where $\overline{\lambda_0}, \overline{a}, \overline{l}, \overline{\delta_0}, \overline{\nu}, \overline{n}$, and I are system constants.

The 1D dispersion relation can be written as

$$k_x^2=\left[2\overline{A_9}\right]^{-1}\left[-\overline{A_{10}}\,(E,n_z)+\left[\overline{A_{10}}^2\,(E,n_z)+4\left(\overline{A_9}\right)\overline{A_{11}}\,(E,n_z)\right]\right]^{1/2}-\left(\frac{n_y\pi}{d_Y}\right)^2, \tag{1.92}$$

where

$$\overline{A_9}=(I_1+\omega_1\omega_3),\quad I_1=I\frac{(\overline{a})^4}{16},$$

$$\overline{A_{10}}\,(E,n_z)=\left[\omega_3E+\omega_1\left[E+\overline{\delta_0}-\omega_4\left(\frac{n_z\pi}{d_z}\right)^2\right]+\omega_2\omega_3\left(\frac{n_z\pi}{d_z}\right)^2+2I_1\left(\frac{n_z\pi}{d_z}\right)^2\right],$$

$$\omega_1=\frac{(\overline{a})^2}{4}\left[\left(\overline{\lambda_0}\right)-\overline{l}\right],\quad \omega_2=\left(\overline{\lambda_0}\frac{(\overline{a})^2}{4}\right),\quad \omega_3=\frac{(\overline{a})^2}{4}(\overline{n}+\overline{\nu}),\quad \omega_4=\frac{(\overline{a})^2}{4}\overline{\nu},\ \text{and}$$

$$\overline{A_{11}}\,(E,n_z)=\left[E\left[E+\overline{\delta_0}-\omega_4\left(\frac{n_z\pi}{d_z}\right)^2\right]+\omega_2\left(\frac{n_z\pi}{d_z}\right)^2\left[E+\overline{\delta_0}-\omega_4\left(\frac{n_z\pi}{d_z}\right)^2\right]-I_1\left(\frac{n_z\pi}{d_z}\right)^4\right].$$

Therefore, (1.92) can be expressed as

$$k_x^2=A_{27}\left(E,n_y,n_z\right), \tag{1.93}$$

where

$$A_{27}\left(E,n_y,n_z\right)=\left[2\overline{A_9}\right]^{-1}\left[-\overline{A_{10}}\,(E,n_z)+\left[\overline{A_{10}}^2\,(E,n_z)+4\left(\overline{A_9}\right)\overline{A_{11}}\,(E,n_z)\right]\right]^{1/2}-\left(\frac{n_y\pi}{d_y}\right)^2.$$

The electron concentration per unit length assumes the form

$$n_0 = \frac{2g_{\mathrm{v}}}{\pi}\sum_{n_x=1}^{n_{x\max}}\sum_{n_y=1}^{n_{y\max}}\left[B_{40}\left(E_{\mathrm{F1D}}, n_x, n_y\right) + B_{41}\left(E_{\mathrm{F1D}}, n_x, n_y\right)\right], \tag{1.94}$$

where $B_{40}\left(E_{\mathrm{F1D}}, n_x, n_y\right) = \sqrt{A_{27}(E_{\mathrm{F1D}}, n_x, n_y)}$ and $B_{41}\left(E_{\mathrm{F1D}}, n_x, n_y\right) = \sum_{r=1}^{s_o} Z_{1\mathrm{D}}(r)\left[B_{40}\left(E_{\mathrm{F1D}}, n_x, n_y\right)\right]$.

The field-emitted current can be written as

$$I = \frac{2g_{\mathrm{v}}ek_{\mathrm{B}}T}{h}\sum_{n_x=1}^{n_{x\max}}\sum_{n_y=1}^{n_{y\max}}\left[F_0(\eta_{27})\exp(-\beta_{27})\right], \tag{1.95}$$

where $\eta_{27} = \dfrac{E_{\mathrm{F1D}} - E_{28}}{k_{\mathrm{B}}T}$. E_{28} is the root of the equation

$$\left[2\overline{A_9}\right]^{-1}\left[-\overline{A_{10}}\left(E_{28}, n_z\right) + \left[\overline{A_{10}}^2\left(E_{28}, n_z\right) + 4\left(\overline{A_9}\right)\overline{A_{11}}\left(E_{28}, n_z\right)\right]\right]^{1/2} - \left(\frac{n_y\pi}{d_Y}\right)^2 = 0, \tag{1.96}$$

$$\beta_{27} = \frac{4}{3}[A_{27}(V_0, n_x, n_y)]^{3/2}\cdot[eF_{sz}A_2'7(V_0, n_x, n_y)]^{-1},$$

$$A_{27}'\left(E, n_y, n_z\right) = \left[2\overline{A_9}\right]^{-1}\left[-\left(\overline{A_{10}}\right)' + \left[\overline{A_{10}}^2\left(V_0, n_z\right) + 4\left(\overline{A_9}\right)\overline{A_{11}}\left(V_0, n_z\right)\right]^{1/2}\cdot\left[\overline{A_{10}}\left(V_0, n_z\right)\left(\overline{A_{10}}\right)' + 2\left(\overline{A_9}\right)\left(\overline{A_{11}}\left(V_0, n_z\right)\right)'\right]\right],$$

$$A_{10}' = (\omega_1 + \omega_3),$$

and

$$\left(\overline{A_{11}}\left(V_0, n_z\right)\right)' = \left[2V_0 + \overline{\delta_0} - \omega_4\left(\frac{n_z\pi}{d_z}\right)^2 + \omega_2\left(\frac{n_z\pi}{d_z}\right)^2\right].$$

1.2.10 *The Field Emission from Quantum Wires of Bismuth Telluride*

The dispersion relation of the conduction electrons in Bi_2Te_3 can be written as [215–217]

$$E(1+\alpha E) = \bar{\omega}_1k_x^2 + \bar{\omega}_2k_y^2 + \bar{\omega}_3k_z^2 + \bar{\omega}_4k_zk_y, \tag{1.97}$$

where $\bar{\omega}_1 = \dfrac{\hbar^2}{2m_0}\bar{\alpha}_{11}, \bar{\omega}_2 = \dfrac{\hbar^2}{2m_0}\bar{\alpha}_{22}, \bar{\omega}_3 = \dfrac{\hbar^2}{2m_0}\bar{\alpha}_{33}$, and $\bar{\omega}_4 = \dfrac{\hbar^2}{2m_0}\bar{\alpha}_{23}$ in which $\bar{\alpha}_{11}, \bar{\alpha}_{22}, \bar{\alpha}_{33}$, and $\bar{\alpha}_{23}$ are system constants.

The 1D electron energy spectrum assumes the form

$$k_x^2 = A_{28}(E, n_y, n_z), \tag{1.98}$$

where $A_{28}(E, n_y, n_z) = \left[E\,(1 + \alpha E) - \bar{\omega}_2 \left(\frac{n_y \pi}{d_y}\right)^2 - \bar{\omega}_3 \left(\frac{n_z \pi}{d_z}\right)^2 - \bar{\omega}_4 \left(\frac{n_y \pi}{d_y}\right) \left(\frac{n_z \pi}{d_z}\right)\right] (\bar{\omega}_1)^{-1}$.

The subband energy (E_{30}) can be expressed as

$$E_{30} = (2\alpha)^{-1}\left[-1 + \sqrt{1 + 4\alpha\theta_{32}(n_y, n_z)}\right], \tag{1.99}$$

where $\theta_{32}(n_y, n_z) = \left[\bar{\omega}_2 \left(\frac{n_y \pi}{d_y}\right)^2 + \bar{\omega}_3 \left(\frac{n_z \pi}{d_z}\right)^2 + \bar{\omega}_4 \left(\frac{n_y \pi}{d_y}\right) \left(\frac{n_z \pi}{d_z}\right)\right]$.

The electron concentration per unit length is given by

$$n_0 = \frac{2g_v}{\pi} \sum_{n_z=1}^{n_{z\max}} \sum_{n_y=1}^{n_{y\max}} \left[B_{42}\left(E_{\mathrm{F1D}}, n_z, n_y\right) + B_{43}\left(E_{\mathrm{F1D}}, n_z, n_y\right)\right], \tag{1.100}$$

where $B_{42}\left(E_{\mathrm{F1D}}, n_z, n_y\right) = \sqrt{A_{28}(E_{\mathrm{F1D}}, n_y, n_z)}$ and $B_{43}\left(E_{\mathrm{F1D}}, n_z, n_y\right) = \sum_{r=1}^{s_o} Z_{1\mathrm{D}}(r)\left[B_{42}B\left(E_{\mathrm{F1D}}, n_z, n_y\right)\right]$.

The field-emitted current in this case can be written as

$$I = \frac{2g_v e k_B T}{h} \sum_{n_z=1}^{n_{z\max}} \sum_{n_y=1}^{n_{y\max}} [F_0(\eta_{28}) \exp(-\beta_{28})], \tag{1.101}$$

where

$$\eta_{28} = \frac{E_{\mathrm{F1D}} - E_{30}}{k_B T}, \quad \beta_{28} = \frac{4}{3}\left[A_{28}\left(V_0, n_y, n_z\right)\right]^{3/2} \cdot \left[eF_{sz}A_2'8(V_0)\right]^{-1}, \quad \text{and}$$

$A_{28}'(V_0) = (\bar{\omega}_1)^{-1}\left[1 + 2\alpha V_0\right]$.

1.2.11 The Field Emission from Quantum Wires of Germanium

It is well known that the conduction electrons of n-Ge obey two different types of dispersion laws since band nonparabolicity has been included in two different ways as given in the literature [218–220].

(a) The energy spectrum of the conduction electrons in bulk specimens of n-Ge can be expressed in accordance with Cardona et al. [218] as

$$E = -\frac{E_{g0}}{2} + \frac{\hbar^2 k_z^2}{2m_{\parallel}^*} + \left[\frac{E_{g0}^2}{4} + E_{g0}k_s^2\left(\frac{\hbar^2}{2m_{\perp}^*}\right)\right]^{1/2}, \tag{1.102}$$

where in this case $m_{\parallel}^*$ and $m_{\perp}^*$ are the longitudinal and transverse effective masses along the $\langle 111\rangle$ direction at the edge of the conduction band, respectively.

The 1D electron energy spectrum assumes the form

$$k_y^2 = A_{29}(E, n_x, n_z), \tag{1.103}$$

where

$$A_{29}(E, n_x, n_z) = \left[\left[\gamma_{15}(E, n_z) - \left(\frac{\hbar^2}{2m_1^*}\right)\left(\frac{n_x\pi}{d_x}\right)^2\right](2m_2^*/\hbar^2)\right],$$

$$\gamma_{15}(E, n_z) = \left[E(1+\alpha E) - (1+2\alpha E)\left(\frac{\hbar^2}{2m_3^*}\right)\left(\frac{n_z\pi}{d_z}\right)^2 + \alpha\left[\left(\frac{\hbar^2}{2m_3^*}\right)\left(\frac{n_z\pi}{d_z}\right)^2\right]^2\right],$$

$$m_1^* = m_{\perp}^*,\ m_2^* = \frac{m_{\perp}^* + 2m_{\parallel}^*}{3} \quad \text{and} \quad m_3^* = \frac{3m_{\perp}^* m_{\parallel}^*}{m_{\perp}^* + 2m_{\parallel}^*}.$$

The quantized energy levels (E_{31}) can be expressed through the equation

$$E_{31} = (2\alpha)^{-1}[-\rho_{91}(n_z) + \sqrt{\rho_{91}(n_z)^2 - 4\alpha\rho_{92}(n_z)}], \tag{1.104}$$

where

$$\rho_{91}(n_z) = \left[1 - 2\alpha\frac{\hbar^2}{2m_3^*}\left(\frac{n_z\pi}{d_z}\right)^2\right] \quad \text{and}$$

$$\rho_{92}(n_z) = \left[\frac{\hbar^2}{2m_3^*}\left(\frac{n_z\pi}{d_z}\right)^2 - \alpha\left[\frac{\hbar^2}{2m_3^*}\left(\frac{n_z\pi}{d_z}\right)^2\right]^2\right].$$

The electron concentration per unit length is given by

$$n_0 = \frac{2g_v}{\pi} \sum_{n_x=1}^{n_{x\max}} \sum_{n_z=1}^{n_{z\max}} [B_{44}(E_{F1D}, n_x, n_z) + B_{45}(E_{F1D}, n_x, n_z)], \tag{1.105}$$

where $B_{44}(E_{F1D}, n_x, n_z) = \sqrt{A_{29}(E_{F1D}, n_x, n_z)}$ and $B_{45}(E_{F1D}, n_x, n_z) = \sum_{r=1}^{s_o} Z_{1D}(r)\,[B_{44}(E_{F1D}, n_x, n_z)]$.

The field-emitted current assumes the form

$$I = \frac{2g_v e k_B T}{h} \sum_{n_x=1}^{n_{x\max}} \sum_{n_z=1}^{n_{z\max}} [F_0(\eta_{29}) \exp(-\beta_{29})], \tag{1.106}$$

where $\eta_{29} = \dfrac{E_{F1D} - E_{31}}{k_B T}$,

$$\beta_{29} = \frac{4}{3}\left[A_{29}(V_0, n_y, n_z)\right]^{3/2} \cdot \left[eF_{sz} A_2' 9(V_0)\right]^{-1}, \text{ and}$$

$$A_{29}'(V_0, n_x, n_z) = \left[\left[1 + 2\alpha V_0 - \left(\alpha \frac{\hbar^2}{m_3^*}\right)\left(\frac{n_z \pi}{d_z}\right)^2\right](2m_2^*/\hbar^2)\right].$$

(b) The dispersion relation of the conduction electron in bulk specimens of n-Ge can be expressed in accordance with the model of Wang and Ressler [220] and can be written as

$$E = \frac{\hbar^2 k_z^2}{2m_{||}^*} + \frac{\hbar^2 k_s^2}{2m_\perp^*} - \bar{c}_1 \left(\frac{\hbar^2 k_s^2}{2m_\perp^*}\right)^2 - \bar{d}_1 \left(\frac{\hbar^2 k_s^2}{2m_\perp^*}\right)\left(\frac{\hbar^2 k_z^2}{2m_{||}^*}\right) - \bar{e}_1 \left(\frac{\hbar^2 k_z^2}{2m_{||}^*}\right)^2, \tag{1.107}$$

where $\bar{c}_1 = \overline{C}\left(2m_\perp^*/\hbar^2\right)^2$, $\overline{C} = 1.4\overline{A}$, $\overline{A} = \frac{1}{4}\left(\hbar^4/E_{g_0} m_\perp^{*2}\right)\left(1 - \dfrac{m_\perp^*}{m_0}\right)^2$, $\bar{d}_1 = \bar{d}\left(\dfrac{4m_\perp^* m_\parallel^*}{\hbar^4}\right)$, $\bar{d} = 0.8\overline{A}$, $\bar{e}_1 = \bar{e}_0\left(2m_\parallel^*/\hbar^2\right)^2$, and $\bar{e}_0 = 0.005\bar{A}$.

The 1D electron energy spectrum assumes the form

$$k_y^2 = A_{30}(E, n_x, n_z), \tag{1.108}$$

where $A_{30}(E, n_x, n_z) = \left[\left[I_{29}(E, n_z) - \left(\dfrac{\hbar^2}{2m_1^*}\right)\left(\dfrac{n_x \pi}{d_x}\right)^2\right](2m_2^*/\hbar^2)\right]$,

$$I_{29}(E,n_z)=\left[2\overline{C_1}\right]^{-1}\left[\overline{A_6}(n_z)+\left[\overline{A_6}^2(n_z)-4\overline{C}_1E+4\left(\overline{C_1}\right)\overline{A_5}(n_z)\right]^{\frac{1}{2}}\right],$$

$$\overline{A_5}(n_z)=\left(\frac{\hbar^2}{2m_3^*}\right)\left(\frac{n_z\pi}{d_z}\right)^2\left[1-\bar{e}_1\left(\frac{\hbar^2}{2m_3^*}\right)\left(\frac{n_z\pi}{d_z}\right)^2\right]\sum_{i=1}^{n}X_i^2,\quad\text{and}$$

$$\overline{A_6}(n_z)=\left[1-\bar{d}_1\left(\frac{\hbar^2}{2m_3^*}\right)\left(\frac{n_z\pi}{d_z}\right)^2\right].$$

The quantized energy levels (E_{32}) can be expressed through the equation

$$E_{32}=\overline{A}_5(n_z)+\left(\frac{1}{4\overline{C}_1}\right)\left[\left[\frac{\overline{C}_1\hbar^2}{m_1^*}\left(\frac{n_x\pi}{d_x}\right)^2\right]^2-2\overline{A}_6(n_z)\frac{\bar{C}_1\hbar^2}{m_1^*}\left(\frac{n_x\pi}{d_x}\right)^2\right]. \tag{1.109}$$

The electron concentration per unit length is given by

$$n_0=\frac{2g_{\mathrm{v}}}{\pi}\sum_{n_x=1}^{n_{x\max}}\sum_{n_z=1}^{n_{z\max}}\left[B_{46}(E_{\mathrm{F1D}},n_x,n_z)+B_{47}(E_{\mathrm{F1D}},n_x,n_z)\right], \tag{1.110}$$

where

$$B_{46}(E_{\mathrm{F1D}},n_x,n_z)=\sqrt{A_{30}(E_{\mathrm{F1D}},n_x,n_z)}\quad\text{and}$$

$$B_{47}(E_{\mathrm{F1D}},n_x,n_z)=\sum_{r=1}^{s_o}Z_{1\mathrm{D}}(r)\left[B_{46}(E_{\mathrm{F1D}},n_x,n_z)\right].$$

The field-emitted current assumes the form

$$I=\frac{2g_{\mathrm{v}}ek_{\mathrm{B}}T}{h}\sum_{n_x=1}^{n_{x\max}}\sum_{n_z=1}^{n_{z\max}}\left[F_0(\eta_{30})\exp(-\beta_{30})\right], \tag{1.111}$$

where $\eta_{30}=\dfrac{E_{\mathrm{F1D}}-E_{32}}{k_BT}$, $\beta_{30}=\dfrac{4}{3}\left[A_{30}\left(V_0,n_y,n_z\right)\right]^{3/2}\cdot\left[eF_{sz}A'_{30}(V_0)\right]^{-1}$,

$$A'_{30}(V_0,n_x,n_z)=(2m_2^*/\hbar^2)I'_{29}(V_0,n_z),\quad\text{and}$$

$$I'_{29}(V_0,n_z)=\left[\left[\overline{A_6}^2(n_z)-4\overline{C}_1V_0+4\left(\overline{C_1}\right)\overline{A_5}(n_z)\right]^{-1/2}\right].$$

1.2.12 The Field Emission from Quantum Wires of Gallium Antimonide

The dispersion relation of the conduction electrons in n-GaSb can be written as [221]

$$E = \frac{\hbar^2 k^2}{2m_0} - \frac{\overline{E'}_{go}}{2} + \frac{\bar{E}'_{go}}{2}\left[1 + \frac{2\hbar^2 k^2}{\overline{E'}_{go}}\left(\frac{1}{m_c} - \frac{1}{m_0}\right)\right]^{\frac{1}{2}}, \tag{1.112}$$

where $\overline{E'}_{go} = \left[E_{go} + \frac{5.10^{-5}T^2}{2(112+T)}\right]$ eV.

Equation (1.112) can be expressed as

$$\frac{\hbar^2 k^2}{2m_c} = I_{16}(E), \tag{1.113}$$

where

$$\begin{aligned} I_{16}(E) = [E + \overline{E'}_{g0} - (m_c/m_0)(\overline{E'}_{g0}/2) - [(\bar{E}'_{g0}/2)^2 \\ + [((\overline{E'}_{g0})^2/2)(1 - (m_c/m_0))] + [(\overline{E'}_{g0}/2)(1 - (m_c/m_0))]^2 \\ + E\overline{E'}_{g0}(1 - (m_c/m_0))]^{1/2}]. \end{aligned}$$

The 1D electron energy spectrum assumes the form

$$k_z^2 = A_{31}(E, n_x, n_y), \tag{1.114}$$

where $A_{31}(E, n_x, n_y) = [I_{16}(E)(2m_c/\hbar^2) - \phi_1(n_x, n_y)]$.

The quantized energy levels (E_{33}) can be expressed through the equation

$$I_{16}(E_{33}) = \left(\frac{\hbar^2}{2m_c}\right)\phi_1(n_x, n_y). \tag{1.115}$$

The electron concentration per unit length is given by

$$n_0 = \frac{2g_v}{\pi}\sum_{n_x=1}^{n_{x\max}}\sum_{n_y=1}^{n_{y\max}}\left[B_{48}\left(E_{F1D}, n_x, n_y\right) + B_{49}\left(E_{F1D}, n_x, n_y\right)\right], \tag{1.116}$$

where

$B_{48}\left(E_{F1D}, n_x, n_y\right) = \sqrt{A_{31}(E_{F1D}, n_x, n_y)}$ and

$B_{49}\left(E_{F1D}, n_x, n_y\right) = \sum_{r=1}^{s_o} Z_{1D}(r)\left[B_{48}\left(E_{F1D}, n_x, n_y\right)\right]$.

The field-emitted current can be written as

$$I = \frac{2g_v e k_B T}{h} \sum_{n_x=1}^{n_{x\max}} \sum_{n_y=1}^{n_{y\max}} [F_0(\eta_{31}) \exp(-\beta_{31})], \tag{1.117}$$

where $\eta_{31} = \frac{E_{F1D} - E_{33}}{k_B T}, \beta_{31} = \frac{4}{3}\left[A_{31}\left(V_0, n_x, n_y\right)\right]^{3/2} \cdot \left[eF_{sz} A'_{31}(V_0)\right]^{-1}$, and $A'_{31}(V_0) = [1 - (m_c/m_0)(\overline{E'}_{g0}/2)[(\overline{E'}_{g0}/2)^2 + [((\overline{E'}_{g0})^2/2)(1 - (m_c/m_0))] + [((\overline{E'}_{g0})^2/2)(1-(m_c/m_0))] + [(\overline{E'}_{g0}/2)(1-(m_c/m_0))]^2 + V_0\overline{E'}_{g0}(1-(m_c/m_0))] - 1/2](2m_c/\hbar^2)$.

1.2.13 The Field Emission from Quantum Wires of II–V Materials

The dispersion relation of the holes are given by [222–224]

$$E = \theta_1 k_x^2 + \theta_2 k_y^2 + \theta_3 k_z^2 + \delta_4 k_x \mp \left[\left\{\theta_5 k_x^2 + \theta_6 k_y^2 + \theta_7 k_z^2 + \delta_5 k_x\right\}^2 + G_3^2 k_y^2 + \Delta_3^2\right]^{\frac{1}{2}} \pm \Delta_3, \tag{1.118}$$

where k_x, k_y, and k_z are expressed in the units of $10^{10}\mathrm{m}^{-1}$,

$\theta_1 = \frac{1}{2}(a_1 + b_1)$, $\theta_2 = \frac{1}{2}(a_2 + b_2)$, $\theta_3 = \frac{1}{2}(a_3 + b_3)$, $\delta_4 = \frac{1}{2}(A + B)$,

$\theta_5 = \frac{1}{2}(a_1 - b_1)$, $\theta_6 = \frac{1}{2}(a_2 - b_2)$, $\theta_7 = \frac{1}{2}(a_3 - b_3)$, $\delta_5 = \frac{1}{2}(A - B)$, and

$a_i (i = 1, 2, 3, 4), b_i, A, B, G_3$, and Δ_3 are system constants.

The 1D electron energy spectrum assumes the form

$$k_z^2 = A_{32,\pm}(E, n_x, n_y), \tag{1.119}$$

where $A_{32,\pm}(E, n_x, n_y) = \alpha_{4,\pm}(n_x, n_y) + \beta_4 E \pm [\beta_5 E^2 + E\beta_{6,\pm}(n_x, n_y) + \beta_{7,\pm}(n_x, n_y)]^{\frac{1}{2}}$,

$$\alpha_{4,\pm}(n_x, n_y) = \left[2\left(\theta_3^2 - \theta_7^2\right)\right]^{-1}\left[2\theta_7\alpha_2(n_x, n_y) - 2\alpha_{1,\mp}(n_x, n_y)\theta_3\right],$$

$$\alpha_{1,\mp}(n_x, n_y) = \theta_1\left(\frac{n_x\pi}{d_x}\right)^2 + \theta_2\left(\frac{n_y\pi}{d_y}\right)^2 + \delta_4\left(\frac{n_x\pi}{d_x}\right) \mp \Delta_3,$$

$$\alpha_2(n_x, n_y) = \left[\theta_5\left(\frac{n_x\pi}{d_x}\right)^2 + \theta_6\left(\frac{n_y\pi}{d_y}\right)^2 + \delta_5\left(\frac{n_x\pi}{d_x}\right)\right],$$

$$\beta_4 = 2\theta_3\left[2\left(\theta_3^2-\theta_7^2\right)\right]^{-1},\quad \beta_5 = \left[2\left(\theta_3^2-\theta_7^2\right)\right]^{-2}\left[4\theta_7^2\right],$$

$$\beta_{6,\pm}(n_x,n_y) = \left[8\theta_3\theta_7\alpha_2(n_x,n_y) - 8\theta_7^2\alpha_{1,\mp}(n_x,n_y)\right]\left[2\left(\theta_3^2-\theta_7^2\right)\right]^{-1},$$

$$\beta_{7,\pm}(n_x,n_y) = \left[2(\theta_3^2-\theta_7^2)\right]^{-2}\left[4\theta_7^2\alpha_2^2(n_x,n_y) - 8\theta_7\theta_3\alpha_2(n_x,n_y)\alpha_{1,\mp}(n_x,n_y)\right.$$
$$\left. + 4\theta_3^2\alpha_3(n_y) + 4\theta_7^2\alpha_{1,\mp}(n_x,n_y) - 4\alpha_3(n_y)\theta_7^2\right],\quad \text{and}$$

$$\alpha_3(n_y) = G_3^2\left(\frac{n_y\pi}{d_y}\right)^2 + \Delta_3^2.$$

The quantized energy levels ($E_{34,\pm}$) can be expressed through the equation

$$E_{34,\pm} = \alpha_{1,\mp}(n_x,n_y) \pm [\alpha_2^2(n_x,n_y) + \alpha_3(n_y)]^{\frac{1}{2}}. \tag{1.120}$$

The electron concentration per unit length is given by

$$n_0 = \frac{g_v}{\pi}\sum_{n_x=1}^{n_{x\max}}\sum_{n_y=1}^{n_{y\max}}\left[B_{49}\left(E_{F1D},n_x,n_y\right) + B_{50}\left(E_{F1D},n_x,n_y\right)\right], \tag{1.121}$$

where $B_{49}\left(E_{F1D},n_x,n_y\right) = \left[\sqrt{A_{32,+}(E_{FID},n_x,n_y)} + \sqrt{A_{32,-}(E_{FID},n_x,n_y)}\right]$ and $B_{50}\left(E_{F1D},n_x,n_y\right) = \sum_{r=1}^{s_o} Z_{1D}(r)\left[B_{49}\left(E_{F1D},n_x,n_y\right)\right]$.

The field-emitted current assumes the form

$$I = \frac{g_v e k_B T}{h}\sum_{n_x=1}^{n_{x\max}}\sum_{n_y=1}^{n_{y\max}}[F_0(\eta_{32,+})\exp(-\beta_{32,+}) + F_0(\eta_{32,-})\exp(-\beta_{32,-})], \tag{1.122}$$

where $\eta_{32,\pm} = \frac{E_{F1D}-E_{34,\pm}}{k_B T}$, $\beta_{32,\pm} = \frac{4}{3}\left[A_{32,\pm}(V_0,n_x,n_y)\right]^{3/2}\cdot\left[eF_{sz}A'_{32,\pm}(V_0,n_x,n_y)\right]^{-1}$, and $A'_{32,\pm}(V_0,n_x,n_y) = \left[\beta_4 \pm \frac{1}{2}\left[2\beta_5 V_0 + \beta_{6,\pm}(n_x,n_y)\right].\left[\beta_5 V_0^2 + \beta_{6,\pm}(n_x,n_y)V_0 + \beta_{7,\pm}(n_x,n_y)\right]^{-\frac{1}{2}}\right]$.

1.3 Result and Discussions

Using (1.5) and (1.12) and taking the energy band constants as given in the Table 1.1, we have plotted the FNFE current from QWs of $CdGeAs_2$ (an example of nonlinear optical materials) as a function of d_y as shown by the dotted plot of Fig. 1.1, in which the plot corresponds to the solid line represents the same for the two-band model of Kane. Figure 1.2 exhibits the plot FNFE current from QWs of n-InSb as a function of film thickness in accordance with the three- and two-band models of

Kane together with the models of Stillman et al., Newson et al., and Palik et al., respectively for the purpose of assessing the influence of dispersion relations on the FNFE current from QWs of III–V semiconductors. Figure 1.3 exhibits the variation of the field-emitted current with electric field which is normal to the two directions of quantizations in the wavevector space of the material for all cases Fig. 1.2. Figure 1.4 presents the FNFE current as function of film thickness for two different

Table 1.1 The numerical values of the energy band constants of few materials

	Materials	Numerical values of the energy band constants
1	(a) The conduction electrons of n-Cadmium Germanium Arsenide can be described by three types of band models	1. The values of the energy band constants in accordance with the generalized electron dispersion relation of nonlinear optical materials (as given by (1.2)) are as follows: $E_{g_0} = 0.57\,\text{eV}$, $\Delta_{\parallel} = 0.30\,\text{eV}$, $\Delta_{\perp} = 0.36\,\text{eV}$, $m_{\parallel}^{*} = 0.034m_0$, $m_{\perp}^{*} = 0.039m_0$, $T = 4\,\text{K}$, $\delta = -0.21$ eV, $g_{\text{v}} = 1$ [47,225], $\varepsilon_{sc} = 18.4\varepsilon_0$[226] ($\varepsilon_{sc}$ and ε_0 are the permittivity of the semiconductor material and free space, respectively), and W(electron affinity) = 4eV [227–229]
		2. In accordance with the three-band model of Kane (as given by (1.13)), the spectrum constants are given by $\Delta = (\Delta_{\|\|} + \Delta_{\perp})/2 = 0.33\text{eV}$, $E_{g_0} = 0.57\text{eV}$, $m_c = (m_{\|\|}^{*} + m_{\perp}^{*})/2 = 0.0365m_0$, and $\delta = 0\text{eV}$
		3. In accordance with two-band model of Kane (as given by (1.19)), the spectrum constants are given by $E_{g_0} = 0.57\,\text{eV}$ and $m_c = 0.0365m_0$
	(b) The conduction electrons of n-Cadmium Arsenide can be described by three types of band models	1. The values of the energy band constants in accordance with the generalized electron dispersion relation of nonlinear optical materials (as given by (1.2)) are as follows: $\lvert E_{g_0}\rvert = 0.095\,\text{eV}$, $\Delta_{\parallel} = 0.27\,\text{eV}$, $\Delta_{\perp} = 0.25\,\text{eV}$, $m_{\parallel}^{*} = 0.00697m_0$, $m_{\perp}^{*} = 0.013933m_0$, $T = 4\,\text{K}$, $\delta = 0.085\,\text{eV}$, $g_{\text{v}} = 1$ [47,225], and $\varepsilon_{sc} = 16\varepsilon_0$ [227–229]
		2. In accordance with the three-band model of Kane (as given by (1.13)), the spectrum constants are given by $\Delta = \left(\Delta_{\|\|} + \Delta_{\perp}\right)/2 = 0.26\,\text{eV}$, $\left\lvert E_{g_0}\right\rvert = 0.095\,\text{eV}$, $m_c = \left(m_{\|\|}^{*} + m_{\perp}^{*}\right)/2 = 0.020903m_0$, and $\delta = 0\,\text{eV}$
		3. In accordance with two-band model of Kane (as given by (1.19)), the spectrum constants are given by $\left\lvert E_{g_0}\right\rvert = 0.095\,\text{eV}$ and $m_c = 0.020903m_0$
2	n-Indium Arsenide	The values $E_{g_0} = 0.36\,\text{eV}$, $\Delta = 0.43\,\text{eV}$, $m_c = 0.026m_0$,$g_{\text{v}} = 1$, $\varepsilon_{sc} = 12.25\varepsilon_0$ [103, 104], and $W = 5.06\,\text{eV}$ [230] are valid for three-band model of Kane as given by (1.13)
3	n-Gallium Arsenide	The values $E_{g_0} = 1.55\,\text{eV}$, $\Delta = 0.35\,\text{eV}$, $m_c = 0.07m_0$,$g_{\text{v}} = 1$, $\varepsilon_{sc} = 12.9\varepsilon_0$ [103, 104], and $W = 4.07\,\text{eV}$ [231] are valid for three-band model of Kane as given by (1.13). The values $a_{13} = -1.97 \times 10^{-37}\,\text{eVm}^4$ and $a_{15} = -2.3 \times 10^{-34}\,\text{eVm}^4$ [106] are valid for the Newson and Kurobe model [106] as given by (1.34)

(continued)

Table 1.1 (continued)

	Materials	Numerical values of the energy band constants
4	n-Gallium Aluminium Arsenide	$E_{g_0} = (1.424 + 1.266x + 0.26x^2)$eV, $\Delta = (0.34 - 0.5x)$eV, $g_v = 1$, $m_c = [0.066 + 0.088x]\, m_0$, $\varepsilon_{sc} = [13.18 - 3.12x]\, \varepsilon_0$ [232], and $W = (3.64 - 0.14x)$eV [233]
5	n-Mercury Cadmium Telluride	$E_{g_0} = (-0.302 + 1.93x + 5.35 \times 10^{-4}(1-2x)T - 0.810x^2 + 0.832x^3)$eV, $\Delta = \left(0.63 + 0.24x - 0.27x^2\right)$ eV, $m_c = 0.1 m_0 E_{g_0}(\text{eV})^{-1}$, $g_v = 1$, $\varepsilon_{sc} = \left[20.262 - 14.812x + 5.22795x^2\right] \varepsilon_0$ [234], and $W = \left(4.23 - 0.813\left(E_{g_0} - 0.083\right)\right)$ eV [235]
6	n-Indium Gallium Arsenide Phosphide lattice matched to Indium Phosphide	$E_{g_0} = \left(1.337 - 0.73y + 0.13y^2\right)$ eV, $\Delta = \left(0.114 + 0.26y - 0.22y^2\right)$ eV, $y = (0.1896 - 0.4052x)/(0.1896 - 0.0123x)$, $m_c = (0.08 - 0.039y)\, m_0$, $g_v = 1$, $\varepsilon_{sc} = [10.65 + 0.1320y]\, \varepsilon_0$, and [231] $W(x, y) = [5.06(1-x)\, y + 4.38(1-x)(1-y) + 3.64xy + 3.75\{x(1-y)\}]$ eV
7	n-Indium Antimonide	$E_{g_0} = 0.2352$ eV, $\Delta = 0.81$ eV, $m_c = 0.01359 m_0$, $g_v = 1$, $\varepsilon_{sc} = 15.56\varepsilon_0$ [103, 104], and $W = 4.72$ eV [230]
8	n-Gallium Antimonide	The values of $E_{g_0} = 0.81$ eV, $\Delta = 0.80$ eV, $P = 9.48 \times 10^{-10}$ eVm, $\bar{\varsigma}_0 = -2.1$, $\bar{v}_0 = -1.49$, $\bar{\omega}_0 = 0.42$, $g_v = 1$ [238], and $\varepsilon_{sc} = 15.85\varepsilon_0$ [239] are valid for the model of Seiler et al. [238] as given by (R1.5).)
9	n-Cadmium Sulphide	$m_{\|}^* = 0.7 m_0$, $m_{\perp}^* = 1.5 m_0$, $C_0 = 1.4 \times 10^{-8}$ eVm, $g_v = 1$ [103, 104], $\varepsilon_{sc} = 15.5\varepsilon_0$ [240], and $W = 4.5$ eV [230]
10	n-Lead Telluride	The values $m_t^- = 0.070 m_0, m_l^- = 0.54 m_0$, $m_t^+ = 0.010 m_0, m_l^+ = 1.4 m_0$, $P_{\|\|} = 141$ meVnm, $P_{\perp} = 486$ meVnm, $E_{g_0} = 190$ meV, $g_v = 4$ [103, 104], $\varepsilon_{sc} = 33\varepsilon_0$ [103, 104, 241], and $W = 4.6$ eV [242, 244] are valid for the Dimmock model [207] as given by (1.70)
		The values $m_1 = 0.0239 m_0, m_2 = 0.024 m_0, m_2' = 0.31 m_0$, and $m_3 = 0.24 m_0$ [243] are valid for the Cohen model [133] as given by (1.60)
11	Stressed n-Indium Antimonide	The values $m_c = 0.048 m_o$, $E_{g_0} = 0.081$ eV, $B_2 = 9 \times 10^{-10}$ eVm, $C_1 = 3$ eV, $C_2 = 2$eV, $\bar{a}_0 = -10$ eV, $\bar{b}_0 = -1.7$ eV, $\bar{d}_0 = -4.4$ eV, $S_{xx} = 0.6 \times 10^{-3}(\text{kbar})^{-1}$, $S_{yy} = 0.42 \times 10^{-3}(\text{kbar})^{-1}$, $S_{zz} = 0.39 \times 10^{-3}(\text{kbar})^{-1}$, $S_{xy} = 0.5 \times 10^{-3}(\text{kbar})^{-1}$, $\varepsilon_{xx} = \sigma S_{xx}$, $\varepsilon_{yy} = \sigma S_{yy}$, $\varepsilon_{zz} = \sigma S_{zz}$, $\varepsilon_{xy} = \sigma S_{xy}$, σ is the stress in kilobar, and $g_v = 1$ [208–211] are valid for the model of Seiler et al. [208–211] as given by (1.76)
12	Bismuth	$E_{g_0} = 0.0153$ eV, $m_1 = 0.00194 m_0$, $m_2 = 0.313 m_0$, $m_3 = 0.00246 m_0$, $m_2' = 0.36 m_0$, $g_v = 3$ [245, 246], $M_2 = 1.25 m_0$, $M_2' = 0.36 m_0$ [247], and $W = 4.34$ eV
13	Mercury Telluride	$m_v^* = 0.028 m_0$, $g_v = 1$, $\varepsilon_{\infty} = 15.2\varepsilon_0$ [248], and $W = 5.5$ eV [249]

(continued)

Table 1.1 (continued)

	Materials	Numerical values of the energy band constants
14	Platinum Antimonide	For valence bands, along the $\langle 100 \rangle$ direction, $\bar{\lambda}_0 = (0.02/4)\text{eV}$, $\bar{l} = (-0.32/4)\text{eV}$, $\bar{\nu} = (0.39/4)\text{eV}$, $\bar{n} = (-0.65/4)\text{eV}$, $\bar{a} = 0.643\,\text{nm}$, $I = 0.30\,(\text{eV})^2$, $\bar{\delta}_0 = 0.02\,\text{eV}$, $g_v = 6$ [214], $\varepsilon_{sc} = 30\varepsilon_0$ [250], and $\phi_w \approx 3.0\,\text{eV}$ [214, 251] For conduction bands, along the $\langle 111 \rangle$ direction, $g_v = 8$ [214, 251], $\bar{\lambda}_0 = (0.33/4)\text{eV}$, $\bar{l} = (1.09/4)\text{eV}$, $\bar{\nu} = (0.17/4)\text{eV}$, and $\bar{n} = (0.22/4)\text{eV}$
15	n-Gallium Phosphide	$m_{\|\|}^* = 0.92m_0$, $m_\perp^* = 0.25m_0$, $k_0 = 1.7 \times 10^{15}\,\text{m}^{-1}$, $\|V_G\| = 0.21\,\text{eV}$, $g_v = 6$ [213], and $W = 3.75\,\text{eV}$ [230]
16	Germanium	$E_{g_0} = 0.785\,\text{eV}$, $m_{\|\|}^* = 1.57m_0$, $m_\perp^* = 0.0807m_0$ [230], $W = 4.14\,\text{eV}$ [231], and $g_v = 4$
17	Tellurium	The values $\psi_1 = 6.7 \times 10^{-16}\,\text{meVm}^2$, $\psi_2 = 4.2 \times 10^{-16}\,\text{meVm}^2$, $\psi_3 = 6 \times 10^{-8}\,\text{meVm}$, and $\psi_4 = (3.6 \times 10^{-8}\,\text{meVm})$ [212] are valid for the model of Bouat et al. [212] as given by (1.81)
18	Graphite	The values $\bar{\Delta} = -0.0002\,\text{eV}$, $\bar{\gamma}_1 = 0.392\,\text{eV}$, $\bar{\gamma}_5 = 0.194\,\text{eV}$, $c_6 = 0.674\,\text{nm}$, $\bar{\gamma}_2 = -0.019\,\text{eV}$, $a_6 = 0.246\,\text{nm}$, $\bar{\gamma}_0 = 3\,\text{eV}$, $\bar{\gamma}_4 = 0.193\,\text{eV}$, $\bar{\gamma_3} = 0.21\,\text{eV}$ [252], and $W = 4.6\,\text{eV}$ [253] are valid for the model of Brandt et al. [252] as given by (R.1.12)
19	Lead Germanium Telluride	The values $g_v = 4$ [254] and $\phi_w \approx 6\,\text{eV}$ [255] are valid for the model of Vassilev [254] as given by (R.1.10)
20	Cadmium Antimonide	The values $a_1 = -32.3 \times 10^{-20}\,\text{eVm}^2$, $b_1 = -60.7 \times 10^{-20}\,\text{eVm}^2$, $a_2 = -16.3 \times 10^{-20}\,\text{eVm}^2$, $b_2 = -24.4 \times 10^{-20}\,\text{eVm}^2$, $a_3 = -91.9 \times 10^{-20}\,\text{eVm}^2$, $b_3 = -105 \times 10^{-20}\,\text{eVm}^2$, $A = 2.92 \times 10^{-10}\,\text{eVm}$, $B = -3.47 \times 10^{-10}\,\text{eVm}$, $G_3 = 1.3 \times 10^{-10}\,\text{eVm}$, $\Delta_3 = 0.070\,\text{eV}$ [222], and $\phi_w \approx 2\,\text{eV}$ [256]
21	Cadmium Diphosphide	The values $\beta_1 = 8.6 \times 10^{-21}\,\text{eVm}^2$, $\beta_2 = 1.8 \times 10^{-21}\,(\text{eVm})^2$, $\beta_4 = 0.0825\,\text{eV}$, $\beta_5 = -1.9 \times 10^{-19}\,\text{eVm}^2$ [257], and $\phi_w \approx 5\,\text{eV}$ [258] are valid for the model of Chuiko [257] and is given by (R.1.20)
22	Zinc Diphosphide	The values $\beta_1 = 8.7 \times 10^{-21}\,\text{eVm}^2$, $\beta_2 = 1.9 \times 10^{-21}\,(\text{eVm})^2$, $\beta_4 = 0.0875\,\text{eV}$, $\beta_5 = -1.9 \times 10^{-19}\,\text{eVm}^2$ [257], and $W \approx 3.9\,\text{eV}$ [258] are valid for the model of Chuiko [257] and is given by (R.1.20)
23	Bismuth Telluride	The values $E_{g_0} = 0.145\,\text{eV}$, $\bar{\alpha}_{11} = 4.9$, $\bar{\alpha}_{22} = 5.92$,$\bar{\alpha}_{33} = 9.5$, $\bar{\alpha}_{23} = 4.22$, $g_v = 6$ [215–217], and $\phi_w = 5.3\,\text{eV}$ [259] are valid for the model of Stordeur et al. [215–217] using (1.97)
24	Carbon Nanotube	The values $a_c = 0.144\,\text{nm}$ [260], $t_c = 2.7\,\text{eV}$ [261], $\bar{r}_0 = 0.7\,\text{nm}$ [262, 263], and $W = 3.2\,\text{eV}$ [265] are valid for graphene band structure realization of carbon nanotube [262, 263]

(continued)

Table 1.1 (continued)

	Materials	Numerical values of the energy band constants
25	Antimony	The values $\alpha_{11} = 16.7$, $\alpha_{22} = 5.98$, $\alpha_{33} = 11.61$, $\alpha_{23} = 7.54$ [265], and $W = 4.63$ eV are valid for the model of Ketterson [265] and are given by (R.1.13) and (R.1.14), respectively
26	Zinc Selenide	$m_{c2} = 0.16m_0$, $\Delta_2 = 0.42$ eV, $E_{g02} = 2.82$ eV [231], and $W = 3.2$ eV [266]
27	Lead Selenide	$m_t^- = 0.23m_0$, $m_l^- = 0.32m_0$, $m_t^+ = 0.115m_0$, $m_l^+ = 0.303m_0$, $P_{\|\|} \approx 138$ meVnm, $P_\perp = 471$ meVnm, $E_{g_0} = 0.28$ eV [267], $\varepsilon_{sc} = 21.0\varepsilon_0$ [231], and $W = 4.2$ eV [268]

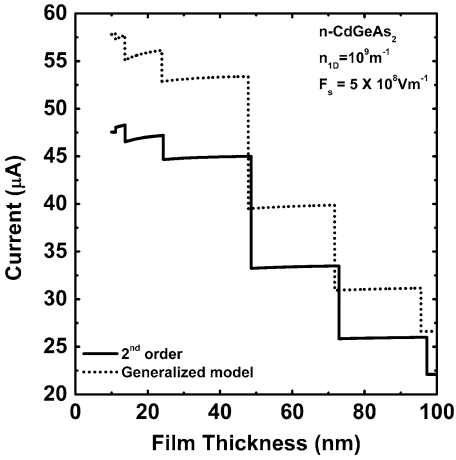

Fig. 1.1 Plot of the FN field emission current as a function of film thickness d_y for QWs of n − $CdGeAs_2$. The *dotted and solid curves* correspond to the generalized and the two-band models of Kane, respectively, where $d_z = 30$ nm

values of alloy composition for QWs of n − $Hg_{1-x}Cd_xTe$. Figure 1.5 shows the carrier concentration dependence of FNFE current from QWs of n − $Hg_{1-x}Cd_xTe$, n-InSb, n-InAs, and n-GaAs, respectively, for the purpose of assessing the influence of different energy band constants on the field-emitted current from QWs of III–V materials. In Fig. 1.6, exhibits the film thickness dependence of FNFE current from QWs of n − $In_{1-x}Ga_xAs_yP_{1-y}$ in accordance with the three- and two-band models of Kane together with the models of Stillman et al., Newson et al., and Palik et al., respectively. Figure 1.7 shows the dependence of FNFE current on alloy composition from QWs of ternary and quaternary materials in accordance with the two-band model of Kane. Figure 1.8 exhibits the film thickness dependence of FNFE current from QWs of II–VI materials taking p-CdS as an example. Figure 1.9 shows the FNFE current as a function of carrier concentration for the case of Fig. 1.8. In Fig. 1.10, we have plotted the FNFE current from QWs of Bismuth as a function of film thickness in accordance with the models of McClure and Choi, Hybrid, Cohen, and Lax, respectively. Figure 1.11 exhibits the variation of the FNFE current as a function of film thickness for QWs of stressed materials taking stressed n-InSb

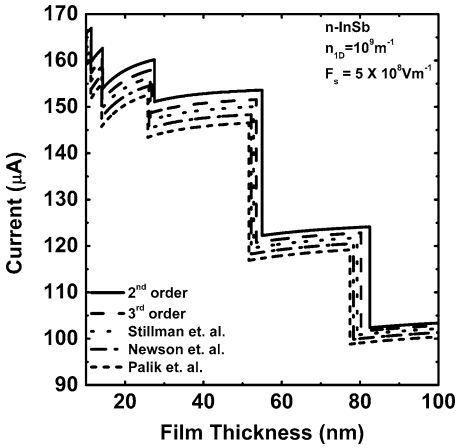

Fig. 1.2 Plot of the FN field emission current as a function of film thickness d_y for QWs of n-InSb in accordance with the three and two-band models of Kane together with the models of Stillman et al., Newson et al., and Palik et al., respectively, where $d_z = 30\,\text{nm}$

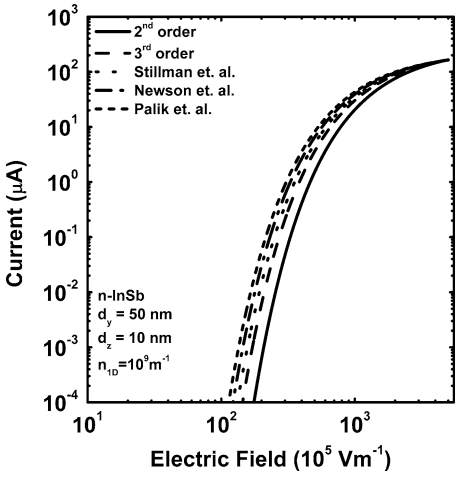

Fig. 1.3 Plot of the FN field emission current as a function of electric field for QWs of n-InSb in accordance with all the cases of Fig. 1.2

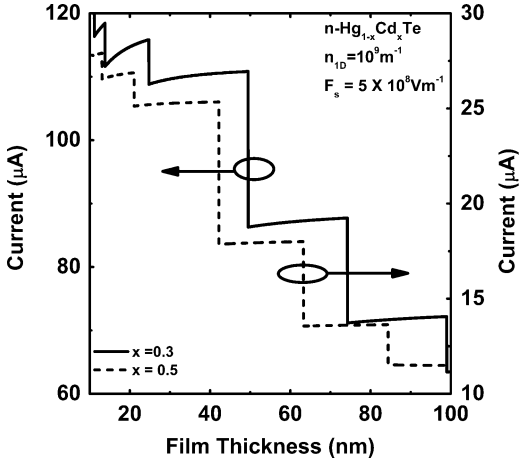

Fig. 1.4 Plot of the FN field emission current as a function of film thickness d_y for QWs of $n - Hg_{1-x}Cd_xTe$ in accordance with the two-band model of Kane for two different values of alloy composition

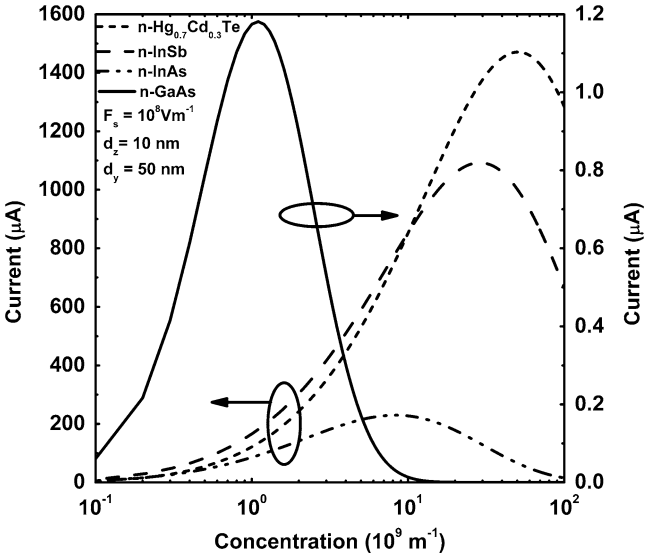

Fig. 1.5 Plot of the FN field emission current as a function of carrier concentration for QWs of n — $Hg_{0.7}Cd_{0.3}Te$, n-InSb, n-InAs, and n-GaAs in accordance with the two-band model of Kane at the lowest subband

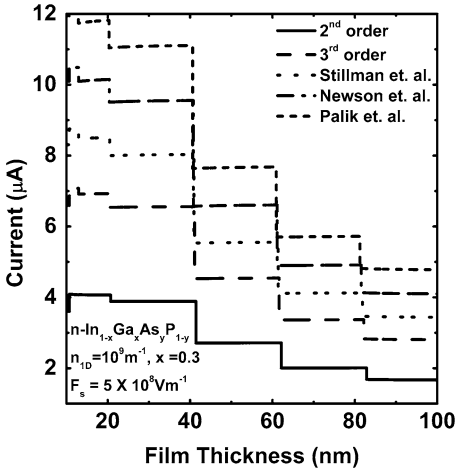

Fig. 1.6 Plot of the field current as a function of film thickness d_y for quantum wires of n — $In_{1-x}Ga_xAs_yP_{1-y}$ in accordance with the three- and two-band models of Kane together with the models of Stillman et al., Newson et al., and Palik et al. respectively, where $d_z = 30\,\text{nm}$

as an example. Figures 1.12 and 1.13 explore the stress dependence of the FNFE current from QWs of stressed n-InSb for different values of doping for the purpose of assessing the influence of carrier concentration on the field-emitted current in this case. In Fig. 1.14, the field-emitted current as a function of film thickness has been plotted for QWs of n-Ge (in accordance with both types of band models of n-Ge), n-GaP,Te, n-PbTe, and p — Bi_2Te_3, respectively. The plot (a) of Fig. 1.15 shows the

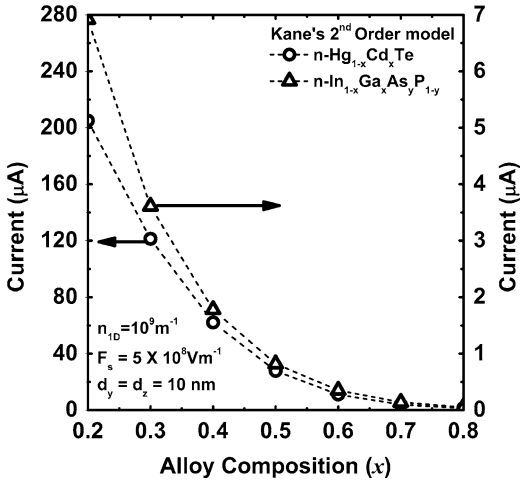

Fig. 1.7 Plot of the field-emitted current as a function of alloy composition for QWs of $n-Hg_{1-x}Cd_xTe$ and $In_{1-x}Ga_xAs_yP_{1-y}$ in accordance with the two-band model of Kane

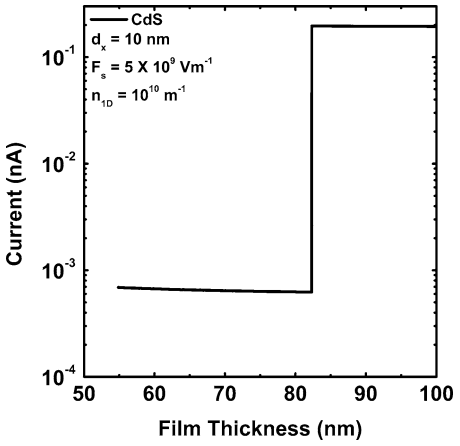

Fig. 1.8 Plot of the field-emitted current as a function of film thickness d_y for QWs of CdS

variation of FNFE current on the electric field for QWs of PbTe and Te, while (b) exhibits the same for QWs of Ge, GaP, and Bi_2Te_3, respectively.

The salient features of the above figures are described as follows:

From Fig. 1.1, we observe that the field emission current exhibits a step-functional decreasing dependence with increase in film thickness for QWs of $n-CdGeAs_2$. The combined influence of the anisotropies of the energy band constants and the crystal field splitting is to enhance the field-emitted current as compared with the same as obtained on the basis of two-band model of Kane in the whole range of thicknesses as considered in Fig. 1.1. The periodicity with respect to the film thickness is same in both the cases and is invariant of the energy band constants. It should be noted that the field-emitted current in general, is a product of two quantities inside the summation signs. One of them is $F_0(\eta_{ij})$, $(i = 1, 2, 3\ldots$ and $j = 1, 2, 3, \ldots)$ and the other one is $\exp(-\beta_{ij})$, where both of them are functions

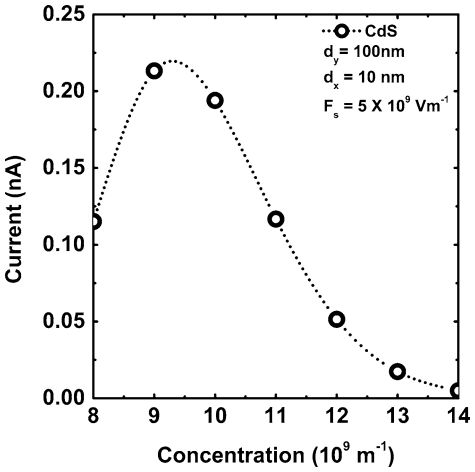

Fig. 1.9 Plot of the field-emitted current as a function of concentration for QWs of CdS

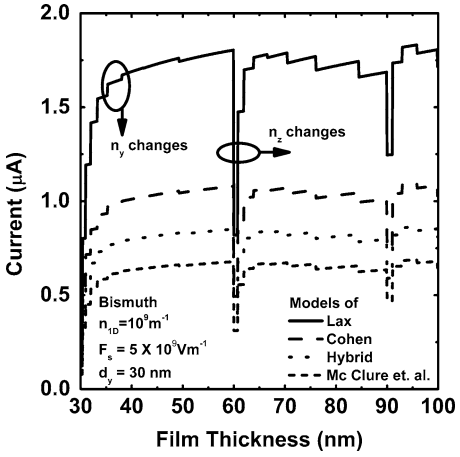

Fig. 1.10 Plot of the field-emitted current as a function of film thickness for QWs of Bi in accordance with the models of Mc Clure and Choi, Hybrid, Cohen, and Lax, respectively

of Fermi energy, effective mass, and various parameters of the system in a complex way. Thus, we observe that field-emitted current depends totally on the product of these two functions within the summation signs and a prefactor outside the summation signs. The product of these two functions ultimately determines the behavior of the field-emitted current. Although we know [247] that the Fermi energy of low-dimensional systems decreases with increasing size, one cannot be always certain that I will decrease with increasing film thickness due to the particular form of field-emitted current in case of QWs. If the rate of increase of $F_0(\eta_{ij})$ overcomes the rate of change of $\exp(-\beta_{ij})$, I will increase, whereas, for the opposite case, I will decrease. This important physical fact determines the magnitude of the field-emitted current and its dependence with respect to any other physical variable.

From Fig. 1.2, we observe that I decrease with increasing film thickness for the three- and two-band models of Kane together with the models of Stillman et al.,

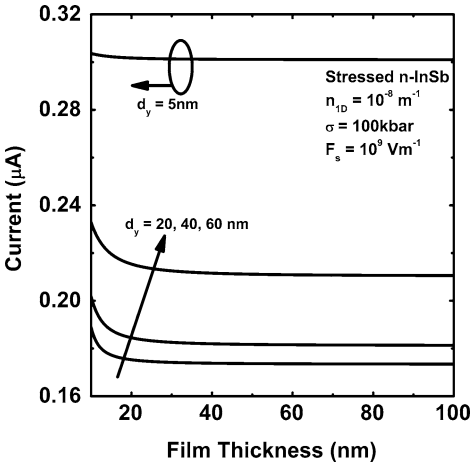

Fig. 1.11 Plot of the field-emitted current as a function of film thickness for QWs of stressed n-InSb for different values of d_y

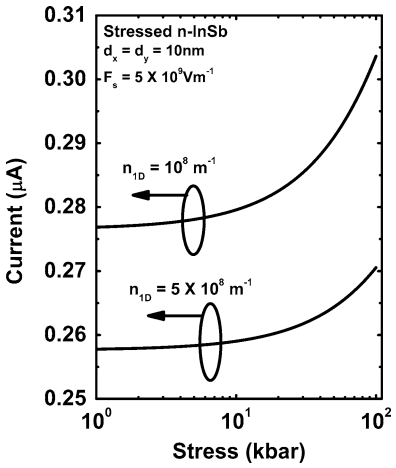

Fig. 1.12 Plot of the field-emitted current as a function of stress for QWs of stressed n-InSb for two different values of carrier concentration as shown

Newson et al., and Palik et al., respectively. The I exhibits different magnitudes which is the direct signature of the dispersion relation on the field-emitted current. Numerical computations reflect the fact that the field-emitted current for a $30 \times 10\,\mathrm{nm}^2$ size quantum wire can reach nearly $160\,\mu\mathrm{A}$ for n-InSb at low temperatures and at a field strength of $5 \times 10^8\,\mathrm{V\,m}^{-1}$ with carrier concentration of $10^9\,\mathrm{m}^{-1}$. From Fig. 1.3, it can be stated that field strength of nearly $10^7\,\mathrm{V\,m}^{-1}$ is sufficient to produce a tenth of microampers. Incidentally, due to the velocity saturation phenomena, we observe that beyond $10^8\,\mathrm{V\,m}^{-1}$, I saturates converging to a unique value and becomes invariant of dispersion relations. The field-emitted current from QWs of $\mathrm{n-Hg}_{1-x}\mathrm{Cd}_x$ Te as function of film thickness has been exhibited in Fig. 1.4 and can be compared with the corresponding cases of earlier figures. It appears that for lower values of film thickness, I increases for a particular subband. As thickness increases, generation of different subbands occurs which

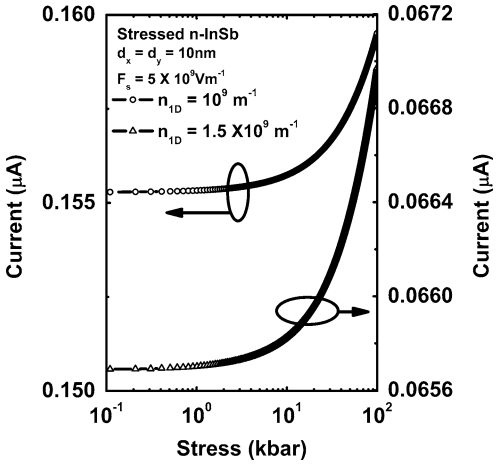

Fig. 1.13 Plot of the field-emitted current as a function of stress for QWs of stressed n-InSb for two different values of carrier concentration as shown

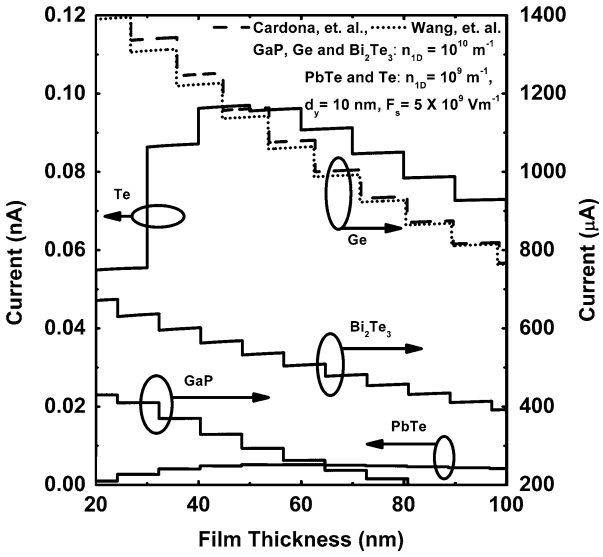

Fig. 1.14 Plot of the field-emitted current as a function of film thickness for QWs of Ge (in accordance with both types of band models), GaP, Bi_2Te_3, PbTe, and Te, respectively

leads to the overall decrease in I. The variation of I over a large range of carrier concentration has been plotted in Fig. 1.5 for the quantum limit case. It appears that I initially increases due to low value of Fermi energy, and as the concentration increases, the magnitude of the current decreases sharply exhibiting a peak. The amount of broadening is highly sensitive to the spectrum parameters of a particular semiconductor. It appears that for n-GaAs, the broadening is more as compared with others as shown in the figure. Figure. 1.6 exhibits the variation of I as function of

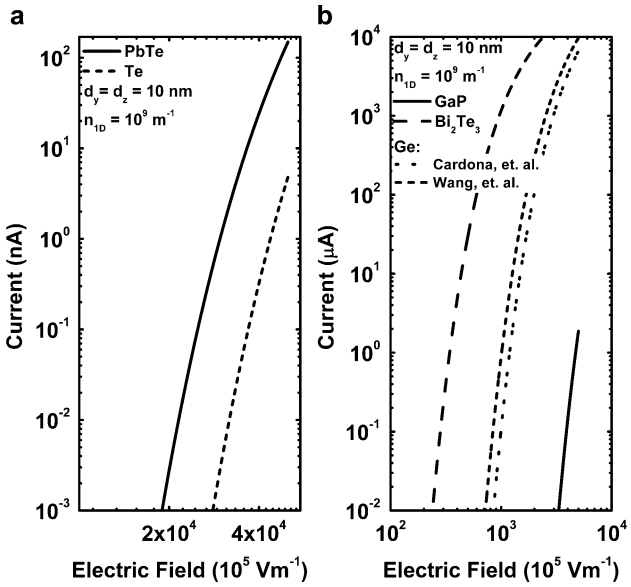

Fig. 1.15 Plot of the field current as a function of electric field for quantum wires of (**a**) PbTe and Te and (b) GaP, Bi_2Te_3, and Ge, respectively

film thickness for QWs of $n - In_{1-x}Ga_xAsP_{1-y}$ in accordance with the three- and two-band models of Kane together with the models of Stillman et al., Newson et al., and Palik et al. respectively. Figure. 1.6 shows almost a constant step-functional dependence of the current for a particular regime of film thickness for all types of band models. This implies that the difference in the Fermi energy and the quantized subband energy is almost invariant of film thickness. From Fig. 1.7, one observes that as alloy composition increases, the field-emitted current decreases for QWs of both ternary and quaternary compounds. For lower values of alloy composition, I from QWs of quaternary semiconductor is more than that of the corresponding ternary one, whereas for higher value of alloy composition, it converges. Step-functional dependence of field-emitted current with film thickness for QWs of CdS has been observed in Fig. 1.8. We note a nearly constant field-emitted current per subband, until a new subband is being occupied. Comparing with the earlier figures on the thickness dependence, we observe in this case an opposite trend because of the fact of overriding of the term $F_0(\eta_{ij})$ by $\exp(-\beta_{ij})$. Figure. 1.9 exhibits the fact that for p-CdS, the field current is of the order of a few nano amperes even at field strength of 5×10^9 V m^{-1}.

Composite oscillations in the field-emitted current from QWs of Bi with film thickness has been exhibited in Fig. 1.10 for the models of McClure and Choi, Hybrid, Cohen and Lax, respectively. We observe that for $n_z = 1$, electrons will be populated in the various other subbands corresponding to n_y. After a certain value of film thickness, when $n_z = 2$, the redistribution of the electrons in the quantized

energy levels is being repeated leading to a composite oscillations. It should be noted that this behavior is a general feature in thickness dependence of field emission from quantum wires. The energy band parameters determine the composite periodicity. The effect of film thickness on the field current in stressed InSb has been plotted in Fig. 1.11 in the quantum limit case, where the current decreases with increase in d_z for different values of d_y. For $d_y = 5\,\text{nm}$, the field-emitted current is highest although is an approximately a constant quantity with respect to d_z. We observe here that the product of the two terms namely $F_0(\eta_{ij})$ and $\exp(-\beta_{ij})$ becomes independent of d_z for large values.

The effect of stress on the field-emitted current has been exhibited in Figs. 1.12 and 1.13 for different values of carrier concentration. From Fig. 1.12, it appears that with the increase in stress, the current increases having a magnitude of few tenths of microamperes. With the increase in carrier degeneracy, the current almost reduces to about 10 times. From Fig. 1.14, we observe that the field current from QWs of Ge (in accordance with the models of Cardona et al. and Wang et al. respectively), Bi_2Te_3, and GaP decreases as film thickness increases because of the fact that the term $\exp(-\beta_{ij})$ dominates over the term $F_0(\eta_{ij})$ in the whole range of thickness as considered here. For QWs of PbTe and Te, the current initially increases since the term $\exp(-\beta_{\text{ij}})$ dominates over the term $F_0(\eta_{ij})$ and then decreases exhibiting the fact that the opposite dominancy exists. For QWs of Ge and Bi_2Te_3, the field current has been observed to be in theorder of hundreds of microampere, where as for other 1D systems as considered in this figures the currents are in the order of few nanoamperes exhibiting the influence of the carrier dispersion relation of a particular semiconductor. In Fig. 1.15 (a), the cut-in electric field for the field currents are in the order of $10^9\,\text{V m}^{-1}$ for QWs of PbTe and Te, while about 10^7–$10^8\,\text{V m}^{-1}$ field strength is sufficient for field current to reach few microamperes.

The influence of quantum confinement is immediately apparent from Figs. 1.1, 1.2, 1.4, 1.6, 1.8, 1.10, 1.11, and 1.14 since the field-emitted current depends strongly on the thickness of the quantum-confined materials in contrast with the corresponding bulk specimens. The current changes with increasing film thickness in an oscillatory way with different numerical magnitudes. It appears from the aforementioned figures that the FNFE exhibits spikes for particular values of film thickness which, in turn, depends on the particular band structure of the specific semiconductor. Moreover, the FNFE from QWs of different compounds can be smaller than of bulk specimens of the same materials, which is also a direct signature of quantum confinement. This oscillatory dependence will be less and less prominent with increasing film thickness. For bulk specimens of the same material, the FNFE will be found to increase continuously with increasing electron degeneracy in a non-oscillatory manner. The appearance of the discrete jumps in the respective figures is due to the redistribution of the electrons among the quantized energy levels when the size quantum number corresponding to the highest occupied level changes from one fixed value to the others.

With varying electron degeneracy, a change is reflected in the FNFE through the redistribution of the electrons among the size-quantized levels. It may be noted that at the transition zone from one subband to another, the height of the peaks

between any two subbands decreases with the increasing in the degree of quantum confinement and is clearly shown in all the curves. It should be noted that although, the FNFE changes in various manners with all the variables as evident from all the figures, the rates of variations are totally band structure dependent.

It is imperative to state that the present investigation excludes the many-body, hot electron, broadening, and the allied effects in the simplified theoretical formalism due to the absence of proper analytical techniques for including them for generalized systems as considered here. We have also approximated the variation of value of the work function from its bulk value in the present system. Our simplified approach will be appropriate for the purpose of comparisons when the methods of tackling the formidable problems after inclusion of the said effects for the generalized systems emerge. The results of this simplified approach get transformed to the well-known formulation of the FNFE for wide gap materials having parabolic energy bands. This indirect test not only exhibits the mathematical compatibility of the formulation but also shows the fact that this simple analysis is more generalized one, since one can obtain the corresponding results for materials having parabolic energy bands under certain limiting conditions from the present derivation. For the purpose of computer simulations for obtaining the plots of FNFE versus various external variables, we have taken very low temperatures since the quantization effects are basically low-temperature phenomena together with the fact that the temperature dependence of all the energy band constants of all the semiconductors and their nanostructures as considered in this chapter are not available in the literature. Our results as formulated in this chapter are valid for finite temperatures and are useful in comparing the results for temperature variations of FNFE after the availability of the temperature dependences of such constants of various dispersion relations in this context. The experimental results for the verification of theoretical formulations of FNFE are still not available in the literature. It is worth noting that the nature of the curves of field-emitted current with various physical variables based on our simplified formulations as presented here would be useful to analyze the experimental results when they materialize. The inclusion of the said effects would certainly increase the accuracy of the results although the qualitative features of FNFE would not change in the presence of the aforementioned effects.

It can be noted that on the basis of the dispersion relations of the various quantized structures as discussed above the effective electron mass,the Debye screening length,the plasma frequency, the activity coefficient, the carrier contribution to the elastic constants, the diffusion coefficient of minority carriers, the third-order nonlinear optical susceptibility, the heat capacity, the dia- and paramagnetic susceptibilities, and the various important dc/ac transport coefficients can be probed for all types of QWs as considered here. Thus, our theoretical formulation comprises the dispersion relation dependent properties of various technologically important quantum-confined semiconductors having different band structures. We have not considered other types of compounds in order to keep the presentation concise and succinct. With different sets of energy band parameters, we shall get different numerical values of the FNFE. The nature of variations of the FNFE as shown here would be similar for the other types of materials and the simplified analysis of

this chapter exhibits the basic qualitative features of the FNFE. It may be noted that the basic aim of this chapter is not solely to demonstrate the influence of quantum confinement on the FNFE for a wide class of quantized materials but also to formulate the appropriate carrier statistics in the most generalized form, since the transport and other phenomena in modern nanostructured devices having different band structures and the derivation of the expressions of many important carrier properties are based on the temperature-dependent carrier statistics in such systems. For the purpose of condensed presentation, the carrier statistics and the FNFE from different QWs as considered in this chapter have been presented in Table 1.2.

1.4 Open Research Problems

The problems under these sections of this monograph are by far the most important part and few open research problems from this chapter till end are being presented. The numerical values of the energy band constants for various semiconductors are given in Table 1.1 for the related computer simulations.

(R.1.1) Investigate the FNFE from all the bulk semiconductors whose respective dispersion relations of the carriers are given in this chapter by converting the summations over the quantum numbers to the corresponding integrations by including the uniqueness conditions in the appropriate cases and considering the effect of image force in the subsequent study in each case.

(R.1.2) Repeat R.1.1 for the bulk semiconductors whose respective dispersion relations of the carriers in the absence of any field are given below:

(a) The electron dispersion law in n-GaP can be written as [269]

$$E = \frac{\hbar^2 k_s^2}{2m_{||}^*} + \frac{\hbar^2 k_s^2}{2m_{\perp}^*} \mp \frac{\bar{\Delta}}{2} \pm \left[\left(\frac{\bar{\Delta}}{2} \right)^2 + P_1 k_z^2 + D_1 k_x^2 k_y^2 \right]^{1/2}, \qquad \text{(R1.1)}$$

where $\bar{\Delta} = 335\,\text{meV}$, $P_1 = 2\times10^{-10}\text{eVm}$, $D_1 = P_1 a_1$, and $a_1 = 5.4\times10^{-10}\text{m}$.

(b) In addition to the Cohen model, the dispersion relation for the conduction electrons for IV–VI semiconductors can also be described by the models of Bangert et al. [270] and Foley et al. [271], respectively.

1. In accordance with Bangert et al. [270], the dispersion relation is given by

$$\Gamma(E) = F_1(E) k_s^2 + F_2(E) k_z^2, \qquad \text{(R1.2)}$$

where $\Gamma(E) \equiv 2E$, $F_1(E) \equiv \dfrac{R_1^2}{E + E_g} + \dfrac{S_1^2}{E + \Delta_c'} + \dfrac{Q_1^2}{E + E_g}$,

Table 1.2 The carrier statistics and the Fowler–Nordheim field emission current from quantum wires of nonlinear optical, III–V, II–VI, Bismuth, IV–VI, stressed materials, Te, n-GaP, $PtSb_2$, Bi_2Te_3, n-Ge, GaSb, and II–V Compounds

Type of materials	The carrier statistics	The Fowler—Nordheim field emission current
1. Nonlinear optical materials	In accordance with the generalized electron dispersion relation as given by (1.2), $n_0 = \frac{2g_v}{\pi}\sum_{n_x=1}^{n_{x\max}}\sum_{n_y=1}^{n_{y\max}}[B_{11}(E_{F1D}, n_x, n_y) + B_{12}(E_{F1D}, n_x, n_y)]$ (1.5)	On the basis of (1.5), $I = \frac{2g_v e k_B T}{h}\sum_{n_x=1}^{n_{x\max}}\sum_{n_y=1}^{n_{y\max}} F_0(\eta_{11})\exp(-\beta_{11})$ (1.12)
2. III–V materials, the conduction electrons of which can be defined by five types of energy wave vector dispersion relations as described in the column of carrier statistics	(a) Three-band model of Kane: In accordance with the three-band model of Kane (1.13), which is the special case of (1.2) $n_0 = \frac{2g_v}{\pi}\sum_{n_x=1}^{n_{x\max}}\sum_{n_y=1}^{n_{y\max}}[B_{13}(E_{F1D}, n_x, n_y) + B_{14}(E_{F1D}, n_x, n_y)]$ (1.16)	On the basis of (1.16), $I = \frac{2g_v e k_B T}{h}\sum_{n_x=1}^{n_{x\max}}\sum_{n_y=1}^{n_{y\max}} F_0(\eta_{12})\exp(-\beta_{12})$ (1.18)
	(b) Two-band model of Kane: In accordance with the two-band model of Kane (1.19), $n_0 = \frac{2g_v}{\pi}\sum_{n_x=1}^{n_{x\max}}\sum_{n_y=1}^{n_{y\max}}[B_{15}(E_{F1D}, n_x, n_y) + B_{16}(E_{F1D}, n_x, n_y)]$ (1.22)	On the basis of (1.22), $I = \frac{2g_v e k_B T}{h}\sum_{n_x=1}^{n_{x\max}}\sum_{n_y=1}^{n_{y\max}} F_0(\eta_{13})\exp(-\beta_{13})$ (1.24)
	(c) The model of Stillman et al.: In accordance with the model of Stillman et al. (1.28), $n_0 = \frac{2g_v}{\pi}\sum_{n_x=1}^{n_{x\max}}\sum_{n_y=1}^{n_{y\max}}[B_{17}(E_{F1D}, n_x, n_y) + B_{18}(E_{F1D}, n_x, n_y)]$ (1.32)	On the basis of (1.32), $I = \frac{2g_v e k_B T}{h}\sum_{n_x=1}^{n_{x\max}}\sum_{n_y=1}^{n_{y\max}} F_0(\eta_{15})\exp(-\beta_{15})$ (1.33)
	(d) The model of Newson and Kurobe: In accordance with the model of Newson and Kurobe (1.34), $n_0 = \frac{2g_v}{\pi}\sum_{n_x=1}^{n_{x\max}}\sum_{n_y=1}^{n_{y\max}}[B_{19}(E_{F1D}, n_x, n_y) + B_{20}(E_{F1D}, n_x, n_y)]$ (1.37)	On the basis of (1.37), $I = \frac{2g_v e k_B T}{h}\sum_{n_x=1}^{n_{x\max}}\sum_{n_y=1}^{n_{y\max}} F_0(\eta_{16})\exp(-\beta_{16})$ (1.39)

	(e) The model of Palik et al.: In accordance with the model of Palik et al. (1.40), $n_0 = \frac{2g_v}{\pi} \sum_{n_x=1}^{n_{x\max}} \sum_{n_y=1}^{n_{y\max}} [B_{21}(E_{F1D}, n_x, n_y) + B_{22}(E_{F1D}, n_x, n_y)]$ (1.43)	On the basis of (1.43), $I = \frac{2g_v e k_B T}{h} \sum_{n_x=1}^{n_{x\max}} \sum_{n_y=1}^{n_{y\max}} F_0(\eta_{16}) \exp(-\beta_{16})$ (1.44)
3. II–VI materials as described by the Hopfield model	In accordance with (1.46), $n_{1D} = \frac{g_v}{\pi\sqrt{B_0}} \sum_{n_x=1}^{n_{x\max}} \sum_{n_y=1}^{n_{y\max}} [t_7(E_{F1D}, n_x, n_y) + t_8(E_{F1D}, n_x, n_y)]$ (1.49)	On the basis of (1.49), $I = \frac{e g_v k_B T}{h} \sum_{n_x=1}^{n_{x\max}} \sum_{n_y=1}^{n_{y\max}} \left[\left\{ F_0 \left\{ (k_B T)^{-1} [E_{F1D} - [G_{3,+}(n_x, n_y)]] \right\} \exp\left(-\overline{\beta}_{016,+}\right) \right\} + F_0 \left\{ (k_B T)^{-1} \left[E_{F1D} - [G_{3,-}(n_x, n_y)] \right] \right\} \times \exp\left(-\overline{\beta}_{016,-}\right) \right]$ (1.48)
4. Bismuth, the carriers of which can be defined by four types of energy band models as described in the column of carrier statistics	(a) The McClure and Choi model: In accordance with (1.50), $n_{1D} = \frac{2g_v}{\pi} \frac{\sqrt{2m_1}}{\hbar} \sum_{n_y=1}^{n_{y\max}} \sum_{n_z=1}^{n_{z\max}} [t_{27}(E_{F1D}, n_y, n_z) + t_{28}(E_{F1D}, n_y, n_z)]$ (1.52)	On the basis of (1.52), $I = \frac{2g_v e k_B T}{h} \sum_{n_z=1}^{n_{z\max}} \sum_{n_y=1}^{n_{y\max}} F_0(\eta_{17}) \exp(-\beta_{17})$ (1.53)
	(b) The Hybrid model: In accordance with (1.55), $n_{1D} = \frac{2g_v}{\pi} \frac{\sqrt{2m_1}}{\hbar} \sum_{n_y=1}^{n_{y\max}} \sum_{n_z=1}^{n_{z\max}} \left[t_{31}(E_{F1D}, n_y, n_z) + t_{32}(E_{F1D}, n_y, n_z) \right]$ (1.57)	On the basis of (1.57), $I = \frac{2g_v e k_B T}{h} \sum_{n_z=1}^{n_{z\max}} \sum_{n_y=1}^{n_{y\max}} F_0(\eta_{18}) \exp(-\beta_{18})$ (1.58)
	(c) The Cohen model: In accordance with (1.60), $n_{1D} = \frac{2g_v}{\pi} \frac{\sqrt{2m_1}}{\hbar} \sum_{n_y=1}^{n_{y\max}} \sum_{n_z=1}^{n_{z\max}} \left[t_{35}(E_{F1D}, n_y, n_z) + t_{36}(E_{F1D}, n_y, n_z) \right]$ (1.62)	On the basis of (1.62), $I = \frac{2g_v e k_B T}{h} \sum_{n_z=1}^{n_{z\max}} \sum_{n_y=1}^{n_{y\max}} F_0(\eta_{19}) \exp(-\beta_{19})$ (1.63)
	(d) The Lax model: In accordance with (1.65), $n_{1D} = \frac{2g_v}{\pi} \frac{\sqrt{2m_1}}{\hbar} \sum_{n_y=1}^{n_{y\max}} \sum_{n_z=1}^{n_{z\max}} \left[t_{37}(E_{F1D}, n_y, n_z) + t_{38}(E_{F1D}, n_y, n_z) \right]$ (1.67)	On the basis of (1.67), $I = \frac{2g_v e k_B T}{h} \sum_{n_z=1}^{n_{z\max}} \sum_{n_y=1}^{n_{y\max}} F_0(\eta_{20}) \exp(-\beta_{20})$ (1.68)

(continued)

Table 1.2 (Continued)

Type of materials	The carrier statistics	The Fowler—Nordheim field emission current
5. IV–VI materials, the carriers of which can be defined by the model of Dimmock	In accordance with the model of Dimmock (1.70), $$n_0 = \frac{2g_v}{\pi}\sum_{n_x=1}^{n_{x\max}}\sum_{n_y=1}^{n_{y\max}}[B_{32}(E_{F1D}, n_x, n_y) + B_{33}(E_{F1D}, n_x, n_y)] \quad (1.73)$$	On the basis of (1.73), $$I = \frac{2g_v e k_B T}{h}\sum_{n_x=1}^{n_{x\max}}\sum_{n_y=1}^{n_{y\max}} F_0(\eta_{22})\exp(-\beta_{22}) \quad (1.74)$$
6. Stressed materials, as defined by the model of Seiler et al.	In accordance with (1.76), $$n_{1D} = \frac{2g_v}{\pi}\sum_{n_y=1}^{n_{y\max}}\sum_{n_z=1}^{n_{z\max}}[B_{34}(E_{F1D}, n_y, n_z) + B_{35}(E_{F1D}, n_y, n_z)] \quad (1.79)$$	On the basis of (1.80), $$I = \frac{2g_v e k_B T}{h}\sum_{n_x=1}^{n_{x\max}}\sum_{n_y=1}^{n_{y\max}} F_0(\eta_{23})\exp(-\beta_{23}) \quad (1.80)$$
7. Tellurium the conduction electrons of which can be defined by the model of Bouat et al	In accordance with (1.81), $$n_0 = \frac{g_v}{\pi}\sum_{n_x=1}^{n_{x\max}}\sum_{n_y=1}^{n_{y\max}}[B_{36,\pm}(E_{F1D}, n_x, n_y) + B_{37,\pm}(E_{F1D}, n_x, n_y)] \quad (1.84)$$	On the basis of (1.84), $$I = \frac{g_v e k_B T}{h}\sum_{n_x=1}^{n_{x\max}}\sum_{n_y=1}^{n_{y\max}}[F_0(\eta_{24,+})\exp(-\beta_{24,+}) + F_0(\eta_{24,-})\exp(-\beta_{24,-})] \quad (1.85)$$
8. n-GaP as described by the Rees model	In accordance with (1.86), $$n_0 = \frac{2g_v}{\pi}\sum_{n_x=1}^{n_{x\max}}\sum_{n_y=1}^{n_{y\max}}[B_{38}(E_{F1D}, n_x, n_y) + B_{39}(E_{F1D}, n_x, n_y)] \quad (1.89)$$	On the basis of (1.89), $$I = \frac{2g_v e k_B T}{h}\sum_{n_x=1}^{n_{x\max}}\sum_{n_y=1}^{n_{y\max}}[F_0(\eta_{26})\exp(-\beta_{26})] \quad (1.89)$$
9. $PtSb_2$, as defined by the Emtage model	In accordance with (1.91), $$n_0 = \frac{2g_v}{\pi}\sum_{n_x=1}^{n_{x\max}}\sum_{n_y=1}^{n_{y\max}}[B_{40}(E_{F1D}, n_x, n_y) + B_{41}(E_{F1D}, n_x, n_y)] \quad (1.94)$$	On the basis of (1.94), $$I = \frac{2g_v e k_B T}{h}\sum_{n_x=1}^{n_{x\max}}\sum_{n_y=1}^{n_{y\max}}[F_0(\eta_{27})\exp(-\beta_{27})] \quad (1.95)$$
10. Bi_2Te_3, which follows the model of Stordeur et al.	In accordance with (1.97), $$n_0 = \frac{2g_v}{\pi}\sum_{n_z=1}^{n_{z\max}}\sum_{n_y=1}^{n_{y\max}}[B_{42}(E_{F1D}, n_z, n_y) + B_{43}(E_{F1D}, n_z, n_y)] \quad (1.100)$$	On the basis of (1.100), $$I = \frac{2g_v e k_B T}{h}\sum_{n_z=1}^{n_{z\max}}\sum_{n_y=1}^{n_{y\max}}[F_0(\eta_{28})\exp(-\beta_{28})] \quad (1.101)$$

11. n-Ge, the conduction electrons of which can be defined by two types of energy band models as described in the column of carrier statistics	(a) In accordance with the model of Cardona et al. (1.102), $n_0 = \frac{2g_v}{\pi} \sum_{n_x=1}^{n_{x\max}} \sum_{n_z=1}^{n_{z\max}} [B_{44}(E_{F1D}, n_x, n_z) + B_{45}(E_{F1D}, n_x, n_z)]$ (1.105)	On the basis of (1.105), $I = \frac{2g_v e k_B T}{h} \sum_{n_x=1}^{n_{x\max}} \sum_{n_z=1}^{n_{z\max}} [F_0(\eta_{29}) \exp(-\beta_{29})]$ (1.106)
	(b) In accordance with the model of Wang and Ressler (1.107), $n_0 = \frac{2g_v}{\pi} \sum_{n_x=1}^{n_{x\max}} \sum_{n_z=1}^{n_{z\max}} [B_{46}(E_{F1D}, n_x, n_z) + B_{47}(E_{F1D}, n_x, n_z)]$ (1.110)	On the basis of (1.110), $I = \frac{2g_v e k_B T}{h} \sum_{n_x=1}^{n_{x\max}} \sum_{n_z=1}^{n_{z\max}} [F_0(\eta_{30}) \exp(-\beta_{30})]$ (1.111)
12. Gallium Antimonide, the carriers of which can be defined by the model of Mathur et al.	In accordance with (1.112), $n_0 = \frac{2g_v}{\pi} \sum_{n_x=1}^{n_{x\max}} \sum_{n_y=1}^{n_{y\max}} [B_{48}(E_{F1D}, n_x, n_y) + B_{49}(E_{F1D}, n_x, n_y)]$	On the basis of (1.116), $I = \frac{2g_v e k_B T}{h} \sum_{n_x=1}^{n_{x\max}} \sum_{n_y=1}^{n_{y\max}} [F_0(\eta_{31}) \exp(-\beta_{31})]$ (1.117)
13. II–V materials, as defined by the model of Yamada	In accordance with (1.118), $n_0 = \frac{g_v}{\pi} \sum_{n_x=1}^{n_{x\max}} \sum_{n_y=1}^{n_{y\max}} [B_{49}(E_{F1D}, n_x, n_y) + B_{50}(E_{F1D}, n_x, n_y)]$ (1.121)	On the basis of (1.121), $I = \frac{g_v e k_B T}{h} \sum_{n_x=1}^{n_{x\max}} \sum_{n_y=1}^{n_{y\max}} [F_0(\eta_{32,+}) \exp(-\beta_{32,+}) + F_0(\eta_{32,-}) \exp(-\beta_{32,-})]$ (1.122)

$$F_2(E) \equiv \frac{2C_5^2}{E+E_g} + \frac{(S_1+Q_1)^2}{E+\Delta_c''},$$

$$R_1^2 = 2.3\times10^{-19}\,(\text{eVm})^2,\ C_5^2 = 0.83\times10^{-19}\,(\text{eVm})^2,\ Q_1^2 = 1.3R_1^2,\ S_1^2 = 4.6R_1^2,$$

$\Delta_c' = 3.07$ eV, $\Delta_c'' = 3.28$ eV, and $g_v = 4$. It may be noted that under the substitution $S_1 = 0$, $Q_1 = 0$, $R_1^2 \equiv \dfrac{\hbar^2 E_g}{m_\perp^*}$, $C_5^2 \equiv \dfrac{\hbar^2 E_g}{2m_{||}^*}$, (R1.2) assumes the form $E(1+\alpha E) = \dfrac{\hbar^2 k_s^2}{2m_\perp^*} + \dfrac{\hbar^2 k_z^2}{2m_{||}^*}$, which is the simplified Lax model.

2. The carrier energy spectrum of IV–VI semiconductors in accordance with Foley et al. [271] can be written as

$$E + \frac{E_g}{2} = E_-(k) + \left[\left[E_+(k) + \frac{E_g}{2}\right]^2 + P_\perp^2 k_s^2 + P_{||}^2 k_z^2\right]^{1/2}, \quad \text{(R1.3)}$$

where $E_+(k) = \dfrac{\hbar^2 k_s^2}{2m_\perp^+} + \dfrac{\hbar^2 k_z^2}{2m_{||}^+}$, $E_-(k) = \dfrac{\hbar^2 k_s^2}{2m_\perp^-} + \dfrac{\hbar^2 k_z^2}{2m_{||}^-}$ represents the contribution from the interaction of the conduction and the valance band edge states with the more distant bands and the free electron term, $1/m_\perp^\pm = \dfrac{1}{2}[1/m_{tc} \pm 1/m_{tv}]$, $\dfrac{1}{m_{||}^\pm} = \dfrac{1}{2}\left[\dfrac{1}{m_{1c}} \pm \dfrac{1}{m_{1v}}\right]$. For n-PbTe, $P_\perp = 4.61\times10^{-10}$ eVm, $P_{||} = 1.48\times10^{-10}$ eVm, $m_0/m_{tv} = 10.36$, $m_0/m_{1v} = 0.75$, $m_0/m_{tc} = 11.36$, $m_0/m_{1c} = 1.20$, and $g_v = 4$.

(c) The hole energy spectrum of p-type zero-gap semiconductors (e.g., HgTe) is given by [272]

$$E = \frac{\hbar^2 k^2}{2m_v^*} + \frac{3e^2}{128\varepsilon_\infty}k - \left(\frac{2E_B}{\pi}\right)\ln\left|\frac{k}{k_0}\right|, \quad \text{(R1.4)}$$

where m_v^* is the effective mass of the hole at the top of the valence band, ε_∞ is the semiconductor permittivity in the high-frequency limit, $E_B \equiv m_0e^2/2\hbar^2\varepsilon_\infty^2$, and $k_0 \equiv m_0e^2/\hbar^2\varepsilon_\infty$.

(d) The conduction electrons of n-GaSb obey the following two dispersion relations:

1. In accordance with the model of Seiler et al. [238]

$$E = \left[-\frac{E_g}{2} + \frac{E_g}{2}\left[1+\alpha_4 k^2\right]^{1/2} + \frac{\bar{\varsigma}_0\hbar^2k^2}{2m_o} + \frac{\bar{v}_0 f_1(k)\hbar^2}{2m_o} \pm \frac{\bar{\omega}_0 f_2(k)\hbar^2}{2m_o}\right], \quad \text{(R1.5)}$$

where $\alpha_4 \equiv 4P^2\left(E_g + \frac{2}{3}\Delta\right)\left[E_g^2\left(E_g + \Delta\right)\right]^{-1}$, P is the isotropic momentum matrix element, $f_1(k) \equiv k^{-2}\left[k_x^2k_y^2 + k_y^2k_z^2 + k_z^2k_x^2\right]$ represents the warping of the Fermi surface, $f_2(k) \equiv \left[\left\{k^2\left(k_x^2k_y^2 + k_y^2k_z^2 + k_z^2k_x^2\right) - 9k_x^2k_y^2k_z^2\right\}^{1/2} k^{-1}\right]$ represents the inversion asymmetry splitting of the conduction band, and $\bar{\varsigma}_0$, $\bar{\nu}_0$, and $\bar{\omega}_0$ represent the constants of the electron spectrum in this case.

2. In accordance with the model of Zhang et al. [273]

$$E = \left[E_2^{(1)} + E_2^{(2)}K_{4,1}\right]k^2 + \left[E_4^{(1)} + E_4^{(2)}K_{4,1}\right]k^4 + k^6\left[E_6^{(1)} + E_6^{(2)}K_{4,1} + E_6^{(3)}K_{6,1}\right], \tag{R1.6}$$

where $K_{4,1} \equiv \frac{5}{4}\sqrt{21}\left[\frac{k_x^4 + k_y^4 + k_z^4}{k^4} - \frac{3}{5}\right]$,

$K_{6,1} \equiv \sqrt{\frac{639639}{32}}\left[\frac{k_x^2k_y^2k_z^2}{k^6} + \frac{1}{22}\left(\frac{k_x^4 + k_y^4 + k_z^4}{k^4} - \frac{3}{5}\right) - \frac{1}{105}\right]$, the coefficients are in eV, the values of k are $10\left(\frac{a}{2\pi}\right)$times those of k in atomic units (a is the lattice constant), $E_2^{(1)} = 1.0239620$, $E_2^{(2)} = 0$, $E_4^{(1)} = -1.1320772$, $E_4^{(2)} = 0.05658$, $E_6^{(1)} = 1.1072073$, $E_6^{(2)} = -0.1134024$, and $E_6^{(3)} = -0.0072275$.

(e) In addition to the well-known band models as discussed in this monograph, the conduction electrons of III–V semiconductors obey the following three dispersion relations:

1. In accordance with the model of Rossler [274]

$$E = \frac{\hbar^2k^2}{2m^*} + \bar{\alpha}_{10}k^4 + \bar{\beta}_{10}\left[k_x^2k_y^2 + k_y^2k_z^2 + k_z^2k_x^2\right] \pm \bar{\gamma}_{10}\left[k^2\left(k_x^2k_y^2 + k_y^2k_z^2 + k_z^2k_x^2\right) - 9k_x^2k_y^2k_z^2\right]^{1/2}, \tag{R1.7}$$

where $\bar{\alpha}_{10} = \bar{\alpha}_{11} + \bar{\alpha}_{12}k$, $\bar{\beta}_{10} = \bar{\beta}_{11} + \bar{\beta}_{12}k$, and $\bar{\gamma}_{10} = \bar{\gamma}_{11} + \bar{\gamma}_{12}k$, in which $\bar{\alpha}_{11} = -2132 \times 10^{-40}\,\mathrm{eVm}^4$, $\bar{\alpha}_{12} = 9030 \times 10^{-50}\,\mathrm{eVm}^5$, $\bar{\beta}_{11} = -2493 \times 10^{-40}\,\mathrm{eVm}^4$, $\bar{\beta}_{12} = 12594 \times 10^{-50}\,\mathrm{eVm}^5$, $\bar{\gamma}_{11} = 30 \times 10^{-30}\,\mathrm{eVm}^3$, and $\bar{\gamma}_{12} = -154 \times 10^{-42}\,\mathrm{eVm}^4$.

2. In accordance with Johnson and Dickey [275], the electron energy spectrum assumes the form

$$E = -\frac{E_g}{2} + \frac{\hbar^2 k^2}{2}\left[\frac{1}{m_0} + \frac{1}{m_{\gamma b}}\right] + \frac{E_g}{2}\left[1 + 4\frac{\hbar^2 k^2}{2m_c'}\frac{\bar{f}_1(E)}{E_g}\right]^{1/2}, \quad \text{(R1.8)}$$

where $\frac{m_0}{m_c'} \equiv P^2\left[\frac{\left(E_g + \frac{2\Delta}{3}\right)}{E_g(E_g + \Delta)}\right]$, $\bar{f}_1(E) \equiv \frac{(E_g + \Delta)\left(E + E_g + \frac{2\Delta}{3}\right)}{\left(E_g + \frac{2\Delta}{3}\right)(E + E_g + \Delta)}$, $m_c' = 0.139 m_0$, and $m_{\gamma b} = \left[\frac{1}{m_c'} - \frac{2}{m_0}\right]^{-1}$.

3. In accordance with Agafonov et al. [276], the electron energy spectrum can be written as

$$E = \frac{\bar{\eta} - E_g}{2}\left[1 - \frac{\hbar^2 k^2}{2\bar{\eta} m^*}\left\{\frac{D\sqrt{3} - 3\overline{B}}{2\left(\frac{\hbar^2}{2m^*}\right)}\right\}\left[\frac{k_x^4 + k_y^4 + k_z^4}{k^4}\right]\right], \quad \text{(R1.9)}$$

where $\bar{\eta} \equiv (E_g^2 + (8/3)P^2k^2)^{1/2}$, $\overline{B} \equiv -21\frac{\hbar^2}{2m_0}$, and $D \equiv -40\left(\frac{\hbar^2}{2m_0}\right)$.

(f) The dispersion relation of the carriers in n-type $Pb_{1-x}Ga_xTe$ with $x = 0.01$ can be written following Vassilev [254] as

$$\left[E - 0.606k_s^2 - 0.0722k_z^2\right]\left[E + \overline{E}_g + 0.411k_s^2 + 0.0377k_z^2\right] = 0.23k_s^2 + 0.02k_z^2 \pm \left[0.06\overline{E}_g + 0.061k_s^2 + 0.0066k_z^2\right]k_s \quad \text{(R1.10)}$$

where $\overline{E}_g (= 0.21\,\text{eV})$ is the energy gap for the transition point, the zero of the energy E is at the edge of the conduction band of the Γ point of the Brillouin zone and is measured positively upwards, k_x, k_y, and k_z are in the units of 10^9m^{-1}.

(g) The energy spectrum of the carriers in the two higher valance bands and the single lower valance band of Te can, respectively, be expressed as [277]

$$\overline{E} = A_{10}k_z^2 + B_{10}k_s^2 \pm \left[\Delta_{10}^2 + (\beta_{10}k_z)^2\right]^{1/2} \text{ and } \overline{E} = \Delta_{||} + A_{10}k_z^2 + B_{10}k_s^2 \pm \beta_{10}k_z, \quad \text{(R1.11)}$$

where $\overline{E}$ is the energy of the hole as measured from the top of the valance and within it, $A_{10} = 3.77 \times 10^{-19}\,\text{eVm}^2$, $B_{10} = 3.57 \times 10^{-19}\,\text{eVm}^2$, $\Delta_{10} = 0.628\,\text{eV}$, $(\beta_{10})^2 = 6 \times 10^{-20}\,(\text{eVm})^2$, and $\Delta_{||} = 1004 \times 10^{-5}\,\text{eV}$ are the spectrum constants.

(h) The dispersion relation for the electrons in graphite can be written following Brandt [252] as

$$E = \frac{1}{2}[E_2 + E_3] \pm \left[\frac{1}{4}(E_2 - E_3)^2 + \eta_2^2 k^2\right]^{1/2}, \tag{R1.12}$$

where $E_2 \equiv \bar{\Delta} - 2\bar{\gamma}_1 \cos\phi_0 + 2\bar{\gamma}_5 \cos^2\phi_0, \phi_0 \equiv c_6 k_z/2, E_3 \equiv 2\bar{\gamma}_2 \cos^2\phi_0$, and $\eta_2 \equiv \left(\frac{\sqrt{3}}{2}\right) a_6(\bar{\gamma}_0 + 2\bar{\gamma}_4 \cos\phi_0)$in which the band constants are $\bar{\Delta}$, $\bar{\gamma}_0$, $\bar{\gamma}_1, \bar{\gamma}_2, \bar{\gamma}_4, \bar{\gamma}_5, a_6$, and c_6, respectively.

(i) The dispersion relation of the conduction electrons in Antimony (Sb) in accordance with Ketterson [265] can be written as

$$2m_0 E = \alpha_{11} p_x^2 + \alpha_{22} p_y^2 + \alpha_{33} p_z^2 + 2\alpha_{23} p_y p_z \tag{R1.13}$$

and

$$2m_0 E = a_1 p_x^2 + a_2 p_y^2 + a_3 p_z^2 + a_4 p_y p_z \pm a_5 p_x p_z \pm a_6 p_x p_y, \tag{R1.14}$$

where $a_1 = \frac{1}{4}(\alpha_{11} + 3\alpha_{22})$, $a_2 = \frac{1}{4}(\alpha_{22} + 3\alpha_{11}\alpha_{22} + 3\alpha_{11})$, $a_3 = \alpha_{33}$, $a_4 = \alpha_{33}$, $a_5 = \sqrt{3}$, and $a_6 = \sqrt{3}(\alpha_{22} - \alpha_{11})$in which $\alpha_{11}, \alpha_{22}, \alpha_{33}$, and α_{23} are the system constants.

(j) The dispersion relation of the holes in p-InSb can be written in accordance with Cunningham [278] as

$$\overline{E} = c_4(1 + \gamma_4 f_4)k^2 \pm \frac{1}{3}[2\sqrt{2}\sqrt{c_4}\sqrt{16 + 5\gamma_4}\sqrt{E_4 g_4 k}], \tag{R1.15}$$

where $c_4 \equiv \hbar^2/2m_0 + \theta_4$, $\theta_4 \equiv 4.7(\hbar^2/2m_0)$, $\gamma_4 \equiv b_4/c_4$, $b_4 \equiv [3/2(b_5) + 2\theta_4]$, $b_5 \equiv 2.4(\hbar^2/2m_0)$, $f_4 \equiv \frac{1}{4}\left[\sin^2 2\theta + \sin^4\theta \sin^2 2\phi\right]$, θ is measured from the positive z-axis, ϕ is measured from positive x-axis, $g_4 \equiv \sin\theta \left[\cos^2\theta + \frac{1}{4}\right.$ $\left.\sin^4\theta \sin^2 2\phi\right]$, and $E_4 = 5 \times 10^{-4}$ eV.

(k) The energy spectrum of the valance bands of CuCl in accordance with Yekimov et al. [279] can be written as

$$E_h = (\gamma_6 - 2\gamma_7)\frac{\hbar^2 k^2}{2m_0} \tag{R1.16}$$

and

$$E_{l,s} = (\gamma_6 + \gamma_7)\frac{\hbar^2 k^2}{2m_0} - \frac{\Delta_1}{2} \pm \left[\frac{\Delta_1^2}{4} + \gamma_7 \Delta_1 \frac{\hbar^2 k^2}{2m_0} + 9\left(\frac{\gamma_7 \hbar^2 k^2}{2m_0}\right)^2\right]^{1/2}, \tag{R1.17}$$

where $\gamma_6 = 0.53, \gamma_7 = 0.07$, and $\Delta_1 = 70$ meV.

(l) In the presence of stress, χ_6 along the $\langle 001\rangle$ and $\langle 111\rangle$ directions, the energy spectra of the holes in semiconductors having diamond structure valance bands can be respectively expressed following Roman [280] et al. as

$$E = A_6k^2 \pm \left[\overline{B}_7^2k^4 + \delta_6^2 + B_7\delta_6\left(2k_z^2 - k_s^2\right)\right]^{1/2} \tag{R1.18}$$

and

$$E = A_6k^2 \pm \left[\overline{B}_7^2k^4 + \delta_7^2 + \frac{D_6}{\sqrt{3}}\delta_7(2k_z^2 - k_s^2)\right]^{1/2}, \tag{R1.19}$$

where A_6, B_7, D_6, and C_6 are inverse mass band parameters in which $\delta_6 \equiv l_7\left(\overline{S}_{11} - \overline{S}_{12}\right)\chi_6$, $\overline{S}_{ij}$ are the usual elastic compliance constants, $\overline{B}_7^2 \equiv (B_7^2 + c_6^2/5)$, and $\delta_7 \equiv (d_8S_{44}/2\sqrt{3})\chi_6$. For gray tin, $d_8 = -4.1\,\text{eV}$, $l_7 = -2.3\,\text{eV}$, $A_6 = 19.2(\hbar^2/2m_0)$, $B_7 = 26.3(\hbar^2/2m_0)$, $D_6 = 31(\hbar^2/2m_0)$, and $c_6^2 = -1112(\hbar^2/2m_0)$.

(m) The dispersion relation of the carriers of cadmium and zinc diphosphides are given by [257]

$$E = \left[\beta_1 + \frac{\beta_2\beta_3(k)}{8\beta_4}\right]k^2 \pm \left\{\left[\beta_4\beta_3(k)\left(\beta_5 - \frac{\beta_2\beta_3(k)}{8\beta_4}\right)k^2\right] + 8\beta_4^2\left(1 - \frac{\beta_3^2(k)}{4}\right) - \beta_2\left(1 - \frac{\beta_3^2(k)}{4}\right)k^2\right\}^{1/2} \tag{R1.20}$$

where $\beta_1, \beta_2, \beta_4$, and β_5 are system constants and $\beta_3(k) = k_x^2 + k_y^2 - 2k_z^2/k^2$.

(R1.3) Investigate the FNFE from quantum wells, wires, and dots of all the semiconductors as considered in R1.1 and R1.2, respectively.

(R1.4) Investigate the FNFE from bulk specimens of heavily doped semiconductors in the presence of Gaussian, exponential, Kane, Halperian, Lax, and Bonch-Burevich types of band tails [103, 104] for all systems whose unperturbed carrier energy spectra are defined in R1.1 and R1.2, respectively.

(R1.5) Investigate the FNFE from quantum wells, wires, and dots of all the heavily doped semiconductors as considered in R1.4.

(R1.6) Investigate the FNFE from bulk specimens of the negative refractive index, organic, magnetic, and other advanced optical materials in the presence of an arbitrarily oriented alternating electric field.

(R1.7) Investigate the FNFE from quantum wells, wires, and dots of the negative refractive index, organic, magnetic, and other advanced optical materials in the presence of an arbitrarily oriented alternating electric field.

(R1.8) Investigate the FNFE from the multiple quantum wells, wires, and dots of semiconductors whose unperturbed carrier energy spectra are defined in R1.1, R1.2, and heavily doped semiconductors in the presences of Gaussian, exponential, Kane, Halperian, Lax, and Bonch-Burevich types of band tails [103, 104] for all systems whose unperturbed carrier energy spectra are defined in the same problems respectively.

(R1.9) Investigate the FNFE from all the appropriate low-dimensional systems of this chapter in the presence of finite potential wells.

(R1.10) Investigate the FNFE from all the appropriate low-dimensional systems of this chapter in the presence of parabolic potential wells.

(R1.11) Investigate the FNFE from all the appropriate systems of this chapter forming quantum rings.

(R1.12) Investigate the FNFE from all the above appropriate problems in the presence of elliptical Hill and quantum square rings.

(R1.13) Investigate the FNFE for the appropriate accumulation layers for all the materials whose unperturbed carrier energy spectra are defined in R1.1and R1.2, respectively.

(R1.14) Investigate the FNFE from wedge shaped, cylindrical, ellipsoidal, conical, triangular, circular, parabolic rotational, and parabolic cylindrical quantum dots in the presence of an arbitrarily oriented alternating electric field for all the materials whose unperturbed carrier energy spectra are defined in R1.1 and R1.2, respectively.

(R1.15) Investigate the FNFE from wedge shaped, cylindrical, ellipsoidal, conical, triangular, circular, parabolic rotational, and parabolic cylindrical quantum dots of the negative refractive index, organic, magnetic, and other advanced optical materials in the presence of an arbitrarily oriented alternating electric field.

(R1.16) Formulate the time delay for all the appropriate systems of this chapter.

(R1.17) Formulate the reflection time for all the appropriate systems of this chapter.

(R1.18) Formulate the minimum tunneling, Dwell and Phase tunneling, Buttiker and Landauer, and intrinsic times for all the appropriate systems of this chapter.

(R1.19) Investigate all the appropriate problems of this chapter for a Dirac electron.

(R1.20) Investigate all the appropriate problems of this chapter by including the many body, image force, broadening, and hot carrier effects, respectively.

(R1.21) Investigate all the appropriate problems of this chapter by removing all the mathematical approximations and establishing the respective appropriate uniqueness conditions.

References

1. R.H. Fowler, L. Nordheim, Proc. Roy. Soc. London A **119**, 173 (1928)
2. A. Van Der Ziel, *Solid State Physical Electronics* (Prentice-Hall, Englewood Cliffs, 1957), p.176
3. B. Mitra, K.P. Ghatak, Phys. Lett. A **357**, 146 (1990)
4. B. Mitra, K.P. Ghatak, Phys. Lett. A **142A**, 401 (1989)
5. K.P. Ghatak, M. Mondal, J. Mag. Mag. Mat. **74**, 203 (1988)
6. K.P. Ghatak, B. Mitra, Phys. Lett.**156A**, 233 (1991)
7. K.P. Ghatak, A. Ghosal, S.N. Biswas, M. Mondal, Proc. SPIE USA **1308**, 356 (1990)
8. V.T. Binh, Ch. Adessi, Phys. Rev. Lett. **85**, 864 (2000)
9. R.G. Forbes, Ultramicroscopy **79**, 11 (1999)

10. J.W. Gadzuk, E.W. Plummer, Rev. Mod. Phys **45**, 487 (1973)
11. J.M. Beebe, B. Kim, J.W. Gadzuk, C.D. Frisbie, J.G. Kushmerick, Phys. Rev. Lett **97**, 026801 (1999)
12. Y. Feng, J.P. Verboncoeur, Phys. Plasmas **12,** 103301 (2005)
13. W.S. Koh, L.K. Ang, Nanotechnology **19**, 235402 (2008)
14. M. Razavy, *Quantum Theory of Tunneling* (World Scientific, Singapore, 2003)
15. S.I. Baranchuk, N.V. Mileshkina, Sov. Phys. Solid State **23**, 1715 (1981)
16. P.G. Borzyak, A.A. dadykin, Sov. Phys. Docklady **27**, 335(1982)
17. S. Bono, R.H. Good, Jr., Surface Sci. **134**, 272 (1983)
18. S.M. Lyth, S.R.P. Silva, Appl. Phys. Lett. **90**, 173124 (2007)
19. C. Xu, X. Sun, Int. J. Nanotechnol. **1**, 452 (2004)
20. S.D. Liang, L. Chen, Phys. Rev. Lett. **101**, 027602 (2008)
21. E.C. Heeres, E.P.A.M. Bakkers, A.L. Roest, M. Kaiser, T.H. Oosterkamp, N. de Jonge, Nano Lett. **7**, 536 (2007)
22. L. Dong, J. Jiao, D.W. Tuggle, J.M. Petty, S.A. Elliff, M. Coulter, Appl. Phys. Lett. **82**, 1096 (2003)
23. S.Y. Li, P. Lin, C.Y. Lee, T.Y. Tseng, J. Appl. Phys. **95**, 3711(2004)
24. N.N. Kulkarni, J. Bae, C.K. Shih, S.K. Stanley, S.S. Coffee, J.G. Ekerdt, Appl. Phys. Lett. **87**, 213115 (2005)
25. K Senthil, K. Yong, Mat. Chem. Phys. **112**, 88 (2008)
26. R. Zhou, H.C. Chang, V. Protasenko, M. Kuno, A.K. Singh, D. Jena, H. Xing, J. Appl. Phys. **101**, 073704 (2007)
27. K.S. Yeong, J.T.L. Thong, J. Appl. Phys. **100**, 114325 (2006)
28. C.H. Oon, S.H. Khong, C.B. Boothroyd, J.T.L. Thong, J. Appl. Phys. **99**, 064309 (2006)
29. . B.H. Kim, M.S. Kim, K.T. Park, J.K. Lee, D.H. Park, J. Joo, S.G. Yu, S.H. Lee, Appl. Phys. Lett. **83**, 539 (2003)
30. Z.S. Wu, S.Z. Deng, N.S. Xu, J. Chen, J. Zhou, J. Chen, Appl. Phys. Lett. **80**, 3829 (2002)
31. Y.W. Zhu, T. Yu, F.C. Cheong, X.J. Xu, C.T. Lim, V.B.C. Tan, J.T.L. Thong, C.H. Sow, Nanotechnology **16**, 88 (2005)
32. Y.W. Zhu, H.Z. Zhang, X.C. Sun, S.Q. Feng, J. Xu, Q. Zhao, B. Xiang, R.M. Wang, D.P. Yu, Appl. Phys. Lett. **83**, 144(2003)
33. S. Bhattacharjee, T. Chowdhury, Appl. Phys. Lett. **95**, 061501 (2009)
34. S. Kher, A. Dixit, D.N. Rawat, M.S. Sodha, Appl. Phys. Lett. **96**, 044101 (2010)
35. I. Shigeo, W. Teruo, O. Kazuyoshi, T. Masateru, U. Satoshi, N. Norio, J. Vac. Sci. Technol. B **13**, 487(2009)
36. C.A. Spindt, I. Brodie, L. Humphrey, E.R. Westerberg, J. Appl. Phys. **47**, 5248 (2009)
37. Q. Fu, A.V. Nurmikko, L.A. Kolodziejski, R.L. Gunshor, J.W. Wu, Appl. Phys. Lett. **51**, 578 (2009)
38. P.M. Petroff, A.C. Gossard, W. Wiegmann, Appl. Phys. Lett. **45**, 620 (1984)
39. J.M. Gaines, P.M. Petroff, H. Kroemar, R.J. Simes, R.S. Geels, J.H. English, J. Vac. Sci. Technol. **B 6**, 1378 (1988)
40. J. Cilbert, P.M. Petroff, G.J. Dolan, S.J. Pearton, A.C. Gossard, J.H. English, Appl. Phys. Lett. **49**, 1275 (1986)
41. T. Fujui, H. Saito, Appl. Phys. Lett. **50**, 824 (1987)
42. H. Sasaki, Jpn. J. Appl. Phys. **19**, 94 (1980)
43. P.M. Petroff, A.C. Gossard, R.A. Logan, W. Weigmann, Appl. Phys. Lett. **41** 635 (1982)
44. H. Temkin, G.J. Dolan, M.B. Panish, S.N.G. Chu, Appl. Phys. Lett. **50**, 413 (1988)
45. I. Miller, A. Miller, A. Shahar, U. Koren, P.J. Corvini, Appl. Phys. Lett. **54**, 188 (1989)
46. L.L. Chang, H. Esaki, C.A. Chang, L. Esaki, Phys. Rev. Lett. **38**, 1489 (1977)
47. K. Less, M.S. Shur, J.J. Drunnond, H. Morkoc, IEEE Trans. Electron. Devices **ED-30**, 07 (1983)
48. G. Bastard, *Wave Mechanics Applied to Semiconductor Heterostructures (*Halsted, Les Ulis, Les Editions de Physique, New York, 1988)

49. M.J. Kelly, *Low Dimensional Semiconductors: Materials, Physics, Technology, Devices* (Oxford University Press, Oxford, 1995)
50. C. Weisbuch, B. Vinter, *Quantum Semiconductor Structures* (Boston Academic Press, Boston, 1991)
51. N.T. Linch, Festkorperprobleme,**23**, 27 (1985)
52. D.R. Sciferes, C. Lindstrom, R.D. Burnham, W. Streifer, T.L. Paoli, Electron. Lett. **19**, 170 (1983)
53. P.M. Solomon, Proc. IEEE, **70**, 489 (1982)
54. T.E. Schlesinger, T. Kuech, Appl. Phys. Lett. **49**, 519 (1986)
55. D. Kasemet, C.S. Hong, N.B. Patel, P.D. Dapkus, Appl. Phys. Lett. **41**, 912 (1982)
56. K. Woodbridge, P. Blood, E.D. Pletcher, P.J. Hulyer, Appl. Phys. Lett. **45**, 16 (1984)
57. S. Tarucha, H.O. Okamoto, Appl. Phys. Lett. **45**, 16 (1984)
58. H. Heiblum, D.C. Thomas, C.M. Knoedler, M.I. Nathan, Appl. Phys. Lett. **47**, 1105 (1985)
59. O. Aina, M. Mattingly, F.Y. Juan, P.K. Bhattacharyya, Appl. Phys. Lett. **50**, 43 (1987)
60. I. Suemune, L.A. Coldren, IEEE J. Quant. Electronic. **24**, 1178 (1988)
61. D.A.B. Miller, D.S. Chemla, T.C. Damen, J.H. Wood, A.C. Burrus, A.C. Gossard, W. Weigmann, IEEE J. Quant. Electron. **21**, 1462 (1985)
62. P. Harrison, *Quantum Wells, Wires and Dots* (John Wiley and Sons, Ltd, 2002)
63. B.K. Ridley, *Electrons and Phonons in Semiconductors Multilayers* (Cambridge University Press, Cambridge, 1997)
64. V.V. Martin, A.A. Kochelap, M.A. Stroscio, *Quantum Heterostructures* (Cambridge University Press, Cambridge, 1999)
65. C.S. Lent, D.J. Kirkner, J. Appl. Phys. **67**, 6353 (1990)
66. F. Sols, M. Macucci, U. Ravaioli, K. Hess, Appl. Phys. Lett. **54**, 350 (1980)
67. C.S. Kim, A.M. Satanin, Y.S. Joe, R.M. Cosby, Phys. Rev. B, **60**, 10962 (1999)
68. S. Midgley, J.B. Wang, Phys. Rev. B **64**, 153304 (2001)
69. T. Sugaya, J.P. Bird, M. Ogura, Y. Sugiyama, D.K. Ferry, K.Y. Jang, Appl. Phys. Lett. **80**, 434 (2002)
70. B. Kane, G. Facer, A. Dzurak, N. Lumpkin, R. Clark, L. PfeiKer, K. West, Appl. Phys. Lett. **72**, 3506 (1998)
71. C. Dekker, Phys. Today **52**, 22 (1999)
72. A. Yacoby, H.L. Stormer, N.S. Wingreen, L.N. Pfeiffer, K.W. Baldwin, K.W. West, Phys. Rev. Lett. **77**, 4612 (1996)
73. Y. Hayamizu, M. Yoshita, S. Watanabe, H.A.L. PfeiKer, K. West, Appl. Phys. Lett. **81**, 4937 (2002)
74. S. Frank, P. Poncharal, Z.L. Wang, W.A. Heer, Science **280**, 1744 (1998)
75. I. Kamiya, I.I. Tanaka, K. Tanaka, F. Yamada, Y. Shinozuka, H. Sakaki, Physica E **13**, 131 (2002)
76. A.K. Geim, P.C. Main, N. LaScala, L. Eaves, T.J. Foster, P.H. Beton, J.W. Sakai, F.W. Sheard, M. Henini, G. Hill et al., Phys. Rev. Lett. **72**, 2061 (1994)
77. A.S. Melinkov, V.M. Vinokur, Nature **415**, 60 (2002)
78. K. Schwab, E.A. Henriksen, J.M. Worlock, M.L. Roukes, Nature **404**, 974 (2000)
79. L. Kouwenhoven, Nature **403**, 374 (2000)
80. S. Komiyama, O. Astafiev, V. Antonov, H. Hirai, Nature **403**, 405 (2000)
81. E. Paspalakis, Z. Kis, E. Voutsinas, A.F. Terziz, Phys. Rev. B **69**, 155316 (2004)
82. J.H. Jefferson, M. Fearn, D.L.J. Tipton, T.P. Spiller, Phys. Rev. A **66**, 042328 (2002)
83. J. Appenzeller, C. Schroer, T. Schapers, A. Hart, A. Froster, B. Lengeler, H. Luth, Phys. Rev. B **53**, 9959 (1996)
84. J. Appenzeller, C. Schroer, J. Appl. Phys. **87**, 31659 (2002)
85. P. Debray, O.E. Raichev, M. Rahman, R. Akis, W.C. Mitchel, Appl. Phys. Lett. **74**, 768 (1999)
86. D. Kasemet, C.S. Hong, N.B. Patel, P.D. Dapkus, Appl. Phys. Lett.**41**, 912 (1982)
87. K. Woodbridge, P. Blood, E.D. Pletcher, P.J. Hulyer, Appl. Phys. Lett. **45**, 16 (1984)
88. S. Tarucha, H.O. Okamoto, Appl. Phys. Lett. **45**, 16 (1984)
89. M.I. Nathan, Appl. Phys. Lett. **47**, 1105 (1985)

90. I. Suemune, L.A. Coldren, IEEE J. Quant. Electronic. **24**, 1178 (1988)
91. J.L. Shay, J.W. Wernick, *Ternary Chalcopyrite Semiconductors – Growth, Electronic Properties and Applications* (Pergamon, London, 1975)
92. J.W. Rowe, J.L. Shay, Phys. Rev. B, **3,** 451 (1973)
93. H. Kildal, Phys. Rev. B, **10,** 5082 (1974)
94. J. Bodnar, in Proc. Int. Conf. of the Physics of Narrow-gap Semiconductors (Polish Science Publishers, Warsaw, 1978)
95. G.P. Chuiko, N.N. Chuiko, Sov. Phys. Semicond. **15**, 739 (1981)
96. K.P. Ghatak, S.N. Biswas, Proc. of SPIE, **1484**, 149 (1991)
97. A. Rogalski, J. Alloys Comp. **371**, 53 (2004)
98. A. Baumgartner, A. Chaggar, A. Patanè, L. Eaves, M. Henini, Appl. Phys. Lett. **92**, 091121 (2008)
99. J. Devenson, R. Teissier, O. Cathabard, A.N. Baranov, Proc. SPIE **6909**, 69090U (2008)
100. B.S. Passmore, J. Wu, M.O. Manasreh, G.J. Salamo, Appl. Phys. Lett. **91**, 233508 (2007)
101. M. Mikhailova, N. Stoyanov, I. Andreev, B. Zhurtanov, S. Kizhaev, E. Kunitsyna, K. Salikhov, Y. Yakovlev, Proc. SPIE **6585**, 658526 (2007)
102. W. Kruppa, J.B. Boos, B.R. Bennett, N.A. Papanicolaou, D. Park, R. Bass, Electron. Lett. **42**, 688 (2006)
103. B.R. Nag, *Electron Transport in Compound Semiconductors* (Springer Verlag, 1980)
104. E.O. Kane, in *Semiconductors and Semimetals*, Vol. 1, Ed. By R.K. Willardson, A.C. Beer (Academic Press, New York, 1966), p. 75
105. G.E. Stillman, C.M. Wolfe, J.O. Dimmock in *Semiconductors and Semimetals*, Ed. R.K. Willardon, A.C. Beer 12 (Academic, New York, 1977), p. 169
106. D.J. Newson, A. Karobe, Semiconductor. Sci. Technol. **3**, 786 (1988)
107. E.D. Palik, G.S. Picus, S. Teither, R.E. Wallis, Phys. Rev. **122**, 475 (1961)
108. P.Y. Lu, C.H. Wung, C.M. Williams, S.N.G. Chu, C.M. Stiles, Appl. Phys. Lett. **49** (1986) 1372
109. N.R. Taskar, I.B. Bhat, K.K. Prat, D. Terry, H. Ehasani, S.K. Ghandhi, J. Vac. Sci. Technol. **7A** (1989) 281
110. F. Koch, *Springer Series in Solid States Sciences*, vol. 53 (Springer-Verlag, Berlin, 1984), pp. 20
111. L.R. Tomasetta, H.D. Law, R.C. Eden, I. Reyhimy, K. Nakano, IEEE J. Quant. Electron. **14** (1978) 800
112. T. Yamato, K. Sakai, S. Akiba, Y. Suematsu, IEEE J. Quantum Electronics **14** (1978) 95
113. T.P. Pearsall, B.I. Miller, R.J. Capik, Appl. Phys. Lett. **28** (1976) 499
114. M.A. Washington, R.E. Nahory, M.A. Pollack, E.D. Beeke, Appl. Phys. Lett. **33** (1978) 854
115. M.I. Timmons, S.M. Bedair, R.J. Markunas, J.A. Hutchby, *Proceedings of the 16th IEEE Photovoltaic Specialist Conference* (IEEE, San Diego, California 666, 1982)
116. J.A. Zapien, Y.K. Liu, Y.Y. Shan, H. Tang, C.S. Lee, S.T. Lee, Appl. Phys. Lett. **90**, 213114 (2007)
117. M. Park, Proc. SPIE **2524**, 142 (1995)
118. S.-G. Hur, E.T. -Kim, J.H. -Lee, G.H. -Kim, S.G. -Yoon, Electrochem. Solid-State Lett. **11**, H176 (2008)
119. H. Kroemer, Rev. of Mod. Phys. **73**, 783 (2001)
120. T. Nguyen Duy, J. Meslage, G. Pichard, J. Crys. Growth, **72**, 490 (1985)
121. T. Aramoto, F. Adurodija, Y. Nishiyama, T. Arita, A. Hanafusa, K. Omura, A. Morita, Solar Energy Mat. Solar Cells, **75**, 211 (2003)
122. H.B. Barber, J. Elect. Mat. **25**, 1232 (1996)
123. S. Taniguchi, T. Hino, S. Itoh, K. Nakano, N. Nakayama, A. Ishibashi, M. Ikeda, Elect. Lett. **32**, 552 (1996)
124. J.J. Hopfield, J. Appl. Phys. **32,** 2277 (1961)
125. R.V. Belosludov, A.A. Farajian, H. Mizuseki, K. Miki, Y. Kawazoe, Phys. Rev. B, **75**, 113411 (2007)

126. J. Heremans, C.M. Thrush, Y.-M. Lin, S. Cronin, Z. Zhang, M.S. Dresselhaus, J.F. Mansfield, Phys. Rev. B **61**, 2921 (2000)
127. D. Shoenberg, Proc. Roy. Soc. (London) **170**, 341 (1939)
128. B. Abeles, S. Meiboom, Phys. Rev. **101**, 544 (1956)
129. B. Lax, J.G. Mavroides, H.J. Zieger, R.J. Keyes, Phys. Rev. Lett. **5**, 241 (1960)
130. Y.-H. Kao, Phys. Rev. **129,** 1122 (1963)
131. R.J. Dinger, A.W. Lawson, Phys. Rev. B, **3**, 253 (1971)
132. J.F. Koch, J.D. Jensen, Phys. Rev. **184**, 643 (1969)
133. M.H. Cohen Phys. Rev. **121**, 387 (1961)
134. S. Takaoka, H. Kawamura, K. Murase, S. Takano, Phys. Rev. B **13**, 1428 (1976)
135. J.W. McClure, K.H. Choi, Solid State Commun. **21**, 1015 (1977)
136. G.P. Agrawal, N.K. Dutta, *Semiconductor Lasers* (Van Nostrand Reinhold, New York, 1993), p. 547
137. S. Chatterjee, U. Pal, Opt. Eng., Bellingham, **32**, 2923 (1993)
138. T.K. Chaudhuri, Int. J. Energy Res. **16**, 481 (1992)
139. J.H. Dughaish, Physica B **322,** 205 (2002)
140. C. Wood, Rep. Prog. Phys. **51**, 459 (1988)
141. K.-F. Hsu, S. Loo, F. Guo, W. Chen, J.S. Dyck, C. Uher, T. Hogan, E.K. Polychroniadis, M.G. Kanatzidis, Science **303**, 818 (2004)
142. J. Androulakis, K.F. Hsu, R. Pcionek, H. Kong, C. Uher, J.J. D'Angelo, A. Downey, T. Hogan, M.G. Kanatzidis, Adv. Mater., Weinheim, Ger. **18**, 1170 (2006)
143. P.F.P. Poudeu, J. D'Angelo, A.D. Downey, J.L. Short, T.P. Hogan, M.G. Kanatzidis, Angew. Chem., Int. Ed. **45**, 3835 (2006)
144. P.F. Poudeu, J. D'Angelo, H. Kong, A. Downey, J.L. Short, R. Pcionek, T.P. Hogan, C. Uher, M.G. Kanatzidis, J. Am. Chem. Soc. **128**, 14347 (2006)
145. J.R. Sootsman, R.J. Pcionek, H. Kong, C. Uher, M.G. Kanatzidis, Chem. Mater. **18**, 4993 (2006)
146. A.J. Mountvala, G. Abowitz, J. Am. Ceram. Soc**. 48**, 651 (1965)
147. E.I. Rogacheva, I.M. Krivulkin, O.N. Nashchekina, A. Yu. Sipatov, V.A. Volobuev, M.S. Dresselhaus, Appl. Phys. Lett. **78**, 3238 (2001)
148. H.S. Lee, B. Cheong, T.S. Lee, K.S. Lee, W.M. Kim, J.W. Lee, S.H. Cho, J.Y. Huh, Appl. Phys. Lett. **85**, 2782 (2004)
149. K. Kishimoto, M. Tsukamoto, T. Koyanagi, J. Appl. Phys. **92**, 5331 (2002)
150. E.I. Rogacheva, O.N. Nashchekina, S.N. Grigorov, M.A. Us, M.S. Dresselhaus, S.B. Cronin, Nanotechnology **14**, 53 (2003)
151. E.I. Rogacheva, O.N. Nashchekina, A.V. Meriuts, S.G. Lyubchenko, M.S. Dresselhaus, G. Dresselhaus, Appl. Phys. Lett. **86**, 063103 (2005)
152. E.I. Rogacheva, S.N. Grigorov, O.N. Nashchekina, T.V. Tavrina, S.G. Lyubchenko, A.Yu. Sipatov, V.V. Volobuev, A.G. Fedorov, M.S. Dresselhaus, Thin Solid Films **493**, 41 (2005).
153. X. Qiu, Y. Lou, A.C.S. Samia, A. Devadoss, J.D. Burgess, S. Dayal, C. Burda, Angew. Chem., Int. Ed**. 44,** 5855 (2005)
154. C. Wang, G. Zhang, S. Fan, Y. Li, J. Phys. Chem. Solids **62**, 1957 (2001)
155. B. Poudel, W.Z. Wang, D.Z. Wang, J.Y. Huang, Z.F. Ren, J. Nanosci. Nanotechnol. **6**, 1050 (2006)
156. B. Zhang, J. He, T.M. Tritt, Appl. Phys. Lett. **88**, 043119 (2006)
157. W. Heiss, H. Groiss, E. Kaufmann, G. Hesser, M. Böberl, G. Springholz, F. Schäffler, K. Koike, H. Harada, M. Yano, Appl. Phys. Lett.**88**, 192109 (2006)
158. B.A. Akimov, V.A. Bogoyavlenskiy, L.I. Ryabova, V.N. Vasil'kov, Phys. Rev. B **61**, 16045 (2000)
159. Ya. A. Ugai, A.M. Samoilov, M.K. Sharov, O.B. Yatsenko, B.A. Akimov, Inorg. Mater. **38**, 12 (2002)
160. Ya. A. Ugai, A.M. Samoilov, S.A. Buchnev, Yu.V. Synorov, M.K. Sharov, Inorg. Mater. **38**, 450 (2002)

161. A.M. Samoilov, S.A. Buchnev, Yu.V. Synorov, B.L. Agapov, A.M. Khoviv, Inorg. Mater. **39**, 1132 (2003)
162. A.M. Samoilov, S.A. Buchnev, E.A. Dolgopolova, Yu.V. Synorov, A.M. Khoviv, Inorg. Mater**. 40**, 349 (2004)
163. H. Murakami, W. Hattori, R. Aoki, Phys. C **269**, 83 (1996)
164. H. Murakami, W. Hattori, Y. Mizomata, R. Aoki, Phys. C **273**, 41 (1996)
165. H. Murakami, R. Aoki, K. Sakai, Thin Solid Films, **27**, 343 (1999)
166. B.A. Volkov, L.I. Ryabova, D.R. Khokhlov, Phys. Usp. **45**, 819 (2002), and references therein
167. F. Hüe, M. Hÿtch, H. Bender, F. Houdellier, A. Claverie, Phys. Rev. Lett. **100**, 156602 (2008)
168. S. Banerjee, K.A. Shore, C.J. Mitchell, J.L. Sly, M. Missous, IEEE Proc., Circuits Devices Syst. **152**, 497 (2005)
169. M. Razeghi, A. Evans, S. Slivken, J.S. Yu, J.G. Zheng, V.P. Dravid, Proc. SPIE, **5840**, 54 (2005)
170. R.A. Stradling, Semicond. Sci. Technol. **6**,*C* 52 (1991)
171. P.K. Weimer, Proc. IEEE, **52**, 608 (1964)
172. G. Ribakovs, A.A. Gundjian, IEEE, J. Quant. Electron. **QE-14**, 42 (1978)
173. S.K. Dey, J. Vac. Sc. Tech. **10**, 227 (1973)
174. S.J. Lynch, Thin Solid Films, **102**, 47 (1983)
175. V.V. Kudzin, V.S. Kulakov, D.R. Pape', S.V. Kulakov, V.V. Molotok, IEEE, Ultrasonics Symposium, **1**, 749 (1997)
176. F. Hatami, V. Lordi, J.S. Harris, H. Kostial, W.T. Masselink, J. Appl. Phys. **97**, 096106 (2005)
177. B.W. Wessels, J. Electrochem. Soc. **122**, 402 (1975)
178. D.W.L. Tolfree, J. Sci. Instrum. **41**, 788, (1964)
179. P.B. Hart, Proc. the IEEE, **61**, 880, 1973
180. M.A. Hines, G.D. Scholes, Adv. Mater. **15**, 1844 (2003)
181. C.A. Wang, R.K. Huang, D.A. Shiau, M.K. Connors, P.G. Murphy, P.W. O'Brien, A.C. Anderson, D.M. DePoy, G. Nichols, M.N. Palmisiano, Appl. Phys. Lett, **83,** 1286 (2003)
182. C.W. Hitchcock, R.J. Gutmann, J.M. Borrego, I.B. Bhat, G.W. Charache, IEEE Trans. Electron. Devices, **46**, 2154 (1999)
183. H.J. Goldsmid, R.W. Douglas, Brit. J. Appl. Phys. **5**, 386 (1954)
184. F.D. Rosi, B. Abeles, R.V. Jensen, J. Phys. Chem. Sol. **10**, 191 (1959)
185. T.M. Tritt (ed.), *Semiconductors and Semimetals, Vols. 69, 70 and 71: Recent Trends in Thermoelectric Materials Research I, II and III* (Academic, New York, 2000)
186. D.M. Rowe (Ed.), *CRC Handbook of Thermoelectrics* (CRC, New York, 1995)
187. D.M. Rowe, C.M. Bhandari, *Modern Thermoelectrics* (Reston, Virginia, 1983)
188. D.M. Rowe (ed.), *Thermoelectrics Handbook: Macro to Nano* (CRC, New York, 2006)
189. H. Choi, M. Chang, M. Jo, S.J. Jung, H. Hwang, Electrochem. Solid-State Lett. **11**, H154 (2008)
190. S. Cova, M. Ghioni, A. Lacaita, C. Samori, F. Zappa, Appl. Opt. **35**, 1956 (1996)
191. H.W.H. Lee, B.R. Taylor, S.M. Kauzlarich, *Nonlinear Optics: Materials, Fundamentals, and Applications* (Technical Digest, 12, 2000)
192. E. Brundermann, U. Heugen, A. Bergner, R. Schiwon, G.W. Schwaab, S. Ebbinghaus, D.R. Chamberlin, E.E. Haller, M. Havenith, *29th International Conference on Infrared and Millimeter Waves and 12th International Conference on Terahertz Electronics*, 283 (2004)
193. A.N. Baranov, T.I. Voronina, N.S. Zimogorova, L.M. Kauskaya, Y.P. Yakoviev, Sov. Phys. Semicond. **19**, 1676 (1985)
194. M. Yano, Y. Suzuki, T. Ishii, Y. Matsushima, M. Kimata, Jpn. J. Appl. Phys. **17**, 2091 (1978)
195. F.S. Yuang, Y.K. Su, N.Y. Li, Jpn. J. Appl. Phys. **30**, 207 (1991)
196. F.S. Yuang, Y.K. Su, N.Y. Li, K.J. Gan, J. Appl. Phys. **68**, 6383 (1990)
197. Y.K. Su, S.M. Chen, J. Appl. Phys. **73**, 8349 (1993)
198. S.K. Haywood, A.B. Henriques, N.J. Mason, R.J. Nicholas, P.J. Walker, Semicond. Sci. Technol. **3**, 315 (1988)
199. C. Young, W.W. Anderson, L.B. Anderson, Trans. Electron Dev., IEEE, **24**, 492 (1977)
200. R.L. Gordon, V.I. Neeley, H.R. Curtin, Proc. IEEE, **54**, 2014 (1966)

201. P.K. Weimer, Proc. IRE, **50**, 1462 (1962)
202. M.J. Lee, S.W. Wright, C.P. Judge, P.Y. Cheung, Display Research Conference, International Conference Record, 211 (1991)
203. M. Abramowitz, I.A. Stegun, *Handbook of Mathematical Functions* (Dover, New York, 1965)
204. A. Haung, *Theoretical Solid State Physics*, vol. 1 (Pergamon, Oxford)
205. S. Flugge, *Practical Quantum Mechanics* (Springer Verlag, Berlin,1974)
206. M. Razavy, *Quantum Theory of Tunneling* (World Scientific, Singapore 2003)
207. J.O. Dimmock in *The Physics of Semimetals and Narrow Gap Semiconductors* Ed. by D.L. Carter, R.T. Bates (Pergamon, Oxford, 1971)
208. D.G. Seiler, B.D. Bajaj, A.E. Stephens, Phys. Rev. B **16**, 2822 (1977)
209. A.V. Germaneko, G.M. Minkov, Phys. Stat. Sol. (b) **184**, 9 (1994)
210. G.L. Bir, G.E. Pikus, *Symmetry and Strain – Induced Effects in Semiconductors* (Nauka, 1972) (in Russian)
211. M. Mondal, K.P. Ghatak, Phys. Stat. Sol. (b) **135**, K21 (1986)
212. J. Bouat, J.C. Thuillier, Surface Science, **73**, 528 (1978)
213. G.J. Rees, Phys. of Compounds, Proc. of the 13th Inter. Nat. Conf. Ed. F.G. Fumi, pp. 1166, North-Holland Company (1976)
214. P.R Emtage, Phys. Rev. **138**, A246 (1965)
215. M. Stordeur, W. Kuhnberger, Phys. Stat. sol. (b), **69**, 377(1975)
216. D.R. Lovett, *Semimetals and Narrow-Bandgap Semiconductor* (Pion, London, 1977)
217. H. Kohler, Phys. Stat. Sol.(b), **74**, 591(1976)
218. M. Cardona, W. Paul, H. Brooks Helv, Acta Phys. **33**, 329 (1960)
219. A.F. Gibson in *"Proceeding of International school of physics "ENRICO FERMI" course XIII*, Ed. R.A Smith, Academic Press, 171 (1963)
220. C.C. Wang, N.W. Ressler, Phys. Rev. **2**, 1827 (1970)
221. P.C Mathur, S. Jain, Phys. Rev. **19**, 1359(1979)
222. M. Singh, P.R. Wallace, S.D. Jog, E. Arushanov, J. Phys. Chem. Solids, **45**, 409 (1984)
223. Y. Yamada, J. Phys. Soc. Japan, **35**, 1600(1973), **37**, 606(1974)
224. J. Cisowski, J.C Portal, E.K Erushanov, J.M Broto, S. Huant, L.C Brumel, Phys.Stat.Sol(b), **121**, 289 (1984)
225. E.A. Arushanov, A.A. Kaynzev, A.N. Natepov, S.I. Radautsan, Sov. Phys. Semicond. **15**, 828 (1981)
226. K.S. Hong, R.F. Speyer, R.A. Condrate, J. Phys. Chem. Solids, **51**, 969 (1990)
227. M. Mondal, S. Banik, K. P. Ghatak, J. Low. Temp. Phys**. 74**, 423 (1989)
228. M.J. Gelten, C.V.M. VanEs, F.A.P. Blom, J.W.F. Jongencelen, Solid State Commun. **33**, 833 (1980)
229. A.A. El-Shazly, H.S. Soliman, H.E.A. El-Sayed, D.A.A. El-Hady, J. Vac. **47**, 53 (1996)
230. S. Adachi, *Properties of Group-IV, III–V and II–VI Semiconductors* (Wiley, New York, 2005)
231. O. Madelung, *Semiconductors: Data Handbook*, 3rd ed. (Springer-Verlag, Berlin, 2003)
232. S. Adachi, J. Appl. Phys. **58**, R1 (1985)
233. S. Adachi, *GaAs and Related Materials: Bulk Semiconductors and Superlattice Properties* (World Scientific, New York, 1994)
234. G.L. Hansen, J.L. Schmit, T.N. Casselman, J. Appl. Phys. **63**, 7079 (1982)
235. J. Wenus, J. Rutkowski, A. Rogalski, IEEE Trans. Elect. Dev. **48**, 1326 (2001)
236. S. Adachi, J. Appl. Phys**. 53**, 8775 (1982)
237. S.K. Sutradhar, D. Chattopadhyay, B.R. Nag, Phys. Rev. (b) **25**, 4069(1982)
238. D.G. Seiler, W.M. Beeker, L.M. Roth, Phys. Rev. **1**, 764 (1970)
239. I.V. Skryabinskii, Yu. I. Ukhanov, Sov. Phys. Solid State, **14**, 2838 (1973)
240. S. Tiwari, S. Tiwari, Cryst. Res. Technol. **41**, 78 (2006)
241. J.R. Lowney, S.D. Senturia, J. Appl. Phys. **47**, 1771 (1976)
242. W.E. Spicer, G.J. Lapeyre Phys. Rev. **139**, A565 (1965)
243. G.M.T. Foley, P.N. Langenberg, Phys. Rev. B, **15**, 4850 (1977)
244. D.R. Lovett, In: *Semimetals and Narrow Band Gap Semiconductors* (Pion, London, 1977)
245. C.C. Wu, C.J. Lin, J. Low. Temp. Phys. **57**, 469 (1984)

246. J. Rose, R. Schuchardt, Phys. Stat. Sol.(b), **117**, 213 (1983)
247. K.P Ghatak, S. Bhattachaya, D. De, *Einstein Relation in Compound Semiconductors and Nanostructures* (Springer Series in Material Sciences, **116**, 2009)
248. V.I. Ivanov-Omskii, A.Sh. Mekhtisev, S.A. Rustambekova, E.N. Ukraintsev, Phys. Stat. Sol. (b) **119**, 159 (1983)
249. H. Kim, K. Cho, H. Song, B. Min, J. Lee, G. Kim, S. Kim, S.H. Kim, T. Noh, Appl. Phys. Lett. **83**, 4619 (2003)
250. R.A. Reynolds, M.J. Brau, R.A. Chapman, J. Phys. Chem. Solids **29**, 755 (1968)
251. J. O'Shaughnessy, C. Smith, Solid State Commun. **8,** 481 (1970)
252. N.B. Brandt, V.N. Davydov, V.A. Kulbachinskii, O.M. Nikitina, Sov. Phys. Sol. Stat. **29**, 1014 (1987)
253. L.M. Viculis, J.J. Mack, O.M. Mayer, H.T. Hahn, R.B. Kaner, J. Mater. Chem. **15**, 974 (2005)
254. L.A. Vassilev, Phys. Stat. Sol. (b), **121**, 203 (1984)
255. D.L. Partin, Superlattices and Microstructures, **1**, 131 (1985)
256. W.J. Turner, A.S. Fischler, W.E. Reese, Phys. Rev. **121**, 759 (1961)
257. G.P. Chuiko, Sov. Phys. Semicond. **19(12)**, 1381 (1985)252
258. W.E. Swank, P.G. Le Comber, Phys. Rev. **153**, 844 (1967)
259. D. Haneman, J. Phys. Chem. Solids, **11**, 205 (1959)
260. N. Wei, G. Wu, J. Dong, Phys. Lett. A **325**, 403 (2004)
261. S. Reich, J. Maultzsch, C. Thomsen, P. Ordejo'n, Phys. Rev. B, **66**, 035412 (2006)
262. M.S. Lundstrom, J. Guo, *Nanoscale Transistors: Device Physics, Modeling and Simulation* (Springer, New York, 2006)
263. J.W. Mintmire, C.T. White, Phys. Rev. Lett. **81**, 2506 (1998)
264. F. Buonocore, F. Trani, D. Ninno, A. Di Matteo, G. Cantele, G. Iadonisi, Nanotechnology, **19**, 025711 (2008)
265. J.B. Ketterson, Phys. Rev. **129**, 18 (1963)
266. R.C. Vilão, J.M. Gil, A. Weidinger, H.V. Alberto, J. Piroto Duarte, N.A. de Campos, R.L. Lichti, K.H. Chow, S.P. Cottrell, S.F.J. Cox, Phys. Rev. B, **77**, 235212 (2008)
267. I. Kang, F.W. Wise, Phys. Rev. B, J. Opt. Soc. Am. B, **14**, 1632 (1997)
268. D. Cui, J. Xu,S.-Y. Xu, G. Paradee, B.A. Lewis, M.D. Gerhold, IEEE Trans. Elect. Dev. **5**, 362 (2006)
269. E.L. Ivchenko, G.E. Pikus. Sov. Phys. Semicond. **13**, 579 (1979)
270. E. Bangert, P. Kastner, Phys. Stat. Sol (b) **61**, 503(1974)
271. G.M.T. Foley, P.N Langenberg, Phys. Rev. B, **15B**, 4850 (1977)
272. V.I. Ivanov-Omskii, A.Sh. Mekhtisev, S.A. Rustambekova, E.N. Ukraintsev, Phys. Stat. Sol. (b) **119**, 159 (1983)
273. H.I. Zhang, Phys. Rev. B, **1**, 3450 (1970)
274. U. Rossler, Solid State Commun. **49**, 943 (1984)
275. J. Johnson, D.H. Dickey, Phys. Rev. **1**, 2676 (1970)
276. V.G. Agafonov, P.M. Valov, B.S. Ryvkin, I.D. Yarashetskin, Sov. Phys. Semiconduct. **12**, 1182 (1978)
277. N.S. Averkiev, V.M. Asnin, A.A. Bakun, A.M. Danishevskii, E.L. Ivchenko, G.E. Pikus, A.A. Rogachev, Sov. Phys. Semicond. **18**, 379 and 402 (1984)
278. R.W. Cunningham,Phys. Rev. **167**, 761(1968)
279. A.I. Yekimov, A.A. Onushchenko, A.G. Plyukhin, AI.L. Efros, J. Expt. Theor. Phys. **88**, 1490 (1985)
280. B.J. Roman, A.W. Ewald, Phys. Rev. B. **5**, 3914 (1972)

http://www.springer.com/978-3-642-20492-0

Fowler-Nordheim Field Emission
Effects in Semiconductor Nanostructures
Bhattacharya, S.; Ghatak, K.P.
2012, XXII, 338 p., Hardcover
ISBN: 978-3-642-20492-0